香港氣象學會

HKMetS BULLETIN, Volume 5, Number 1, 1995

HONG KONG METEOROLOGICAL SOCIETY

BULLETIN

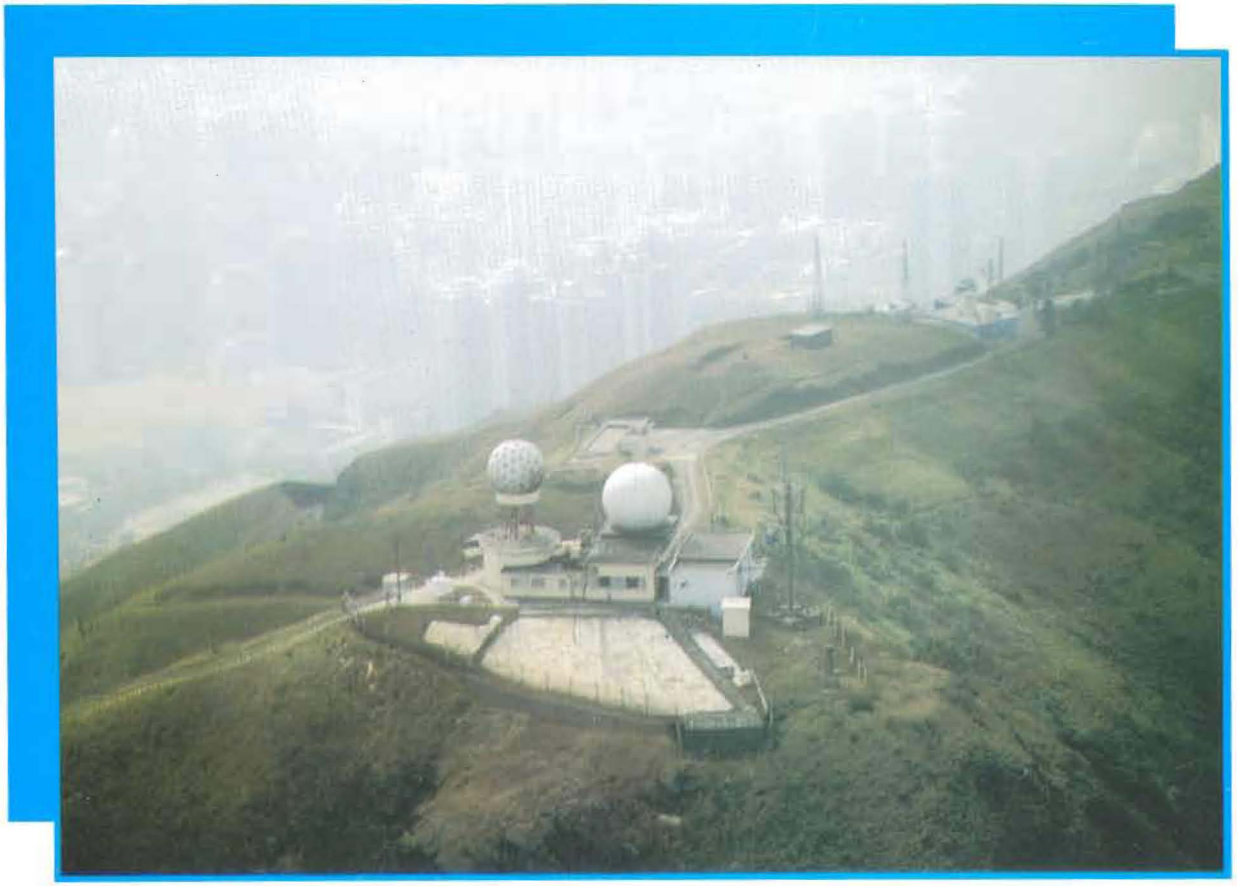

ISSN 1024-4468

ISSN 1024-4468

About the cover

The cover picture shows an aerial view of The Royal Observatory Hong Kong's Tate's Cairn radar station overlooking Kowloon to the southwest. The radome on the left houses the Digital Weather Weather Radar installed in 1983 and the subject of an article by S.K. Wong and K.L. Ho in *HKMetS Bulletin Vol. 4, No. 2*. The Doppler Weather Radar is housed in the protective radome on the left. See the article by B.Y. Lee, O. Wong, C.M. Cheng, S.C. Tai & Y.S. Hung in this issue for more details.

The Hong Kong Meteorological Society Bulletin is the official organ of the Society, devoted to editorials, articles, news, activities and announcements of the Society.

Members are encouraged to send any articles, media items or information for publication in the Bulletin.

For guidance see the "INFORMATION FOR CONTRIBUTORS" in the inside back cover.

Advertisements for products and/or services of interest to members of the Society are accepted for publication in the Bulletin.

For information on formats and rates please contact the Society Secretary at the address below.

Views expressed in the articles or any correspondence are those of the authors alone and do not necessarily represent those of the Society.

The mention of specific products and/or companies does not imply there is any endorsement by the Society or its office bearers in preference to others which are not so mentioned.

SUBSCRIPTION RATES

Two issues per volume.

Institutional rate:

HK$ 300 per volume.

Individual rate:

HK$ 150 per volume.

Published by

The Hong Kong Meteorological Society

c/o Royal Observatory, 134A Nathan Road, Kowloon, Hong Kong.

香港氣象學會 HKMetS BULLETIN, Vol. 5, Number 1, 1995

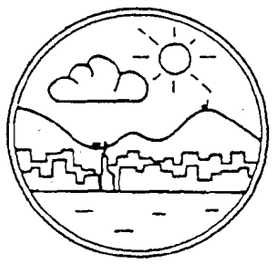

HONG KONG METEOROLOGICAL SOCIETY

BULLETIN

CONTENTS

Editorial

This issue of the *Bulletin* contains three papers on widely varying aspects of the atmospheric environment in Hong Kong.

The first paper, by Ronald Sequeira of the City University of Hong Kong, investigates the relationships between the chemical properties of rainwater collected at a rural site in the New Territories and the prevailing meteorological and human activities taking place. In it he draws attention to an apparent connection between the quality of rainwater and the prevailing meteorological conditions which gives rise to the rainfall and links this, not only to variations in atmospheric conditions, but also to the associated changes in human activity which take place in response to those conditions. While the *connection* may indeed prove to be *apparent*, as implied by the title, this paper is certain to raise new questions which should provide an impetus for further investigation.

The second paper continues the annual review of tropical cyclone activity in the Western North Pacific Ocean started in *Bulletin Vol.3 No.1*. As in previous issues, the paper documents all storms occurring in the region providing information about tracks, changing weather conditions and resulting impacts on the areas affected. Special emphasis is also placed on those storms affecting Hong Kong.

The third paper may be considered a follow-up to that by S.K. Wong and K.L. Ho of the Royal Observatory, Hong Kong (*Bulletin Vol.4 No.2*) which provided a brief history of the weather radars used by the Royal Observatory for the last 35 years. In this new paper, B.Y. Lee and his colleagues document the new Doppler Weather Radar recently installed at the Tate's Cairn facility, focussing on the capabilities of the system and the potential advantages for forecasting as this new data is now available.

The next section of this *Bulletin* provides our readers, as in the previous *Bulletin*, with the latest issue, Number 6 of *The United Nations Climate Change Bulletin*. This organ is published quarterly (Issue 6 in 1st quarter 1995) by the interim secretariat for the UN Climate Change Convention, the Secretariat of the UNEP/WMO Intergovernmental Panel on Climate Change (IPCC) and the UNEP/WMO Information Unit on Climate Change (IUCC). It provides articles and information of a general nature concerning the subject of climate change.

The remainder of the *Bulletin* contains the regular features *News and Announcements*, *Hong Kong Weather Reviews*, *Meeting Reviews* and *Calendar of Coming Events*. The *News and Announcements* section contains much useful information including the 1995 Atlantic Hurricane Season and Sahel Rainfall forecasts made by Colorado State University meteorologists. *Hong Kong Weather Reviews* focusses on Autumn 1994 and Winter 1994-95 in Hong Kong, providing an overview of the season and a more detailed monthly summary of weather events.

The Editorial Board expresses their thanks to the contributors and hope that you, the reader, find this issue useful and informative. We welcome all comments and suggestions for items to be included as well as news and contributions of articles related to your own activities.

Bill Kyle, Editor-in-chief

Ronald Sequeira

Department of Biology and Chemistry

City University of Hong Kong

On an Apparent Connection of the Electrical Conductivity of Rainwater with Severe Storms and Urban Activity in Hong Kong

ABSTRACT

Results of the analysis of seventeen daily, bulk rainfall samples from an elevated, vegetated, rural area in Hong Kong during the summer of 1993 are presented. The balance between the total inorganic cations and anions was satisfactory to excellent, with a single exception. However, the electrical conductivity calculated on the basis of the assumption that the rain samples are *infinitely dilute* only accounts for 34 to 80 percent of the experimentally measured value for thirteen of the samples. A significant observation is that the inorganic composition of the remaining four samples accounts, within experimental error, for the measured conductivity. It is observed that these rainfall episodes are associated with the influence on the territory of major tropical storms, and in one case, with the period that immediately followed the passage of one such storm.

It is tentatively suggested that bulk rainwater at the rural site is normally affected by charged particles of anthropogenic origin not included in the list of the analyzed inorganic ions, and therefore, probably largely organic. The direct impact of storms virtually clears the urban air of such particles. This is believed to be due partly to the arrival of the maritime (unpolluted air) which flushes out the urban air, and partly due to the hoisting of the severe storm signal (#8 or higher) which brings the usually hectic urban activities in the territory to a virtual halt.

Introduction

Rainwater is often considered to be a dilute aqueous solution to which the Kohlrausch *law of the independent migration of ions* (Barrow, 1979) should, in principle, be applicable. Indeed, the electrical conductivity of rainwater has been reported for numerous locations in the world for about two decades now (NOAA-WMO-EPA) with very few attempts to explain its measured value on the basis of the observed ionic composition, the notable exceptions being studies on U.S. precipitation with ionic strength predominantly below 0.1 mM (Miles and Yost, 1982), and a regression analysis of Alpine snow chemistry data (Puxbaum *et al.*, 1991).

A study of *event* type of samples in Venice (Argese and Bianchini, 1989) appears to suggest that filtration of even wet-only deposition is necessary for the approximate agreement between the calculated and measured conductivities, λ_K and λ_m, respectively. The above authors, however, also speculate that the unfiltered samples show changes in conductivity with time (days to several weeks) because of the slow dissolution of mineral constituents from soil particles in the water with a simultaneous disappearance of the H^+ ion. However, the Δ H values given in data presented in Table 1 of their paper apparently disagree (often with respect to the sign, let alone the magnitude) with the $\Delta \lambda_m$ for almost all data sets presented, thus lending very little support to their tentative explanation.

In the present paper, the chemical composition of seventeen, unfiltered, bulk daily rainwater samples collected at a rural location, Kadoorie Agricultural Research Centre (KARC), Shek Kong, New Territories, Hong Kong during the summer of 1993 are presented. The samples were collected during a variety of rainfall event situations associated with troughs and tropical cyclone activity. The station (Figure 1) is suitable as an urban background site for Hong Kong since it has no localized sources of air pollution. The measured electrical conductivity, λ_m is compared with that calculated from the inorganic ionic composition determined analytically, λ_K. The anion-to-cation ratio (R_1 *i.e.* $\Sigma - / \Sigma +$) and the pH variation are also presented.

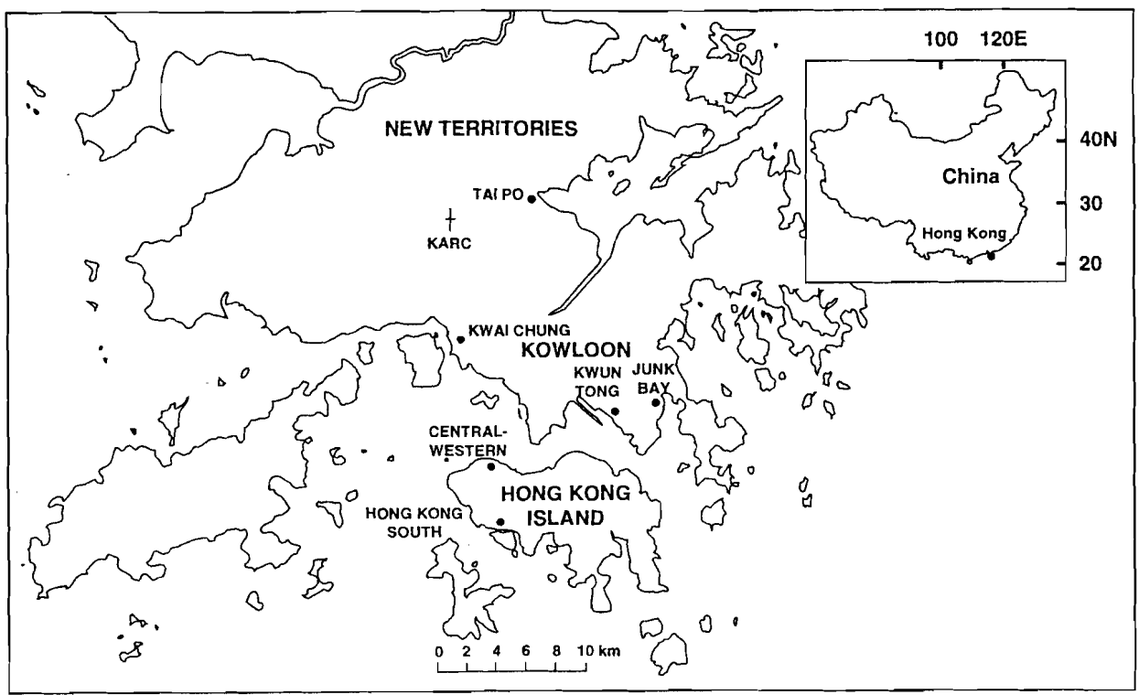

Figure 1. Map of Hong Kong and vicinity showing the rural sampling site: Kadoorie Agricultural Research Centre, KARC (+). The inset shows the position of Hong Kong relative to China

Sampling, Analysis & Calculations

The University of Hong Kong has been carrying out daily and weekly collections of bulk rainwater at Kadoorie Agricultural Research Centre (KARC) since April 1989 employing an all polyethylene funnel-and-bottle assembly as the collector. Some important results on the pH of the samples have already been presented and published (Peart, 1993: Sequeira and Peart, 1995).

Daily rain samples were usually collected at 0900 hr, labelled, and their date of collection and volume recorded. Their pH and electrical conductivity were measured immediately at the on-site KARC laboratory employing a PHM-83 (combined) glass electrode and the conductivity was measured with a CG-858 Schott-Gerate direct-reading conductivity meter.

During the summer 1993 season a number of the samples were collected during severe rainstorm conditions. The details are given in Table 1. In relation to the present study these severe storms could be classified into three separate categories. **Type I** events consist of widespread heavy rainfall associated with a lingering trough of low pressure over the region. These mainly led to the issue of rainstorm warnings by the Royal Observatory of heavy or very heavy rainfall and resulting, respectively, in the hoisting of the Red (R) or Black (B) rainstorm warning signals (*see* Table 1 and Figure 2).

Type II events encompass rainfall associated with tropical storms (TS), typhoons (T) and related severe weather systems which directly influenced the Territory of Hong Kong. Rainfall related to TS Koryn, T Becky and T Dot are included in this category (*see* Table 1 and Figures 3 to 5).

Lastly, **Type III** events were associated with storms of Type II which did not directly influence the Territory but nevertheless indirectly brought rainfall (*see* Table 1 and Figures 6 and 7).

After initial measurements of pH and electrical conductivity were taken the daily samples were collected from the on-site laboratory and analyzed for NH^+, Na^+, K^+, Cl^-, NO_3^- and SO_4^{2-} employing an Ion Chromatograph and for Mg and Ca by the Inductively Coupled Plasma (ICP-AES) technique. Samples awaiting analysis were refrigerated at 277K.

Table 1. Summary of important tropical and other storms, 1993 (Source: Royal Observatory, Hong Kong)

Storm	Dates	Rainfall (mm)		Remarks
		Territory	Shek Kong	
Convective and related rain systems	June 10-11	up to 270 (11th)	Heavy (>100)	torrential rain and thunderstorms (**R**)
	16	up to 260 (16th)	Heavy (>100)	as above (**R** ; **B**)
TS Koryn LP_c = 935 hPa **Vm** = 175 kmh^{-1}	June 26-28	24 to 27	57.5	peaked on 27th; signals **#1**, **#3**, **#8NE**, **#8SE** hoisted
STS Lewis	July 10-13	67 to 141	75 *est.*	minimal impact; only signal **#1** hoisted
T Abe LP_c = 950 hPa **Vm** = 160 kmh^{-1}	Sept 13-14	0 to 65.5	13	as above; approached territory from eastern side and departed from north
STS Becky	Sept 16-18	88.5 to 141	104.5	hit territory with full force crossing from south and leaving toward west signals **#1**, **#3**, **#8NE**, **#8SE** hoisted
T Dot LP_c = 965 hPa **Vm** = 140 kmh^{-1}	Sept 23-27	278 to 770	278	developed from area of disturbance in South China Sea; approached HK from southwest, left from west; peaked 26th; signal **#1**, **#3**, **#8SE** hoisted

The symbols denote the following:

R ; **B** - **R**ed and **B**lack rainstorm warning issued on **heavy** to **locally very heavy** rainfall;
TS, **STS**, **T** - Tropical Storm, Severe Tropical Storm, Typhoon respectively;
LP_c - lowest central pressure; **Vm** - maximum winds off centre; **#1** - standby signal;
#3 - strong wind signal; **#8NE** / **#8SE** - gale or storm signal from direction indicated

The bicarbonate ion $[HCO_3^-]$ concentration was estimated only when required (pH > 5) from the expression (Sequeira, 1988):

$$[HCO_3^-] = [H_2CO_3] \cdot 10^{pH-pK_1} \qquad (1)$$

where $[H_2CO_3]$ is a constant based on the temperature, partial pressure of atmospheric CO_2 and on Henry's Law: $pK_1 = -\log K_1$, where K_1 is the first dissociation constant of H_2CO_3. The calculation of the "total" ionic conductivity (due to the **n** significantly-to-appreciably abundant ions which are considered), λ_K, is carried out employing the following expression:

$$\lambda_K = \Sigma^n [\,|z|\, M^{z\pm}]_j \cdot \lambda_{ij} \qquad (2)$$

where, the quantity inside the square brackets is the equivalent concentration of the ionic species M_j whose charge (common valence) is $+z$; $|\ |$ is the *modulus* and λ_{ij} is the equivalent ionic conductance of the j^{th} species in solution. Standard $_{ij}$ values were used (Barrow, 1979) in the calculation.

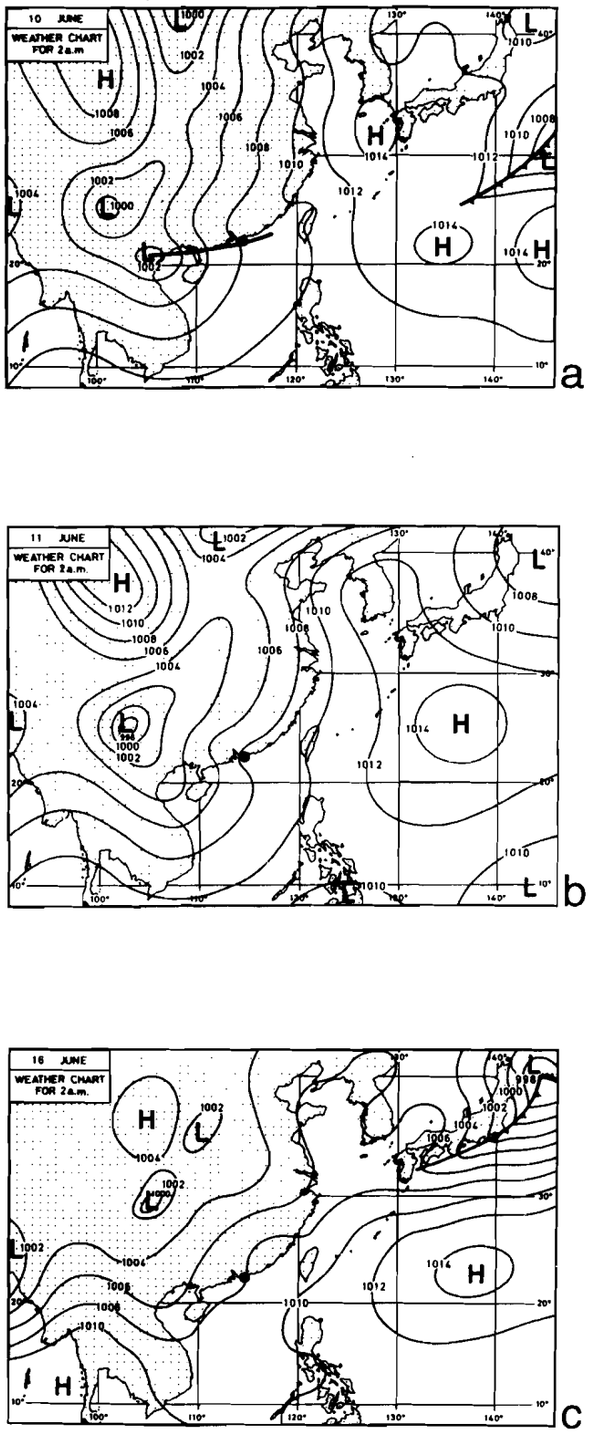

Figure 2 Daily Weather Maps for (a) 10th; (b) 11th; and (c) 16th June, 1993 associated with heavy rainfall in Hong Kong. Courtesy: Royal Observatory, Hong Kong.
(the location of Hong Kong is indicated by the dot (●) on the southeast coast of China)

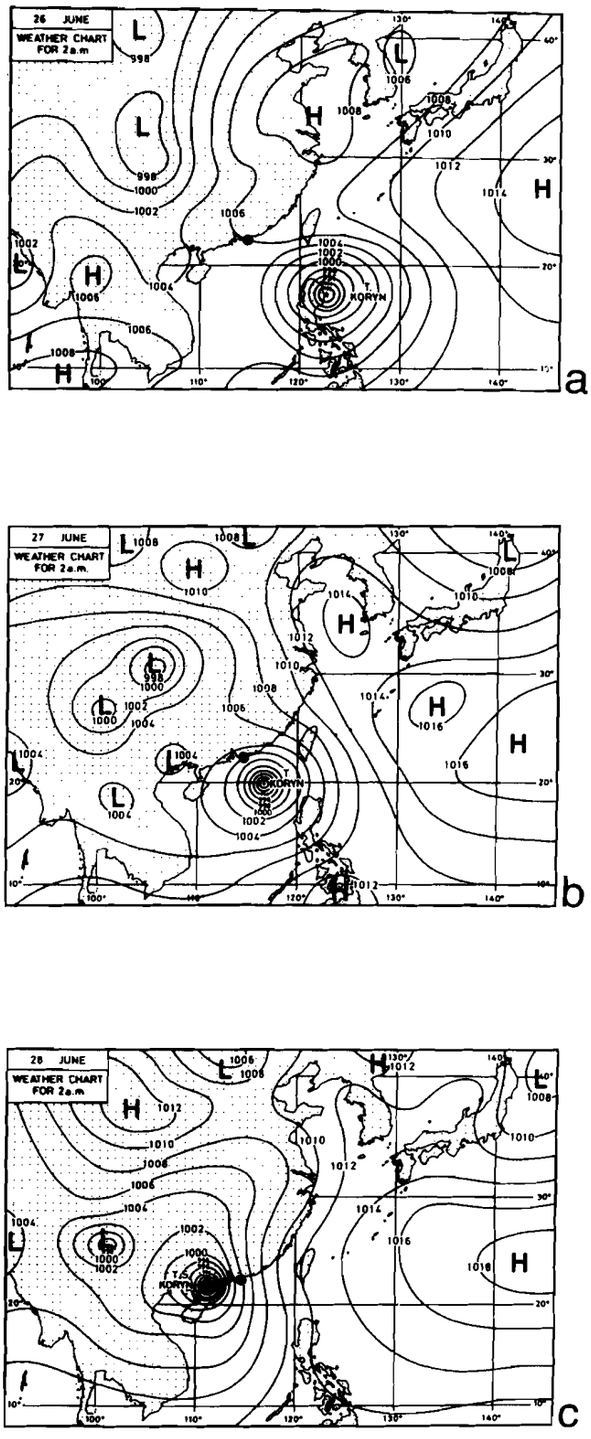

Figure 3 Daily Weather Maps for (a) 26th; (b) 27th; and (c) 28th June, 1993 showing the approach of Tropical Storm Koryn towards Hong Kong. Courtesy: Royal Observatory, Hong Kong. (the location of Hong Kong is indicated by the dot (●) on the southeast coast of China)

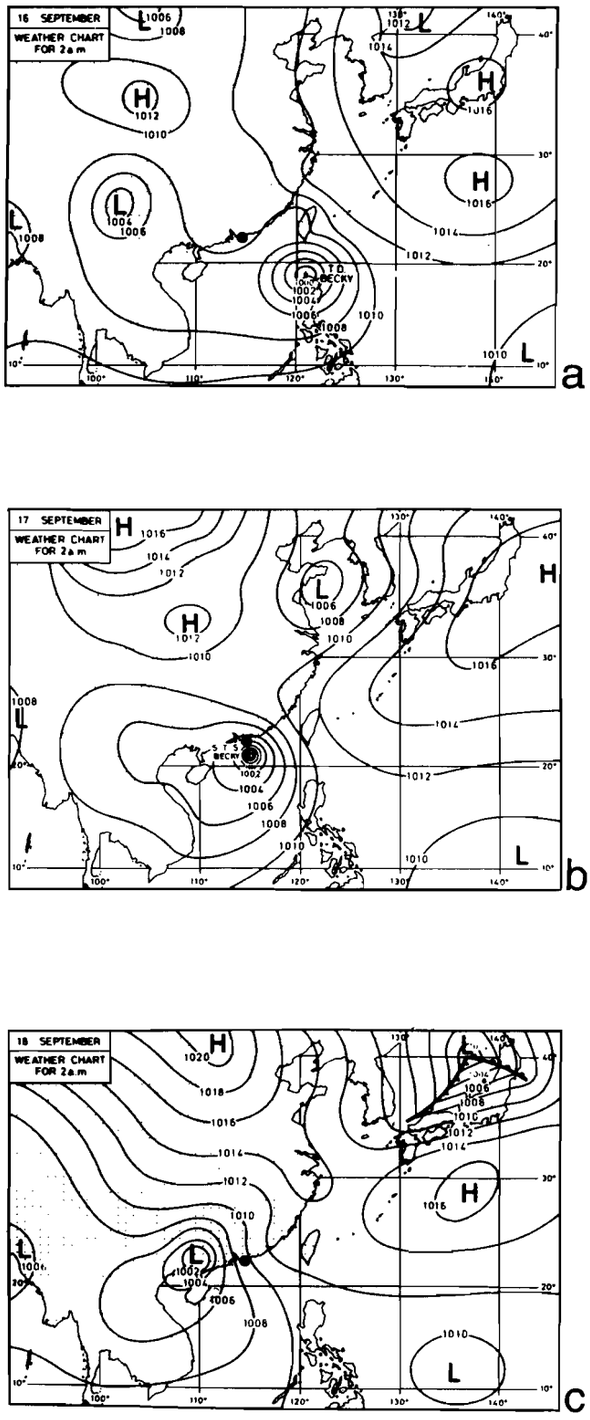

Figure 4 Daily Weather Maps for (a) 16th; (b) 17th; and (c) 18th September, 1993 showing the approach of Typhoon Becky towards Hong Kong. Courtesy: Royal Observatory, Hong Kong. (the location of Hong Kong is indicated by the dot (●) on the southeast coast of China)

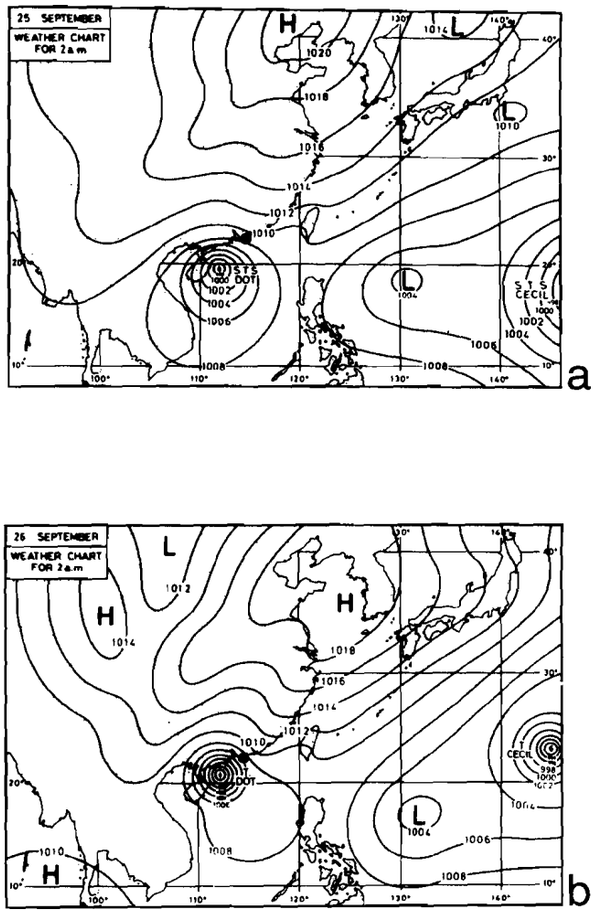

Figure 5 Daily Weather Maps for (a) 25th; and (b) 26th September, 1993 showing the approach of Typhoon Dot towards Hong Kong. Courtesy: Royal Observatory, Hong Kong. (the location of Hong Kong is indicated by the dot (●) on the southeast coast of China)

Results and Discussion

pH

The pH of the rainwater samples varies between 4.07 and 5.51 (Figure 8). The relatively higher values are apparently associated with the passage of typhoons which hit the territory with full force, not after landfall. (*see* Figures 3 - 5) However, one tropical storm, *Koryn (TS-K)*, shows rainfall with a slightly lower pH around 4.9. It may be observed that there is no consistency in the apparent relationship between the rainfall amount and the pH, a conclusion also reached by us in another recent study (Sequeira and Lung, 1995).

Yet, mostly a relatively higher pH is observed when the tropical storms hit, which may indicate that there is a flushing of the relatively more acidic urban air, usually present over Hong Kong, by a predominantly maritime airmass associated with tropical storms and typhoons. Table 1 does show consistently heavy rainfall during tropical storms when the pH of the rainwater is greater than 5. Finally, there is an indication that the expected cleansing of the local air by two widespread episodes in rapid succession (12 and 17 June samples) of territory-wide rainfall not associated with tropical storms results in the holding of the pH almost steady at around 4.8 (*see* Table 1 and Figure 8).

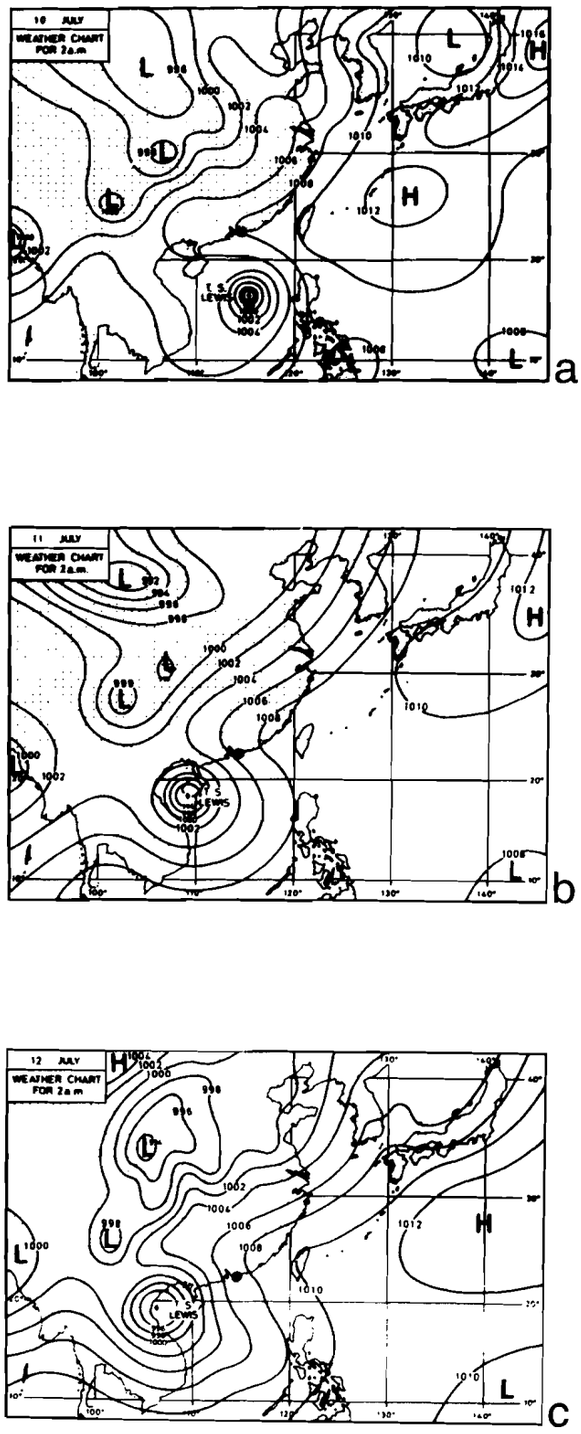

Figure 6 Daily Weather Maps for (a) 10th; (b) 11th; and (c) 12th July, 1993 showing the approach of Tropical Storm Lewis towards Hong Kong. Courtesy: Royal Observatory, Hong Kong. (the location of Hong Kong is indicated by the dot (●) on the southeast coast of China)

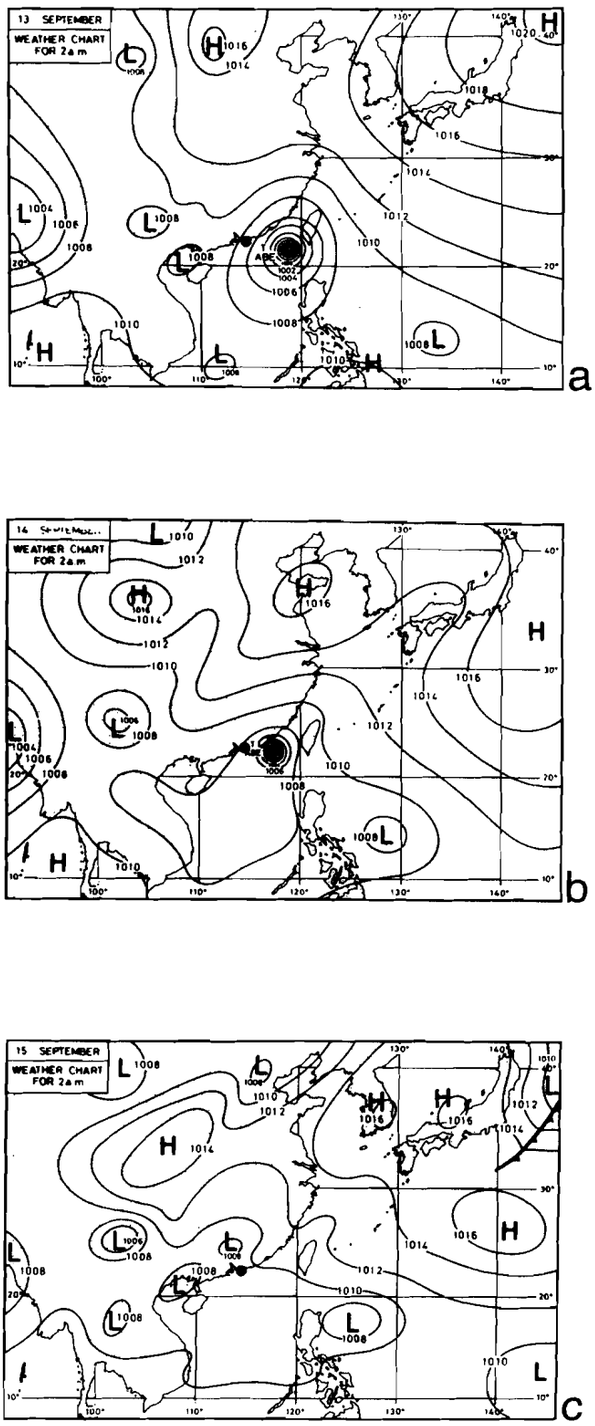

Figure 7 Daily Weather Maps for (a) 13th; (b) 14th; and (c) 15th September, 1993 showing the approach of Typhoon Abe towards Hong Kong. Courtesy: Royal Observatory, Hong Kong.
(the location of Hong Kong is indicated by the dot (●) on the southeast coast of China)

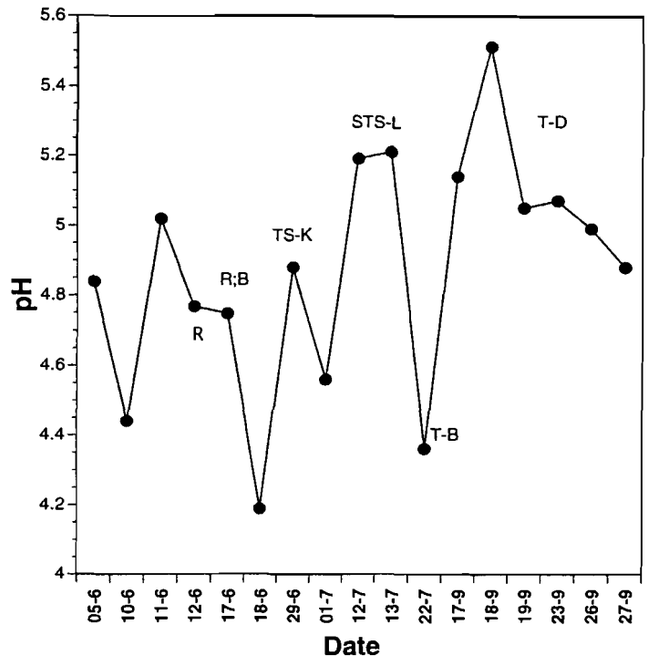

Figure 8 *Variation of the pH of daily summer rainwater samples at Kadoorie Agricultural Research Centre, Shek Kong, Hong Kong, 1993.*
R ; B = Red and Black rainstorm warning signal; TS-K = Tropical storm Koryn;
STS-L = Severe tropical storm Lewis; T-B = Typhoon Becky; T-D = Typhoon Dot

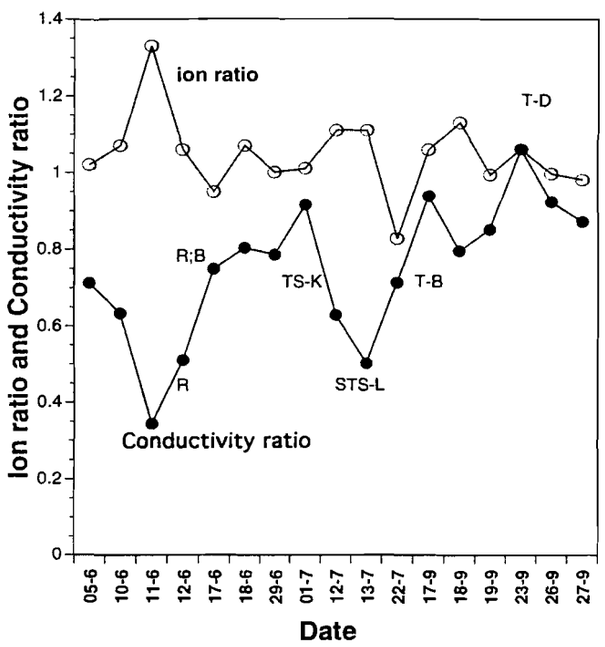

Figure 9 *Variations of ion ratio and the ratio of the calculated-to-measured conductivity for daily summer rainwater at Kadoorie Agricultural Research Centre, Shek Kong, Hong Kong, 1993.*
R ; B = Red and Black rainstorm warning signal; TS-K = Tropical storm Koryn;
STS-L = Severe tropical storm Lewis; T-B = Typhoon Becky; T-D = Typhoon Dot

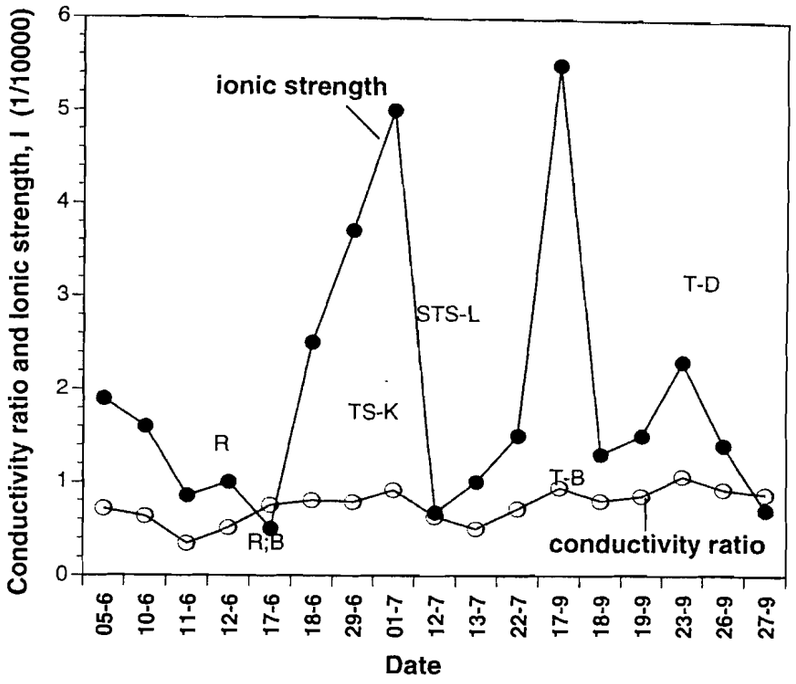

Figure 10 Variations of ionic strength (I) and the ratio of the calculated-to-measured conductivity for daily summer rainwater at Kadoorie Agricultural Research Centre, Shek Kong, Hong Kong, 1993. R ; B = Red and Black rainstorm warning signal; TS-K = Tropical storm Koryn; STS-L = Severe tropical storm Lewis; T-B = Typhoon Becky; T-D = Typhoon Dot

Ionic strength

The Ionic strength, I, of the rainwater samples calculated in the usual manner was found to be below 10^{-4} M for all individual ionic species and of the same order, mostly around 10^{-4} M for their sum. Specifically, the I values for the solutions were calculated to be in the range of 0.5 to 5 x 10^{-4} M, with a median of 1.5 x 10^{-4} M and a mean of approximately 1.9 x 10^{-4} M. The total ion loadings were found to be well below 20 mg l^{-1} with an arithmetic mean of about 4 mg l^{-1}.

On account of the low I alues involved, one is more or less justified in assuming that: (i) the ionic activity coefficients are bracketed by r_i = 0.9 - 1.0 (Hem, 1992); and (ii) the partial ionic conductivities obtained as the product of the equivalent ionic concentrations and the corresponding limiting equivalent ionic conductances when summed up as in Equation 2 to yield λ_K, ought to closely approximate the experimentally measured conductivity of the rainwater, λ_m, as expected from Kohlrausch's law of the *independent migration of ions* (Barrow, 1979).

Ion ratio versus onductivity ratio

The chemical composition is found to indicate satisfactory ion balance, with the range of the ion ratio, R_I, being 0.827 - 1.13 for sixteen of the seventeen samples and between 0.95 and 1.06 for twelve of them (*see* Figure 9). The median value was 1.02 and the aritmetic average 1.028. This is the best R_I range one can expect within experimental limitations. Furthermore, among the remaining five samples, only sample #3 had an awkwardly high R_I value of 1.33, due to very low concentration of ions. However, Figure 9 shows that there is no systematic connection between R_I and the conductivity ratio, R_λ.

Conductivity ratio

The measured conductivity values (Figure 10) ranged from 9 to 47 μS cm^{-1}, with a median at around 19 μS cm^{-1} and an arithmetic mean of 21.3 μS cm^{-1}. The ratio of the calculated-to-measured conductivity, R_λ, is quite variable from sample to sample, with the lowest value at approximately 0.34 and the highest value 1.06.

A total of thirteen samples showed R_λ between 0.34 and 0.8. On the other hand, the remaining four values of R_λ range from 0.915 to 1.06 and are associated with the passage of tropical cyclones, or in one case, rainfall immediately following such storms (*see* Table 1 and Figure 10; *also refer to* Figures 3-5 for the accompanying surface weather maps).

When we consider the samples in temporal sequence (Figure 10), there is a noticeable *improvement* in the R_λ value from 0.343 to around 0.48 (sample of 12-6-93) which apparently occurred due to the torrential territory-wide storm rainfall on 10th and 11th June, in response to which the Red rainstorm warning signal was hoisted (*see* Table 1). This weather is known to have been brought about by a lingering trough of low pressure close to the southern coast of Guangdong on those days (Figure 2a and b). The R_λ value then rose to around 0.8 (sample of 17-6-93) under the severe weather conditions which soon prevailed over the territory once more on 16th June. This time both the Red and Black rainstorm warning signals were hoisted in succession (*see* Figure 2c).

Severe tropical storms such as STS Lewis or other Type III tropical storms such as Typhoon Abe, however can be seen to have had little influence. This is likely because they passed by the territory with only the the #1 standby signal being hoisted (*see* Table 1 and Figures 6, 7 and 10). As a result there did not seem to have been any significant reduction in local urban, anthropogenic activity although such storms can be associated with significant rainfall as was the case with STS Lewis (Table 1).

In marked contrast Type II storms such as TS Koryn (TS-K) and Typhoons Becky (T-B) and Dot (T-D) which hit Hong Kong with full force (Table 1 and Figures 3 to 5) raised the R_λ value to even higher levels, reaching the expected value around 1 (1.06) for T-D for the first time for the summer samples (Figure 10). The very direct influence of the two typhoons Becky and Dot is evidenced in the hoisting of the #8 gale or storm signals.

Finally, the data in Figure 10 does not indicate that the better conductivity ratio (approaching 1) during rainfall associated with Type II storms is due to low ionic strength accompanying such storms. In fact, the relatively higher wind force during the stronger tropical storms is, in general, associated with a much greater sea salt content and hence above normal I values, up to about 5 x 10^{-4} M. However, in reference to our recent work (Sequeira and Lung, 1995), this apparent anomaly needs further clarification. This is presented in the following section.

Conclusion

Based on the results of this study it is proposed that the reason for the value of the conductivity ratio, $R_\lambda < 1$ for rainwater composition in rural Hong Kong, under normal weather conditions during the 1993 rainy season, is possibly the typical urban air which contains significant amounts of extraneous electrical charge of continental origin. In all probability this charge is carried by organic water-soluble material and/or some unmeasured organic ions.

It is also concluded that Type III tropical storms, such as STS Lewis and T Abe, which do not influence Hong Kong strongly as they approach the territory have a different influence on rainwater compared to Type II storms, such as T Becky or T Dot, which directly influence the territory with a strong, relatively unpolluted, maritime flow. These latter storms also bring with them a higher wind force, as evidenced by the hoisting of the #8 gale or storm signal by the Royal Observatory. This has the effect of further helping to cleanse the atmosphere of anthropogenic pollutants due to the temporary cessation of most anthropogenic activities in the territory. There thus appears to be a considerable reduction in urban aerosol emissions, leading to the condition of R approaching 1 at rural sites, such as Shek Kong, which is far enough from the sea coast for the ionic strength to remain sufficiently small thus validating the Kohlrausch law.

Acknowledgements

The following people are acknowledged for their role in this work. The laboratory staff of the Kadoorie Agricultural Research Centre, The University of Hong Kong, Mrs Dorothy Yau and Mrs. K.W. Chan, carried out the daily sample collection and made careful measurements of pH and conductivity on those samples kindly made available by Dr. Mervyn Peart of the Department of Geography and Geology, The University of Hong Kong. Miss Law Wai Fong carried out the chemical instrument analysis on the samples and Miss Vivian Lei, Miss Yeung Chui Ling and Mr. Lai Kim Hung assisted in the preparation of the manuscript. Part of this reasearch was supported by a grant from the Croucher Foundation.

References

ARGESE, E. and A.G. BIANCHINI, 1989: Chemical and Physical Characteristics of Rainfall in Venice: Influence of the Sampling Method on the Reliability of the Data. *The Sci. Total Environ.*, **83**, 287-298.

BARROW, G. M., 1979: *Physical Chemistry*, McGraw-Hill, New York, 832 p.

HEM, J. D., 1992: *Study and Interpretation of the Chemical Characteristics of Natural Water*, U.S.G.S. Water Supply Paper 2254, U.S. Govt. Printing Office, Washington D.C., 263 p.

MILES L.J., and K.J. YOST, 1982: Quality Analysis of U.S.G.S. Precipitation Chemistry Data for New York. *Atmos. Environ.*, **16**, 2889-2898.

NOAA-WMO-EPA: *Global Monitoring of the Environment for Selected Atmospheric Constituents, 1973 - Present*, Environmental Data and Information Series, National Climate Center, Asheville, NC, USA.

PEART, M. R., 1993: Acid precipitation in Hong Kong. *in* Kyle, W.J. & C.P. Chang (Eds.), Proceedings 2nd International Conference on East Asia & Western Pacific Meteorology & Climate, World Scientific, Singapore, 585-592.

PUXBAUM, H., A. KOVAR and M. KALINA, 1991: Chemical composition and fluxes of wet deposition at elevated sites (700-3100 m a.s.l.) in the eastern Alps (Austria). *in* Davies, T.D. *et al.* (Eds.), NATO ASI Series Vol. G28, Seasonal Snowpacks, Springer-Verlag, Heidelberg.

SEQUEIRA, R., 1988: On the net transfer of carbon dioxide from liquid precipitation to the atmosphere. *Geophys. Res. Lett.*, **15**, 273-276.

SEQUEIRA, R., and F. LUNG, 1995: A critical analysis and interpretation of the pH, ion loadings and electrical conductivity of rainwater from the territory of Hong Kong. *Atmos. Environ. (in press).*

SEQUEIRA, R., and M.R. PEART, 1995: Analysis of the pH of daily rainfall at a rural site in Hong Kong, 1989-1993. *The Sci. Total Environ.*, **159**, 177-183.

Bill Kyle

Department of Geography & Geology

The University of Hong Kong

1994 Tropical Cyclone Summary for the Western North Pacific Ocean (west of 180 degrees)

Information employed in the compilation of this section is derived from warnings and other published material issued by U.S. National Hurricane Center, Miami; U.S. Central Pacific Hurricane Center, Hawaii; U.S. Naval Western Oceanography Center, Hawaii; U.S. Joint Typhoon Warning Center, Guam; Japanese Meteorological Agency, Tokyo; Philippine Meteorological Service, Manila; and Royal Observatory, Hong Kong.

*Storms marked *, **, ***, **** caused the #1, #3, #8, or #9/10 Tropical Cyclone Signal respectively to be hoisted in Hong Kong. Track maps, courtesy of the Royal Observatory, are provided for these storms.*

Keywords:

Tropical Cyclone, Tropical Depression, Tropical Storm, Hurricane, Typhoon

Tropical Depression

The year 1994 began with the remnants of Typhoon Nell (9337) moving in a west to south-westerly course across the South China Sea towards the Malay Peninsula. These dissipated near 7N 113E, about 800 km east-southeast of Ho Chi Minh City on 2 January.

Tropical Storm (9401)

Tropical Depression 01W formed just north of Palau, near 8N 134E, on 4 January. Moving west-northwest at about 30 km h^{-1} in the direction of the Philippines, the system reached tropical storm strength and a peak intensity of 65 km h^{-1} later that day. The storm followed a generally west-northwest track into the central Philippines where it quickly dissipated on 6 January. This storm was assigned to tropical storm status by the Philippine Meteorological Service but intensity estimates from both the Joint Typhoon Warning Center, Guam and the Japanese Meteorological Agency listed it at depression status. Although this system was of minimal tropical storm intensity at best, it caused 35 deaths in the Philippines. Approximately 50 people were reported missing and more than 16,000 were forced to seek refuge in shelters. The deaths were primarily from landslides due to heavy rain which also blocked roads in some provinces. Floods were also reported to have destroyed three bridges.

Typhoon Owen (9402)

Tropical Depression 02W formed near 12N 134E, about 550 km north of Palau, on 31 March. Initially moving west-northwest, the system turned west at about 13 km h^{-1} on 1 April as it reached tropical storm strength. Owen continued west on 2 April and then it changed direction the next day as it reached typhoon strength. At that time Owen was near the east coast of Mindanao in the Philippine Islands moving west-southwest with 140 km h^{-1} winds. This was to be the peak intensity reached by the storm. Guiuan on Samar Island reported 83 km h^{-1} sustained winds at 1900 UTC on 3 April. Owen tracked in a westward direction across the southern Philippines on 4 April while maintaining its typhoon strength and thus wreaking havoc there. On Cebu flash floods severely affected nore than 7,000 people living in coastal villages. The cyclone then turned west-northwest into the South China Sea on the evening of 5 April and weakened to a tropical storm. Owen maintained a track in a northwest direction the following day before beginning to recurve north-east on 7 April. While moving north-northeast on 8 April towards the Luzon Strait Owen

weakened further to a minimal tropical storm. This weakening process continued and Owen dissipated over water near 19N 118E, approximately 580 km north-northwest of Manila, on 9 April. Press reports indicate 3 people were killed and 14 others were missing due to the impact of Owen in the Philippines.

Typhoon Page (9403)

A large disturbance began brewing near the island of Yap on 9 May. Two days later reports from Yap and satellite imagery revealed the presence of a new tropical depression in the Western Pacific Ocean. Tropical depression 03W developed more or less 250 km north-northeast of Yap, near 11.5N 139E, at 1800 UTC on 11 May. It slowly became better organized, and was named Page at 1200 UTC on 12 May near 13.5N 138E, when it was located around 500 km north of Yap. The general motion of Page then was north-northwest at 20 km h^{-1} and it was already in the process of recurving into the westerlies. The system then developed at a modest rate and by 0600 UTC on 14 May, Page became a typhoon near 17N 135E, when it was about 1100 km west-northwest of Guam and moving on a northward track. A peak intensity of 165 km h^{-1} was reached near 21.5N 138E, close to 450 km southwest of Iwojima, at 1200 UTC on 15 May. Page then began moving to the northeast just ahead of a frontal boundary. It then slowly began to lose strength over cooler waters and became extratropical on the 17 May near 30N 147E, 920 km southeast of Tokyo, as it continued to move harmlessly northeastward across the North Pacific Ocean at 35 km h^{-1}.

Tropical Depression Deling (9404)

This system was given the name Deling by the Philippine Meteorological Service. Tropical depression Deling formed near 12N 127E, about 380 km northeast of Cebu, on 24 May. Initially moving west-northwest, the system turned west the next day as it moved across the Philippine Islands. Deling then moved into the South China Sea later on 25 May, and accelerated west-northwest the following day. The system made landfall in central Vietnam late on 26 May and quickly dissipated. The maximum sustained winds in this cyclone have been estimated at 55 km h^{-1}. Although there were no reports of significant winds or pressures, Deling produced heavy rains over the central and southern Philippines. The resulting heavy flooding killed five people and left one missing in Davao City. According to press reports a further 2,000 people were forced to evacuate their homes in that city.

Tropical Depression

A tropical depression formed near 19N 118E, 250 km southeast of Dongsha, on 27 May. Moving in a generally northeast direction, the depression merged with a frontal system east of Taiwan the next day near 24N 123E. Maximum sustained winds in this short-lived depression were estimated at 55 km h^{-1}.

****Tropical Storm Russ (9405)**

Tropical Depression 05W formed in the South China Sea about 290 km south of Hong Kong near 20N 114E on 3 June. Dongsha reported 61 km h^{-1} sustained winds and a minimum pressure of 99.63 kPa at 0900 UTC that day. Russ was nearest to Hong Kong at the time of its formation around 1400 HKT on 3 June. The system initially drifted east at about 13 km h^{-1} and did not pose any immediate threat to the territory. This motion continued the next day as the cyclone reached tropical storm intensity. Ship 8LVN reported 67 km h^{-1} winds at 0300 UTC 4 June. Russ passed about 60 km south of Dongsha early on 5 June and slowed down significantly later that morning enabling deepening to severe tropical storm intensity about 380 km southeast of Hong Kong. It then started drifting west-southwest on 5 June with 55 km h^{-1} winds bringing it back closer to Hong Kong. The Stand By Signal #1 was raised at 1010 HKT that morning when Russ was about 330 km to the southeast. At that time the weather in Hong Kong was mainly fine with moderate winds from the northeast. Figure 1 shows Russ about 24 hours after the Stand By Signal #1 was raised.

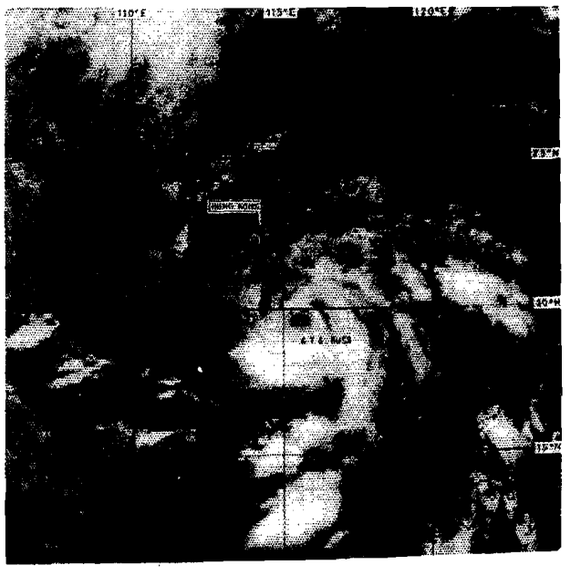

Figure 1 GMS-4 Visible Image of Tropical Storm Russ (9405) over the South China Sea to the southeast of Hong Kong at 03:00 UTC, 6 June, 1994

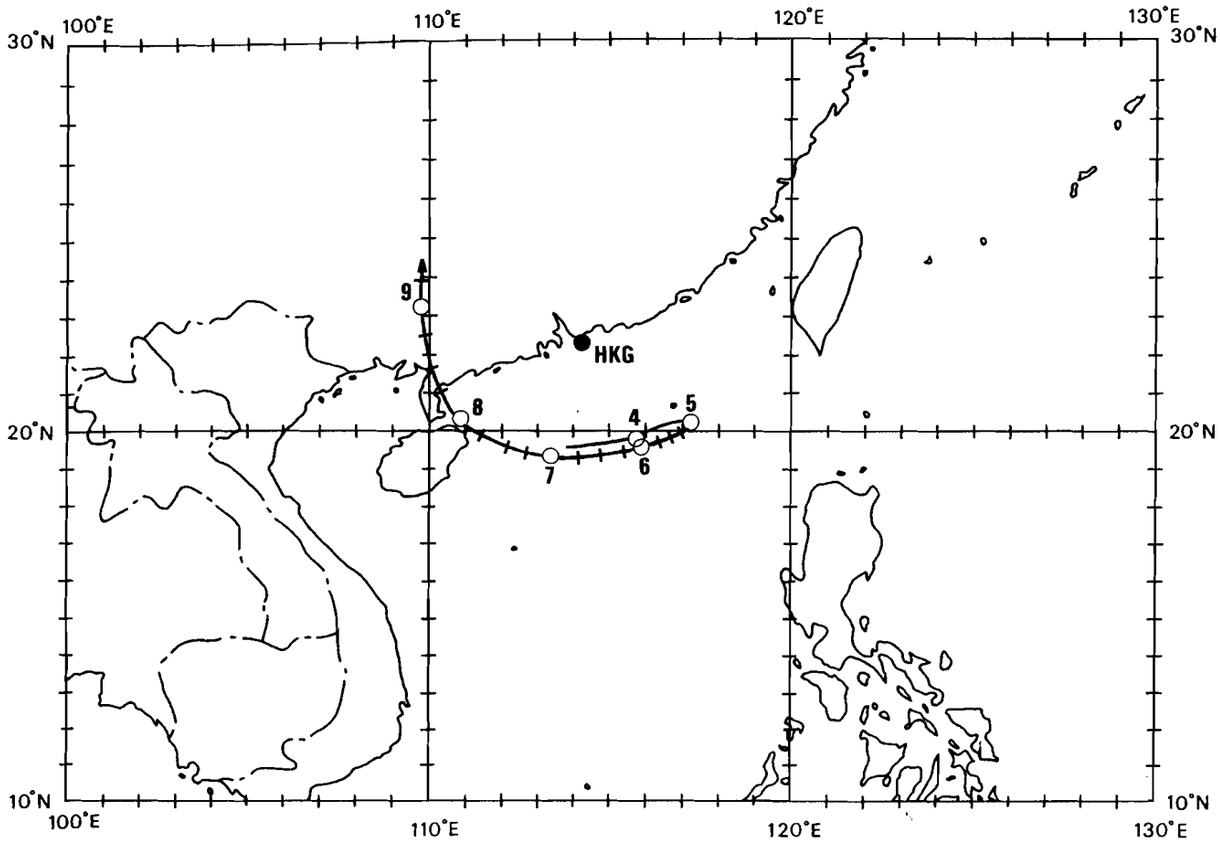

Figure 2 Track of Tropical Storm Russ (9405), 3 - 9 June, 1994 (after Royal Observatory, Hong Kong)

The storm continued to move on a westerly track on 6 June and winds gradually strengthened from the east leading to the hoisting of the Strong Wind Signal #3 at 2030 HKT that evening. The lowest sea-level pressure of 100.28 kPa was recorded at the Royal Observatory two and a half hours earlier when Russ was to the south-southeast. Russ turned west-southwestwards and briefly weakened to tropical storm intensity early on 7 June when it was about 330 km south of Hong Kong. Weather conditions deteriorated in Hong Kong with showers starting that day. The system turned more to the northwest later on 7 June as it intensified again reaching a peak intensity of 100 km h^{-1}. As Russ continued to move away from the territory winds locally moderated and all signals were lowered at 1545 HKT that afternoon. Nevertheless, showery conditions prevailed for another two days. There are no reports of injury in Hong Kong due to Russ although a ship was reported to be in difficulties about 200 km southeast of Hong Kong. Russ continued to move northwest and then north-northwest just to the east of Hainan Dao and the Leizhou Peninsula and made landfall over the coast of southern Guangdong near Zhanjiang, China on 8 June. The storm maintained its peak intensity to landfall, and then it rapidly weakened. Zhanjiang reported a minimum pressure of 98.06 kPa at 0900 UTC 8 June, while Haikou on Hainan reported a pressure of 98.97 kPa at 0000 UTC the same day. While there were no reports of sustained tropical storm-force winds at any land station, higher winds probably occurred between reports. Russ weakened to a tropical depression and dissipated over southern China on 9 June. The storm and its associated heavy rains inflicted heavy losses in southern China. In Hainan one person was reported dead and five injured, 2,400 hectares of farmland were flooded and irrigation works were damaged. Guangdong suffered the most with 59 people killed, 684 injured and 16 othere reported missing. Nearly 700,000 houses were reported damaged leaving 253,000 people homeless. Flash floods were reported to have devasted some 530,000 hectares of farmland. In the hardest hit Chinese cities of Zhanjiang and Maoming communications, telecommunications, electricity asnd water supplies were subject to considerable disruption. Total economic loss for the province was put at RMB 5.8 thousand million. Guangxi also lost 14 people with another 37 injured. Some 35,000 homes were reported damaged and around 170,000 hectares of farmland destroyed. Economic loss in that province was estimated at

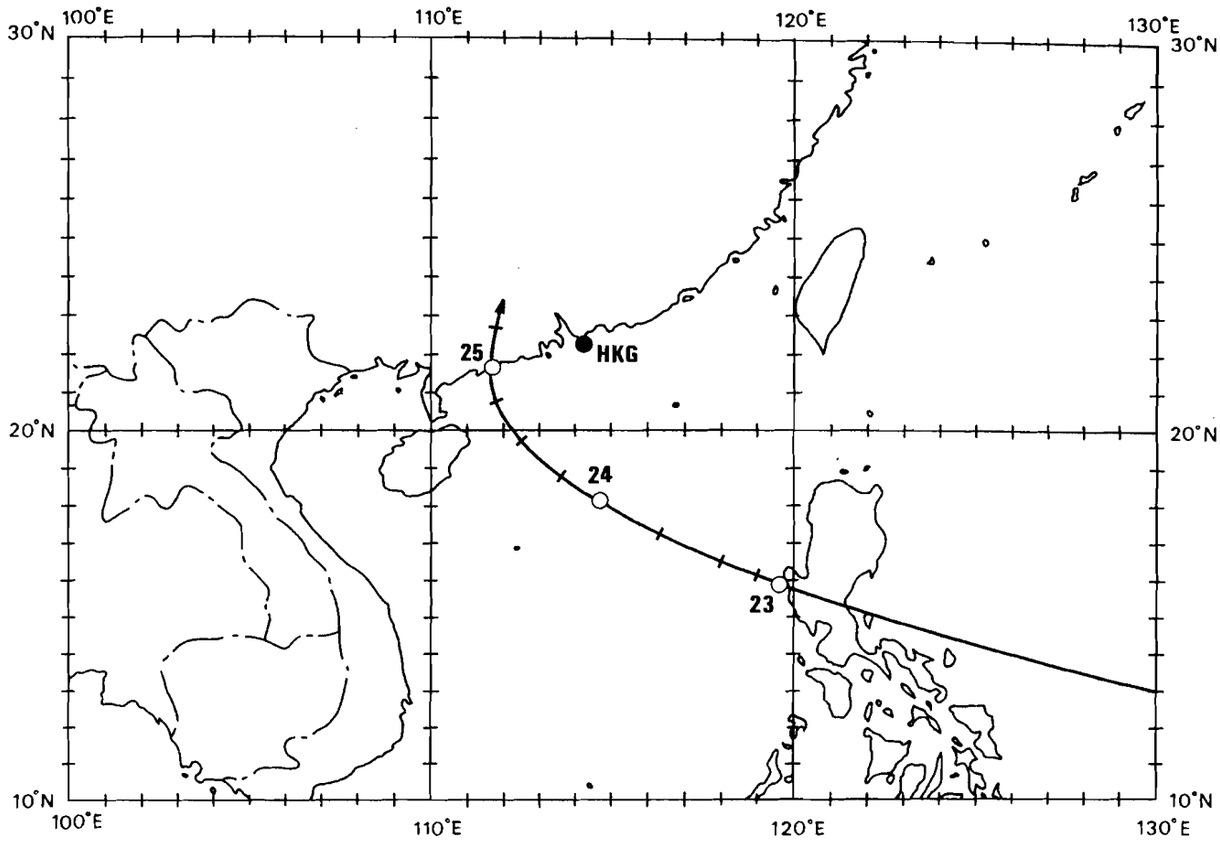

Figure 3 Track of Tropical Storm Sharon (9406), 22 - 25 June, 1994 (after Royal Observatory, Hong Kong)

RMB 480 million. Despite these losses heavy rains from the storm helped ease a drought over parts of southern China. Figure 4 shows the track of Tropical Storm Russ over the northern part of the South China Sea and southwest China during its lifetime.

**Tropical Storm Sharon (9406)

Tropical Depression 06W formed near 12N 135E, approximately 450 km northwest of Yap, on 21 June. The system moved in a generally west-northwest direction from its development towards Luzon in the Philippines which it crossed on 23 June. While there were no significant wind or pressure reports from the Philippines, heavy rains produced flooding that caused two deaths. Heavy rain in Luzon associated with the storm also promoted mudflows around the slopes of Mount Pinatubo which also disrupted traffic on main roads in the area. Sharon reached tropical storm intensity upon entering the South China Sea about 210 km northwest of Manila on the afternoon of 23 June. The storm gathered strength as it passed over water and reached a peak intensity of 95 km h^{-1} to the southwest of Dongsha early on 24 June. In Hong Kong the Stand By Signal #1 was hoisted at 1050 HKT that day when Sharon was about 430 km south of the territory. At the time the weather was dominated by showers and winds were moderate to fresh easterly. The storm turned to the northwest and then to north-northwest during 24 June so that winds in the territory became southeasterlies which were occasionally strong offshore. Sharon made landfall in southern China on the morning of 25 June around 0000 UTC as a minimal tropical storm and dissipated over land later that day. Yangjiang, China reported a minimum pressure of 99.85 kPa at 0000 UTC 25 June as Sharon made landfall. There were no reports of tropical storm force winds. The #1 signal was lowered at 0630 HKT that morning just prior to landfall. Sharon was closest to Hong Kong at 1400 HKT that afternoon when it was about 250 km to the west-northwest. During its passage a Chinese fishing vessel with 11 fishermen on board sank near Tathong Channel and another boat was freed from its moorings in Kwun Tong typhoon shelter. Five people were reported injured in Central. Four people lost their lives in Guangdong due to Sharon and in Yangjiang and Maoming more than 6,700 houses collapsed and 50,000 others were reported damaged. Heavy rains from the storm also worsened flooding over parts of southern China with a total of 120,000

hectares of farmland affected. Figure 3 shows the track of Sharon across Luzon and the South China Sea.

Tropical Depression

A tropical depression formed about 520 km southwest of Manila near 12N 117E on 26 June. It moved west across the South China Sea to Vietnam, where it made landfall and dissipated on 28 June. Maximum sustained winds in this system were estimated at 55 km h^{-1}.

Tropical Depression (9407)

Tropical Depression 07W formed on 2 July 250 km southeast of Dongsha near 19N 118E. The system tracked west-northwest across the South China Sea through the next day before turning north and moving into China on 4 July. The depression quickly dissipated over land. There are no reports of damage or casualties.

Typhoon Tim (9408)

Tropical Depression 08W formed near 13N 130E, about 980 km east of Manila, on 7 July. Initially moving to the north-northwest at about 13 km h^{-1}, the system turned northwest the next day and reached tropical storm intensity. Tim continued northwest and rapidly intensified becoming a typhoon on 9 July when it was about 960 km southeast of Taibei. The storm continued to intensify reaching a peak of 230 km h^{-1} before it made landfall over Taiwan about 175 km south of Taibei on the evening of 10 July. Taibei reported 102 km h^{-1} sustained winds with gusts to 152 km h^{-1} at 1400 UTC 10 July. Hsinchu reported a minimum pressure of 97.10 kPa at the same time. The storm inflicted serious damage on the island. Press reports indicate that at least nineteen people died, a further 67 were injured and eleven others missing. A mainland Chinese freighter with 97 on board ran aground near Suao. Around 50,000 hectares of farmland were flooded and some 300 buildings collapsed. Widespread electricity failure affected around 2 million households. Domestic and international air traffic was also disrupted by the inclement weather. Total damage was estimated at NT$ 2 thousand million. Tim then moved west over the Taiwan Straits towards the coast of eastern China with winds estimated between 140-210 km h^{-1}. The storm made landfall over Fujian about 130 km south-southwest of Fuzhou on 11 July. Xiamen, China reported a minimum pressure of 98.25 kPa at 2100 UTC 10 July. Tim continued northwest into eastern China and dissipated rapidly over land. Tim also seriously affected Fujian claiming three lives, flooding 140,000 hectares of farmland and forcing 3,000 factories to shutdown due to loss of electric power. Total economic loss was put at RMB 1.5 thousand million.

Tropical Storm Vanessa (9409)

Tropical Depression 09W formed approximately 550 km west-northwest of Manila near 16N 116E on 9 July as Tim headed towards Taiwan. The system reached tropical storm intensity later that day as it remained quasi-stationary. Vanessa then started moving north-northeast through the South China Sea on 10 July in response to Typhoon Tim approaching Taiwan. At this time the storm was packing 85 km h^{-1} winds which turned out to be its peak intensity. There are several ship reports of 45-75 km h^{-1} winds and air pressures below 100 kPa in association with Vanessa. The storm continued north-northeast on 11 July as it rapidly weakened, and it dissipated later that day in the Taiwan Straits near 23N 119W, some 180 km southeast of Xiamen.

Typhoon Walt (9410)

Tropical Depression 10W formed some 960 km east-southeast of Manila near 11N 129E on 14 July. Initially moving northwest, the system continued this motion through 15 July as it headed towards Luzon in the Philippines. Walt turned and adopted an east-northeast track the next day as it reached tropical storm strength. and continued on this track with 110 km h^{-1} winds on 17 July. The system moved generally northeast to north-northeast through 20 July reaching typhoon intensity on 18 July some 900 km south-southeast of Okinawa. There followed a period of rapid strengthening to a peak intensity of 240 km h^{-1} on 19 July. Walt turned northwest on 21 July, followed by a westward turn the next day as it weakened to a tropical storm. The storm passed near buoy 21004 on 22 July, which reported 82 km h^{-1} sustained winds at 0100 UTC and a pressure of 97.57 kPa at 0600 UTC that day. Walt then slowed to an erratic drift near 30N 132E on 23 July, followed by a north-northeast drift toward southwestern Japan the next day with 100 km h^{-1} winds. At this time the storm was just south of Japan and Muruotomisaki reported 91 km h^{-1} sustained winds at 2100 UTC 24 July. The storm turned north-northwest across southwestern Japan on 25 July, with Shimiza reporting a 98.55 kPa pressure at 0300 UTC. Walt turned west into the East China Sea on 26 July as it weakened to a depression. The system drifted west from that time until it dissipated near 34N 127E, just south of Korea near Cheju Do, on 28 July. There are no reports of damage or casualties.

Tropical Storm Yunya (9411)

Tropical Depression 11W formed over the South China Sea near 16N 118E, about 350 km west-northwest of Manila, on 18 July. Initially moving northeast, the system reached tropical storm intensity later that day before tracking across the northwest corner of Luzon Island in the Philippines. Vigan reported a pressure of 99.28 kPa at 2300 UTC 18 July. Yunya then moved northeast into the Philippine Sea on 19 July as it reached a peak intensity of 85 km h^{-1}. It turned east on 20 July as it weakened to a depression about 700 km northeast of Manila and dissipated over water around 860 km southeast of Okinawa later that day near 21N 134E. This system brought heavy rain and mudslides to the Philippines resulting in the death of eight people and the evacuation of thousands of others.

Typhoon Zeke (9412)

Tropical Depression 12W formed nearly 540 km southwest of Iwojima close to 22N 137E on 17 July. Initially moving in an east-northeasterly direction at 23 km h^{-1} passing close to Iwo Jima on the evening of 18 July, this general motion continued the next day. The depression reached tropical storm strength on 19 July and maintained 65-75 km h^{-1} sustained winds until 20 July. Zeke turned northeast on that dayy, then it turned north on 21 July as it reached a peak intensity of 120 km h^{-1}. This was based on a 120 km h^{-1} ship report near the centre. Zeke continued north into higher latitudes the next day as it weakened to a tropical storm some 1,600 km northeast of Iwo Jima, then it turned north-east on 24 July. Zeke continued to move northeast across the open Pacific with 75 km h^{-1} winds. The storm became extratropical on 25 July near 44N 162E, 1650 km east of Sapporo, Japan.

Tropical Depression (9413)

This system was the subject of a warning by the Joint Typhoon Warning Center, Guam. Tropical Depression 13W formed approximately 250 km east of Guam near 14N 174E on 25 July. Moving north-northwest, it dissipated the next day near 19N 145E, about 250 north of Guam. Maximum sustained winds in this short-lived system were estimated at 55 km h^{-1}.

Tropical Depression

The Japanese Meteorological Agency issued a warning on this system. The depression formed near 16N 147E, about 370 km northeast of Guam, on 25 July, apparently from the same area of disturbed weather that spawned 13W. The depression moved north through 27 July, then it turned north-northwest on 28 July. The system dissipated close to Hachijojima, near 33N 140E, on 29 July. Maximum sustained winds in this system were estimated at 55 km h^{-1}. Ship JPKN reported 80 km h^{-1} sustained winds and a pressure of 99.5 kPa at 0600 UTC 28 July. It is not known whether this wind report is representative of the true strength of the system.

Tropical Storm Brendan (9414)

A tropical depression formed almost 830 km east-northeast of Manila near 16N 129E on 26 July. Moving west, the system reached minimal tropical storm intensity later that day. This system was named as a tropical storm by the Philippine Meteorological Service. However, it was not designated a storm (14W) by the Joint Typhoon Warning Center or the Japanese Meteorological Agency until 30 July. The storm turned northwest on 27 July, then it began a northward drift the following day. Ship WDZW reported 59 km h^{-1} sustained winds and a pressure of 99.97 kPa at 0600 UTC 28 July. The storm continued north on 29 July, then it accelerated across Okinawa on 30 July. Naha on Okinawa reported a minimum pressure of 99.5 kPa around 1600 UTC on that day. There are no reports of damage or casualties from the Ryukyu Islands. Brendan continued to move north at 27 km h^{-1} on the following day approaching the west coast of the Korean peninsula with 85 km h^{-1} winds. Cheju Island, Korea reported 69 km h^{-1} sustained winds and a pressure of 99.5 kPa at 1800 UTC 31 July. Brendan turned northeast and moved across the Korean peninsula on 1 August leaving a trail of destruction in its wake. Press reports from Korea indicate that Brendan's passage caused 8 deaths and twenty people were reported missing. Some 200,000 people had to be evacuated and 66,000 vessels took shelter during the passage of the storm. Brendan turned east and entered the Sea of Japan the same day weakening to a depression as it headed towards Japan. The system moved across northern Honshu, Japan late in the evening of 2 August and dissipated near 41N 149E, some 1000 km northeast of Tokyo, the next day.

Tropical Storm Amy (9415)

Tropical depression 15W formed and developed very rapidly from a persistent area of low pressure in Beibu Wan near 19N 108E, about 250 km west-southwest of Haikou, Hainan Island on 29 July. The system initially drifted east towards Hainan but reversed its direction the next morning as it re-entered Beibu Wan. Drifting west on 30 July it reached a peak intensity of 75 km h^{-1}.

Amy continued west at 15 km h^{-1} into Vietnam on 31 July and dissipated. Dongfang, China reported 56 km h^{-1} winds and a pressure of 98.74 kPa at 0600 UTC 29 July as Amy intensified. There are no reports of damage or casualties.

Tropical Storm Caitlin (9416)

As Brendan approached Korea another tropical depression formed about 1180 km east-southeast of Gaoxiong, near 19N 131E, on 31 July. The system was initially moving west, and this motion continued through 2 August. The depression reached tropical storm strength on 2 August, strengthening to a peak intensity of 100 km h^{-1} prior to moving west-northwest at 25 km h^{-1} across Taiwan the next day. Ship DQFS reported 82 km h^{-1} sustained winds at 0000 UTC 4 August. Kaohsiung International Airport on Taiwan reported 59 km h^{-1} sustained winds with gusts to 78 km h^{-1} at 0802 UTC 3 August. Chiang Kai-Shek Airport near Taipei reported a 98 km h^{-1} gust at 1200 UTC that day. Hsinchu, Taiwan reported a minimum pressure of 99.18 kPa at 1100 UTC 3 August. Heavy rain associated with Caitlin triggered numerous flash floods on the island and over 1,100 people were reported stranded. Electricity supply to 100,000 households was interrupted and air and land traffic disrupted. Press reports indicate that at least 10 people were killed on Taiwan with 4 missing. Loss in agricultural products alone was put at NT$ 620 million. Caitlin continued west across the Taiwan Strait making landfall over mainland China about 70 km southwest of Xiamen on 4 August and moved west-northwest inland and dissipated. Xiamen, China reported a 99.24 kPa pressure at 2100 UTC on 3 August.

Typhoon Doug (9417)

Tropical Depression 17W formed near 15N 145E, about 180 km north of Guam, on 1 August. The system moved west through 3 August, and on that day it strengthened to both tropical storm and typhoon status while maintaining a forward motion of 20 km h^{-1}. Doug continued west on 4 August, then it turned west-northwest the next day. The typhoon moved northwest on 6 August as it reached a peak intensity of 250 km h^{-1}. The storm moved north-northwest to near Taiwan on 7 August, passing just north of the northeast tip of the island. Maximum sustained winds had decreased to 175 km h^{-1} by that time. Doug seriously affected Taiwan and the southwestern Ryukyu Islands. Ishigakijima, Japan reported 96 km h^{-1} sustained winds at 1200 UTC 7 August. Chiang Kai-Shek Airport, Taiwan reported 80 km h^{-1} sustained winds with gusts to 111 km h^{-1} at 1800 UTC, while Hulien, Taiwan reported a gust to 137 km h^{-1} at 2000 UTC. Hulien also reported a pressure of 96.5 kPa at 1800 UTC. In Taiwan 26 people were killed with 41 injured and 4 reported missing. About 125 houses collapsed and another 450 or so were damaged. Some 100,000 people were deprived of electricity and water during the storm. Flood-related losses were estimated at NT$ 4 thousand million. Doug turned north-northeast on 8 August, and this general motion continued the next day as it weakened to a tropical storm. Shengsi, China reported 74 km h^{-1} sustained winds with a pressure of 98.55 kPa at 0600 UTC 9 August. Doug continued north-northeast on 10 August and weakened further. Then it slowed to an east-northeast drift over the Yellow Sea on 11 August and began making a clockwise loop turning southwest the next day in response to Typhoon Ellie approaching from the southeast. The system weakened further to a depression as it continued this track making landfall over eastern China about 100 km north-northwest of Shanghai on 12 August, and dissipating over land later that day. Doug also played a role in the crash of a Korean Air jet on Cheju Island, Korea. The plane tried to land while winds were sustained near 65 km h^{-1}. Fortunately, none of the 160 passengers and crew on board were killed.

Typhoon Ellie (9418)

While Typhoon Doug was closing in on Taiwan another tropical depression formed 400 km east-northeast of Iwo Jima, near 26N 145E, on 7 August from a low pressure system that had moved south from near Japan. The system drifted slowly west on 8 August as it reached tropical storm strength. During Ellie's initial development near Iwo Jima the island reported a minimum pressure of 98.9 kPa from 0500-0800 UTC on 9 August, with sustained winds of 67 km h^{-1} and gusts to 98 km h^{-1} at 1500 UTC the same day. Ellie moved west-southwest on 9 August, then it became nearly stationary near 23N 139E, about 310 km southwest of Iwo Jima, the next day. Ellie then turned northwest with a forward speed of 20 km h^{-1} on 11 August as it reached typhoon intensity some 500 km southeast of Kagoshima, Japan. This track continued the next day before Ellie moved west-northwest through the northern Ryukyu Islands reaching a peak intensity of 140 km h^{-1} on 13 August. The typhoon continued this track through the Yellow Sea on 14 August packing 120 km h^{-1} winds. Ellie at this time affected southern Japan as well as continuing to affect the Ryukyu islands. Tanegashima Island, Japan, reported a minimum pressure of 98.32 kPa at 2100 UTC 12 August. Kanoya, Japan, reported 80 km h^{-1} sustained

winds with gusts to 115 km h^{-1} at 0200 UTC 13 August. Ellie turned north as it weakened to a tropical storm on 15 August, and the system made landfall in northeastern China the next day. Ellie became extratropical later that day near 43N 126E, approximately 100 km southeast of Changchun, China. Dalian, China reported a minimum pressure of 99.12 kPa at 2100 UTC 15 August. Chengshantou, China reported a minimum pressure of 99.14 kPa at 1800 UTC the same day, with 91 km h^{-1} sustained winds at 1500 UTC. There are no reports of damage or casualties anywhere along Ellie's track.

Tropical Storm Li

Former Hurricane Li weakened to a tropical storm as it moved west at 20 km h^{-1} across the International Dateline near 12N on 12 August. Li began life as Tropical Depression 08E in the Eastern North Pacific around 3000 km east-southeast of Honolulu near 13N 126W on 31 July. Initially moving west-northwest, the system turned west the following day. The depression continued west until it moved into the Central North Pacific some 2150 km east-southeast of Honolulu near 12N 140W on 3 August. Maximum sustained winds during the depression's track through the Eastern North Pacific were 55 km h^{-1}. The system continued west until it dissipated near 11N 156W, more or less 1150 km south-southeast of Honolulu on 5 August. While this ended the first part of it's life, the remains of Tropical Depression 8E continued to move west to the south of the Hawaiian Islands. The system regenerated to tropical storm intensity when it was near 14N 167W, about 1250 km southwest of Honolulu, on 8 August and was named Li. Li followed a general westward track gradually strengthening to a peak of 120 km h^{-1} on 11 August. Li weakened to a tropical storm as it moved west across the International Dateline the next day before turning west-northwest on 13 August with 65 km h^{-1} winds. The storm turned north-northwest on 15 August as it weakened to a depression, then it slowed to an erratic drift the next day. Li then continued to drift aimlessly until it dissipated some 3400 km west-southwest of Honolulu near 17N 170E on 18 August.

Typhoon Fred (9419)

Tropical Depression 19W formed near 18N 145E, about 500 km north of Guam on 14 August one day after Li entered the Western North Pacific Ocean. It initially moved west at about 20 km h^{-1}, and this track continued the next day as the cyclone reached tropical storm strength. Fred moved west-southwest on 16 August as it reached typhoon strength some 1000 km west-northwest of Guam. It turned west-northwest the next day and continued this track through 19 August, when it reached a peak intensity of 240 km h^{-1}. The typhoon moved north-northwest through the southern Ryukyu Islands on 20 August with 215 km h^{-1} winds. Ishigakijima Island, Japan, reported a minimum pressure of 94.16 kPa at 1200 UTC 20 August, with sustained winds of 93 km h^{-1} at 1800 UTC. Higher winds and lower pressures occurred between the 3 hourly observations. Miyakojima Island, Japan, reported 98 km h^{-1} sustained winds and a pressure of 96.79 kPa at 1200 UTC the same day. There are no reports of damage or casualties from the Ryukyu Islands. However, the circulation of Fred seriously affected Taiwan as it crossed the East China Sea. Three people were killed, one was injured and two were reported missing. Almost NT$ 22 million of agricultural products were destroyed. Electricity supply, telephone service and land transport were also severely disrupted, the latter being particularly affected by landslides brought by the heavy rain associated with the storm. Fred turned west-northwest with 150 km h^{-1} winds on 21 August and moved towards Zhejiang making landfall about 50 km south of Wenzhou near midnight local time that day. Funding, China, reported a minimum pressure of 97.85 kPa at 1500 UTC 21 August, while Shipu, China reported 95 km h^{-1} sustained winds at 1200 UTC the same day. The system continued further inland, weakening the following morning and degenerating rapidly to an area of low pressure early the next day. Fred caused serious problems in Zhejiang with press reports indicating that more than 1,000 people were killed and 490 others were missing. Over 96,000 houses were destroyed and a further 700,000 damaged. Agricultural destruction was also severe with the loss of some 140,000 hectares of farmland, 425 hectares of fish farms and 367,000 head of various livestock. Irrigation works, dykes, power lines and telecommunication facilities were also badly damaged or destroyed. At sea some 700 fishing vessels sank and 900 others were reported damaged. direct economic loss was estimated at RMB 7.5 thousand million.

Typhoon Gladys (9420)

Tropical Depression 20W formed near 24N 175E on 22 August. Initially moving northeast, the system turned west the next day. This general motion continued through 27 August. The system reached tropical storm intensity on 24 August and typhoon intensity on 25 August. Gladys passed near Minamitorishima Island, which reported 83 km h^{-1} sustained winds at 1200 UTC 25 August. The cyclone reached a first peak intensity of 130

km h^{-1} on 26 August, then it weakened to a tropical storm the next day. Gladys turned west-southwest on 28 August with 65 km h^{-1} winds. Gladys turned west on 29 August while maintaining minimal tropical storm strength, and this motion continued the next day as Gladys started to re-intensify. Gladys regained typhoon strength some 500 km east-southeast of Taibei on 31 August reaching a second peak intensity of 165 km h^{-1} later that day. The storm also turned west-northwest at this time. Gladys continued west-northwest across Taiwan and into China on 1 September, making it yet another in a series of tropical cyclones that have plagued that region. The storm weakened to a low pressure system over China the next day. Gladys moved across central Taiwan with the central core missing the reporting stations. Chiang Kai Shek airport in Taipei reported 56 km h^{-1} sustained winds with gusts to 98 km h^{-1} at 0300 UTC 1 September. Hulien reported a minimum pressure of 99.2 kPa at the same time. Press reports indicate that 6 people were killed on Taiwan with 51 injured and one reported missing. Torrential rain associated with the storm disrupted land traffic in many places. Electricity supply to over 600,000 households was also cut. Agricultural losses were estimated at NT$ 400 million. At sea a freighter ran aground in northern Taiwan though fortunately all 40 crew members were rescued. In China, Mazu reported 65 km h^{-1} sustained winds at 1200 UTC 1 September, while Pingtan reported a minimum pressure of 99.24 kPa at the same time. In Fujian over 30,000 people had to leave their homes during the landfall of Gladys as serious flooding was reported in many places, damaging houses and inundating cropland. Power supply to Fuzhou was also interrupted.

**Tropical Storm Harry (9421)

Originating from a disturbed area near Luzon Tropical Depression 21W formed over the South China Sea about 430 km north-northwest of Manila, near 18N 119E, on 25 August. The system initially drifted west but soon turned west-northwestwards travelling at a steady 19 km h^{-1}. In Hong Kong the Stand By Signal #1 was hoisted at 2250 HKT when Harry was about 600 km to the southeast. The storm continued to intensify further as it tracked across the northern part of the South China Sea. The weather in Hong Kong deteriorated early on 26 August as squally showers associated with the outermost rainbands began to affect the territory. Winds continued to strengthen from the east that day and the Strong Wind Signal #3 was hoisted at 1615 HKT when Harry was about 340 km to the south. Figure 4 shows Harry around 1400 HKT time when the outermost rainbands were affecting the territory.

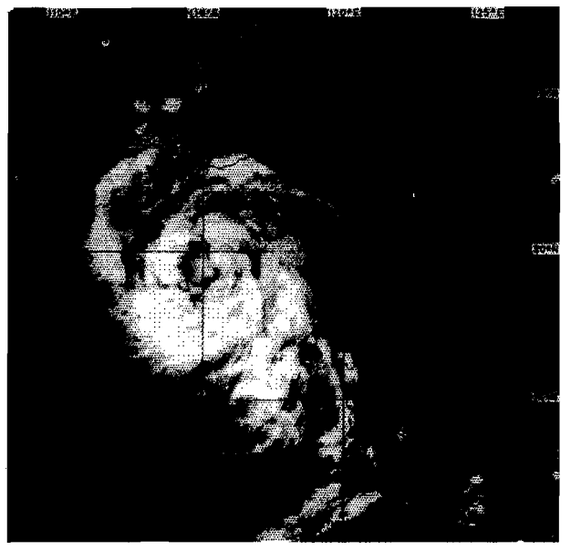

Figure 4 GMS-4 Visible Image of Tropical Storm Harry (9421) over the South China Sea to the south of Hong Kong at 0600 UTC on 26 August, 1994

The storm came closest to Hong Kong around 2300 HKT that evening when it was about 270 km to the south. The Royal Observatory recorded the lowest sea level pressure at 0400 HKT on 27 August. Around this time Harry took on a more westerly track heading towards the Leizhou Peninsula and away from Hong Kong so all signals were lowered at 1145 HKT. The adverse weather during the passage of Harry produced a collision between a hoverferry and a catamaran off Stonecutter's Island with two passengers being injured in the incident. One person died while swimming in heavy seas in Sai Kung. As Harry moved away from Hong Kong it continued to intensify reaching a peak intensity of 110 km h^{-1} just before skirting the southern tip of Leizhou Peninsula on 27 August. The storm brought heavy rain to Zhangjiang and caused extensive damage with the loss of 90,000 hectares of sugar cane, 13,000 hectares of paddy, 16,600 houses, 50 km of river embankments and 370 irrigation work sites. Total loss was estimated at RMB 484 million. Harry also adversely affected Hainan Dao with Haikou reporting a minimum pressure of 99.0 kPa at 1500 and 1800 UTC 27 August. Harry weakened the following morning and moved westward across Beibu Wan into Vietnam on 28 August with 85 km h^{-1} winds. It made landfall about 160 km east of Hanoi and continued inland weakening rapidly and dissipated the next day. Phu Lien reported a pressure of 99.4 kPa at 1800 UTC 28 August and Mong Cai reported 56 km h^{-1} sustained winds at 1200 UTC the same day. There are no reports of damage from Vietnam. The track of Harry

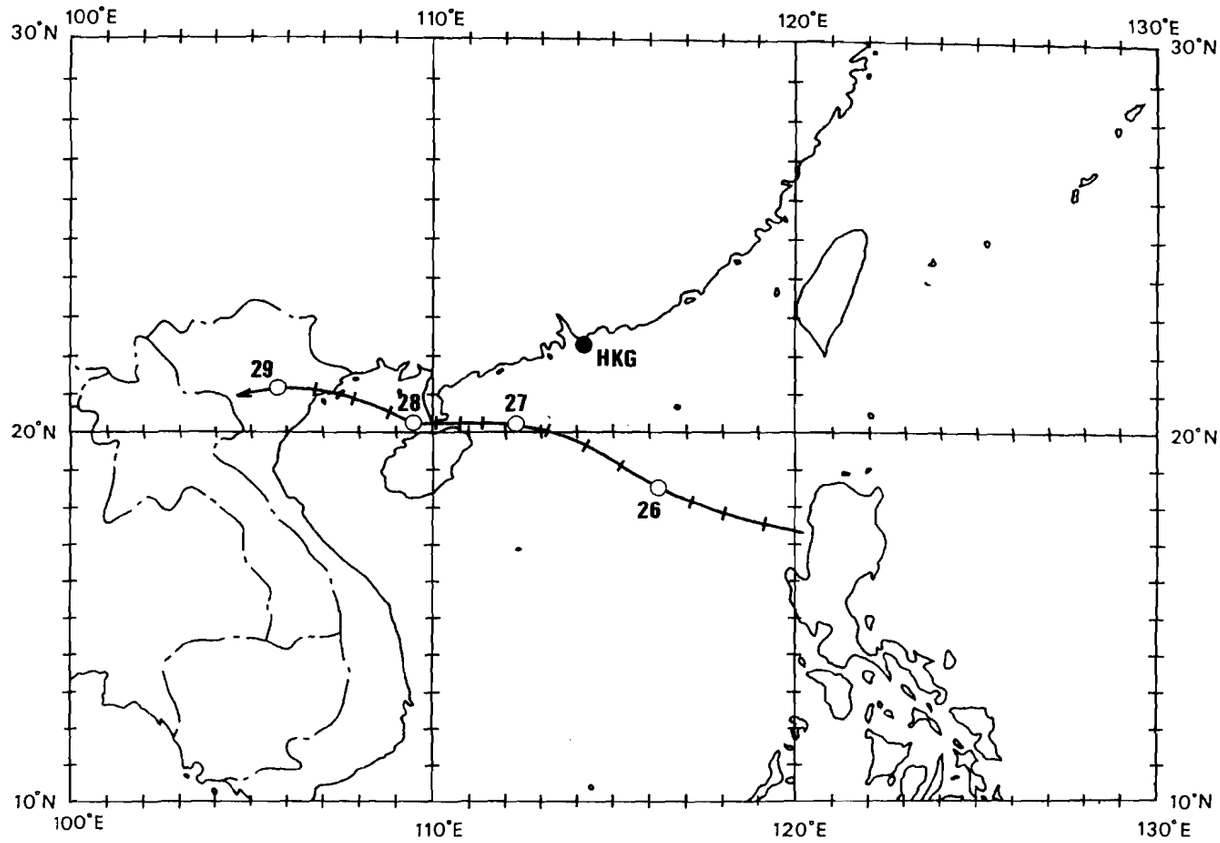

Figure 5 Track of Tropical Storm Harry (9421), 25 - 29 August, 1994 (after Royal Observatory, Hong Kong)

across the South China Sea is presented in Figure 5 above. ,

Typhoon Ivy (9422)

A tropical depression formed near 20N 165E, about 190 km west-northwest of Wake Island, on 27 August. Initially moving west, the system turned north-northwest at 16 km h^{-1} with 85 km h^{-1} winds the next day as it reached tropical storm strength. Ivy turned north-northwest on 29 August, and this motion continued the next day as the storm continued to intensify. Ivy turned north on 31 August as it reached typhoon intensity and later a peak intensity of 140 km h^{-1}. The cyclone recurved to take a north-northeast track on 1 September. It weakened to a tropical storm on 3 September and became extratropical near 45N 170E, almost 2,300 km east-northeast of Sapporo on 4 September.

Typhoon John

Former Hurricane John entered the Western North Pacific near 22N on 28 August while moving west-northwest at 12 km h^{-1} with 175 km h^{-1} winds and was renamed Typhoon John. John began life as Tropical Depression 10E which formed on 11 August in the Eastern North Pacific near 12N 97W, about 620 km south-southeast of Acapulco. This was the second such storm in 1994 which formed in that region and which eventually entered the Western North Pacific, the first being Li. The system reached tropical storm strength later that day while moving west. John turned west-northwest on 12 August and maintained this motion the next day while reaching a peak intensity of 110 km h^{-1}. John turned west on 14 August, and generally maintained this track through 18 August as a poorly-organized storm with 75-95 km h^{-1} winds. The storm began to intensify again on 19 August while continuing west, and reached hurricane intensity the next day. Further strengthening followed, and by the time John reached 140W late on 20 August it was packing 185 km h^{-1} winds. John crossed 140W and entered the Central North Pacific near 15N, some 2,000 km east-southeast of Honolulu, at about 0000 UTC 21 August, moving west with the same intensity. Strengthening continued, and following a general westward track through 23 August, John reached a peak intensity of 275 km h^{-1}. Although the satellite intensity estimates for John were as high or higher than for Hurricane Emilia earlier in the season, the lowest pressure measured by

reconnaissance aircraft was 92.9 kPa at 0128 UTC 23 August. This is higher than Emilia's 92.6 kPa. The storm turned west-northwest on 24 August as it weakened, and this track continued until it moved into the Western North Pacific on 28 August. While in the Central North Pacific John passed just north of Johnston Island on 26 August with 155-165 km h^{-1} winds. The island reported sustained winds of 91 km h^{-1} with gusts to 119 km h^{-1} at 0236 UTC with a minimum pressure of 98.54 kPa at 0436 UTC. Lower pressures and higher winds probably occurred between the hourly observations. John's winds dropped to 130 km h^{-1} later on 26 August, then they increased again to 205 km h^{-1} on 27 August. When John crossed the International Dateline some 750 km south-southwest of Midway Island on 28 August it was packing 185 km h^{-1} winds. This track was maintained the next day as John weakened, then turned northeast on 31 August, and weakened further to a tropical storm. John slowed to an east-northeast drift on 1-2 September, then it drifted southeast on 3 September. By the next day the storm was near 26N 178E, about 500 km west-southwest of Midway Island, moving in an east-southeast direction. The maximum sustained winds were estimated at 65 km h^{-1} by the Joint Typhoon Warning Center and the Japanese Meteorological Agency, but ship WFLG suggests the system was stronger. It reported 102 km h^{-1} sustained winds with a pressure of 99.12 kPa at 1500 UTC 4 September. John turned northwest the next day, then it moved west-northwest on 6 September. Maximum sustained winds during this period were 90-100 km h^{-1}. The storm turned east-northeast on 7 September as its winds weakened to 75 km h^{-1}, and this track continued as John moved towards the Dateline on 8 September. The storm strengthened during that day and when it again crossed the International Dateline and re-entered the Central North Pacific near 32N 180W, 490 km north northwest of Midway Island, on 9 September the maximum sustained winds had increased to 100 km h^{-1}. The storm quickly regained hurricane status, with winds increasing to 150 km h^{-1} later that day. John accelerated north-east while weakening, and finally became extratropical approximately 1,650 km north northeast of midway Island, near 42N 170W on 10 September. John set a world record for tropical cyclone longevity. It lasted for 30 days which breaks the old record of 27.25 days set by Atlantic Hurricane Ginger in September - October 1971. During John's lifetime, fourteen other tropical cyclones formed and died:

Hurricane Ileana (Eastern North Pacific)
Tropical Depression 12E (Eastern North Pacific)
Tropical Storm Beryl (Atlantic)
Typhoon Fred (Western North Pacific)
Hurricane Chris (North Atlantic)
Tropical Depression (North Indian Ocean)
Typhoon Gladys (Western North Pacific)
Tropical Storm Harry (Western North Pacific)
Typhoon Ivy (Western North Pacific)
Tropical Depression (Western North Pacific)
Tropical Depression Five (Atlantic)
Hurricane Kristy (Eastern and Central North Pacific)
Tropical Storm Joel (Western North Pacific)
Tropical Storm Mele (Central North Pacific)

The National Hurricane Center, the Central Pacific Hurricane Center, and the Joint Typhoon Warning Center issued a total of 120 advisories on John.

Tropical Depression

This system was the subject of a warning issued by the Philippine Meteorological Service. A tropical depression formed near 10N 133E, about 990 km east of Cebu, on 29 August. Moving west, the system dissipated the next day near 11N 129E, 550 km east of Cebu. Maximum sustained winds in this system were estimated at 55 km h^{-1}.

Tropical Storm Joel (9423)

Tropical depression 24W formed in the South China Sea near 16N 114E, 220 km east-southeast on 3 September. Initially moving at 20 km h^{-1} to the west-northwest, the system turned west the next day as it reached tropical storm strength with 65 km h^{-1} winds. Joel then drifted northwest and performed a counter-clockwise loop on 5 September. It intensified to a tropical storm the next day about 280 km south-southeast of Haikou and moved west-northwest across Hainan Island as it reached a peak intensity of 83 km h^{-1}. Joel moved northwest into northern Vietnam on 7 September and dissipated. The storm affected southern China and northern Vietnam. Yaxian, China reported a minimum pressure of 99.06 kPa at 0600 UTC 6 September. Dongfang, China reported 65 km h^{-1} sustained winds at 1200 UTC the same day. Bach Longvi, Vietnam reported 87 km h^{-1} sustained winds and a pressure of 98.97 kPa at 0600 UTC 7 September. There are no reports of damage or casualties.

Typhoon Kinna (9424)

Tropical Depression 24W formed 430 km south of Iwo Jima Island, near 21N 142E, on 5 September. The system reached tropical storm intensity later that day as it moved northwest at 10 km h^{-1}. Kinna turned north-northwest on 6 September, and this motion continued the next

day as Kinna passed west of Iwo Jima, which reported 44 km h^{-1} sustained winds with gusts to 83 km h^{-1} at 0000 UTC 7 September. The storm turned north on 8 September, and this general motion continued through 10 September. During this time Kinna deepened rapidly and reached typhoon strength on 9 September, and a peak intensity of 150 km h^{-1} the next day. The storm turned north-northeast with 130 km h^{-1} winds and accelerated to 30 km h^{-1} on 11 September when it was east of Japan. Kinna continued north-northeast and became extratropical the next day near 42N 152E when it was about 880 km east of Sapporo.

**Tropical Storm Luke (9425)

A tropical depression, 25W, formed in the Philippine Sea about 760 km east of Manila, near 14N 128E, on 7 September. Initially moving west, the system reached tropical storm intensity the next day according to the Japanese Meteorological Agency. Ship JQCU reported 72 km h^{-1} winds with a pressure of 100.05 kPa at 0600 UTC 8 September. The Joint Typhoon Warning Center, however, did not name the system until 11 September. The storm turned west-northwest during that day and this motion continued for about 24 hours before the motion became more westerly as the system approached the northeast tip of Luzon Island. Luke moved west into the Luzon Straits on 10 September and maintained this course until it entered the South China Sea at an intensity of 75 km h^{-1}. Initially Luke headed northwestwards towards Dongsha. In Hong Kong the Stand By Signal #1 was hoisted at 0750 HKT on 11 September when Luke was about 600 km to the east-southeast and local winds were light northerlies. Luke passed near Dongsha that evening at which time it turned west-southwestwards towards Hainan Dao. The Strong Wind Signal #3 was hoisted at 2230 HKT on 11 September when Luke was about 240 km to the southeast and winds from the east had strengthened appreciably with the approach of the storm closer to Hong Kong. Luke came closest to the territory, 230 km to the south-southeast, about 0200 HKT on 12 September. The lowest sea-level pressure of 100.39 kPa was recorded at the Royal Observatory around 0400 HKT when the storm was about 400 km to the east-southeast. Strong winds, occasionally reaching gale force, and squally showers prevailed at this time. As Luke moved away all signals were lowered at 1150 HKT that morning although heavy showers continued to affect Hong Kong for the remainder of the day. Luke continued a general west-southwest motion with a speed of 20 km h^{-1} on 12 September as it reached a peak intensity of 100 km h^{-1}. Figure 6 shows Luke at around 1400 HKT on 12 September when the storm was heading for Hainan Dao. The storm made landfall about 100 km south of Haikou on the evening of 12 September and moved across Hainan Dao and into Beibu Wan on 13 September with 55-65 km h^{-1} winds. Qionghai on Hainan Dao reported a minimum pressure of 99.65 kPa at 1500 UTC 12 September. Luke produced considerable damage in Hainan with direct economic losses amounting to over RMB 100 million. More than 3,000 houses were damaged and 45,000 acres of farmland destroyed. There were also reports of damage to roads, bridges, power plants and reservoirs. Luke weakened to a tropical depression just before making landfall over northern Vietnam later that day and dissipated over Vietnam on 14 September. This storm was yet another in a series of cyclones which moved across Hainan Dao and into Vietnam. Bach Longvi, Vietnam reported 65 km h^{-1} sustained winds at 0600 UTC 13 September along with a minimum pressure of 100.3 kPa. There are no reports of damage or casualties from Vietnam. Figure 7 shows the track of Luke across the South China Sea.

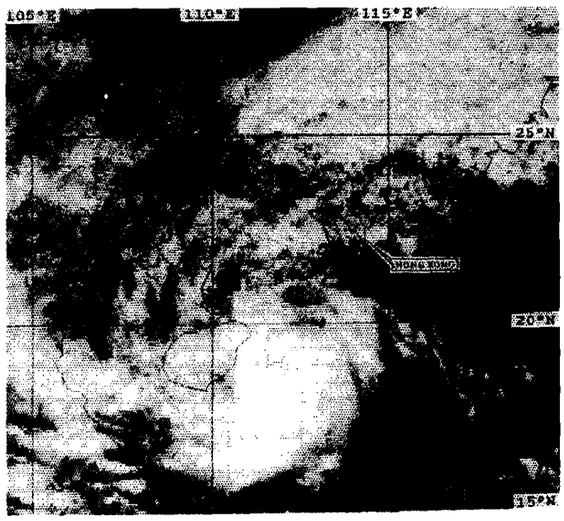

Figure 6 GMS-4 Visible Image of Tropical Storm Luke (9425) heading towards Hainan Dao at 0600 UTC 12 September, 1994

Typhoon Melissa (9426)

Tropical Storm Melissa rapidly developed in the Marshall Islands 600 km west of Kwajalein, near 9N 162E, on 11 September. Initially moving west, the storm turned northwest the next day. Melissa turned north-northeast on 13 September as it reached typhoon intensity and this track continued the next day as rapid intensification occurred. Melissa turned north-northwest on 15 September as it reached a peak intensity of 270

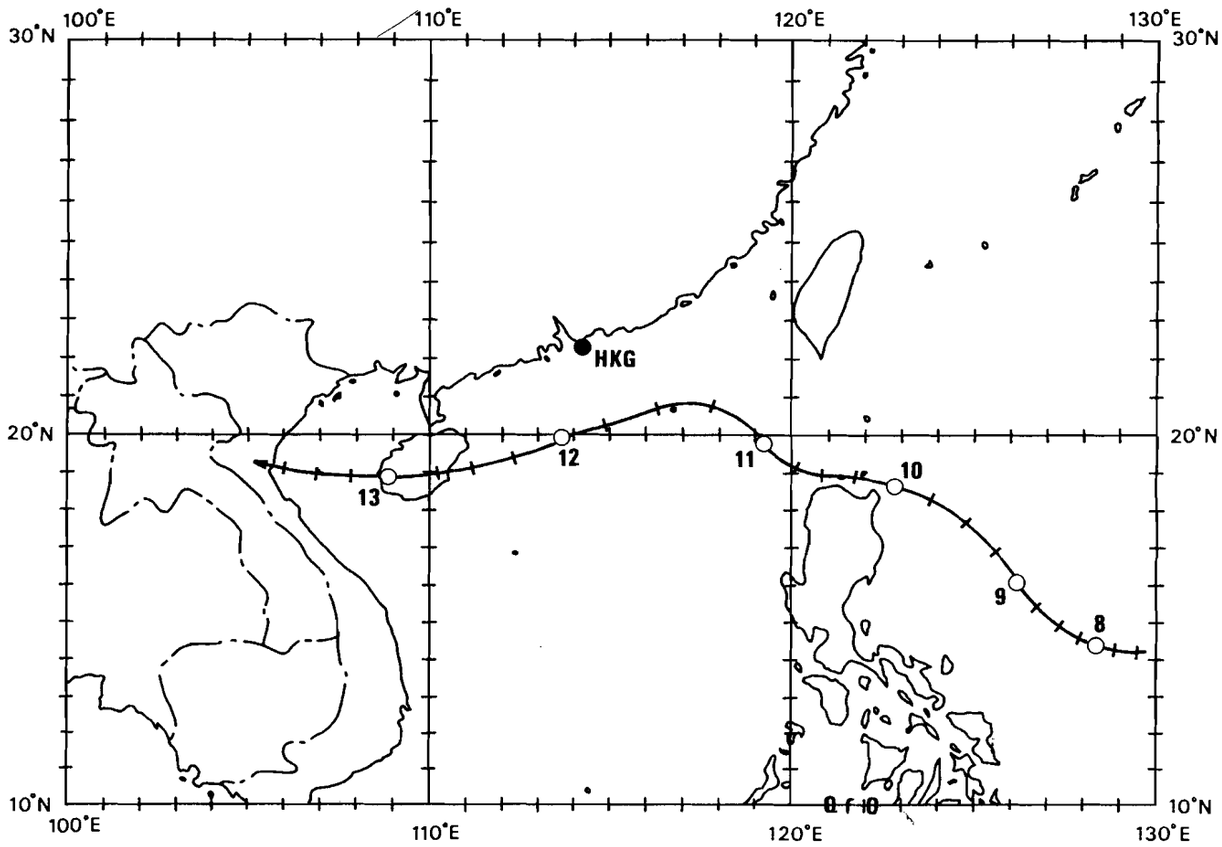

Figure 7 Track of Tropical Storm Luke (9425), 7 - 14 September, 1994 (after Royal Observatory, Hong Kong)

km h^{-1}. This track continued although Melissa steadily weakened during this time, with the typhoon weakening to a tropical storm on 18 September when east of northern Japan with 110 km h^{-1} winds. Melissa was a large system with tropical storm force winds covering a 550-1100 km diameter region during much of the storm's life. Minamtorishima Island reported a minimum pressure of 98.51 kPa at 1500 UTC 16 September, even though Melissa's closest approach was about 300 km. Maximum reported winds were below tropical storm strength. Ship OYSN2 reported a pressure of 97.25 kPa at 1200 UTC 18 September, with maximum sustained winds of 89 km h^{-1} six hours later. The storm turned north-northeast and became extratropical 700 km east of Sapporo on 19 September near 43N 150E. In Japan at least three people were killed, nine were injured and seven were reported missing.

Tropical Storm Nat (9427)

Tropical Depression 27W formed near 14N 144E, about 100 km northeast of Guam on 15 September. Initially moving east-northeast, the system passed near Guam and Saipan later that day. The unusual east-northeast motion was due to flow around Typhoon Melissa. Nat was still a poorly organized depression when it passed through the Mariana Islands. Agana, Guam reported a peak gust of 61 km h^{-1} at 1900 UTC 15 September, while Rota Island reported a pressure of 99.7 kPa at 2000 UTC the same day. The depression continued east-northeast the next day as it reached tropical storm strength. Nat turned north-northeast on 17 September as it reached a peak intensity of 85 km h^{-1}. The cyclone then turned north-northwest the next day with 75 km h^{-1} winds. Nat continued this motion on 19 September as winds again increased to 85 km h^{-1}, then it turned north the next day while weakening. Nat turned northeast on 21 September, and this track continued as it weakened to a depression on 22 September. The system dissipated later that day near 31N 152E, some 1,250 km east-southeast of Tokyo. Nat passed through the Marianas early in its life, but there are no reports of damage or casualties.

Typhoon Orchid (9428)

Tropical Depression 28W formed about 850 km west of Guam, near 14N 137E, on 17 September. Initially moving east, the system continued this track the next day as it reached tropical storm

strength. This was assigned by the Japanese Meteorological Agency when the system was southwest of Guam moving east with 65 km h^{-1} winds. The system was named Orchid by the Joint Typhoon Warning Center on 19 September as it turned north at 15 km h^{-1} about 90 km west of the southern Mariana Islands. Orchid passed just west of the Mariana Islands, but there are no reports of significant strong winds or low pressures. There are also no reports of damage or casualties. The storm turned northwest on 20 September, and this motion continued the next day as it reached typhoon intensity. The typhoon interacted with a monsoon surge on 22 September, and this caused a west-southwestward motion. It assumed a north-northwest motion the next day. Orchid continued to move slowly north to north-northwest reaching a peak intensity of 250 km h^{-1} on 25 September to the south of Japan. Orchid turned northwest on 26 September while maintaining 230-240 km h^{-1} winds, then it turned north the next day. It turned north-northeast on 28 September, and this track continued as the storm moved across Japan and into the Sea of Japan on 29-30 September. The system weakened to a tropical storm on 29 September, and it became extratropical some 160 km southeast of Vladivostok, Russia, near 42N 133E, later the next day. Orchid affected much of Japan. Muruotomisaki reported 119 km h^{-1} sustained winds and a pressure of 97.97 kPa at 0600 UTC 29 September. Owase reported a minimum pressure of 97.27 kPa at 1200 UTC, while Nagoya reported a peak gust of 128 km h^{-1} at 1400 UTC. Press reports indicate three people were killed with 32 hurt due to Orchid's passage. However, the storm appears to have brought much welcome rain to Japan, which was suffering from a summer drought.

Typhoon Pat (9429)

Pat began with the formation of Tropical Depression 29W near 16N 167E, 370 km south of Wake Island on 21 September. Initially moving west-southwest, the system reached tropical storm strength later that day. Pat then turned north-northwest on 22 September as it reached typhoon strength, and this general motion continued the next day as it reached a peak intensity of 175 km h^{-1}. Pat turned west-northwest on 24 September as it slowly weakened. On 25 September, Pat and the newly-formed Tropical Storm Ruth rotated around each other in a Fujiwhara interaction. Pat's track changed from a rapid west-northwest motion to a southwest motion. Rapid weakening occurred at this time and sustained winds decreased. Pat and Ruth were southeast of Japan rotating around each other with both systems having 85 km h^{-1} winds. The two systems merged into one storm about 1,150 km northeast of Iwo Jima Island, near 31N 150E, on 26 September. Which of the two centers actually absorbed the other is uncertain, as the Japanese Meteorological Agency called the merged system Pat while the Joint Typhoon Warning Center called it Ruth. The combined Pat/Ruth turned northeast on 27 September with 75-85 km h^{-1} winds, and the system became extratropical the next day near 40N 159E, about 1,750 km east-northeast of Tokyo. This merger of two tropical cyclones is unusual. The last such recorded occurrence in the Western North Pacific was in 1986, when Typhoon Tip absorbed the remains of Typhoon Georgette.

Tropical Storm Ruth (9430)

An area of low pressure deepened to become Tropical Depression 30W near 20N 156E, about 1,100 km west of Wake Island on 24 September. The system initially moved northeast passing southeast of Miamtorishima Island as it developed. The island reported a minimum pressure of 99.8 kPa, but reported winds stayed below tropical storm strength. The depression reached tropical storm strength the next day as it began to interact with Pat and the storms rotated around each other. Ruth's northeastward motion changed to northward and then to rapidly west-northwestward during the day with 85 km h^{-1} winds. The two systems merged into one storm near 31N 150E, about 1,100 km northeast of Iwo Jima Island, on 26 September. Which of the two centers actually absorbed the other is uncertain as mentioned above in the report on Typhoon Pat. The combined Pat/Ruth turned northeast on 27 September with 75-85 km h^{-1} winds, and became extratropical the next day near 40N 159E, 1,750 km east-northeast of Tokyo.

Tropical Depression (9431)

Tropical Depression 31W formed some 1,120 km north-northwest of Wake Island, near 28N 161E, on 29 September. Initially moving west-northwest, the system became nearly stationary the next day near 30N 159E, around 1,400 km northwest of Wake Island. The depression started a general northwestward drift on 1 October and continued this track to the southeast of Japan at its peak intensity of 55 km h^{-1}. The depression turned east-northeast on 3 October, and this motion continued the next day. The cyclone turned back westward on 5 October, dissipating on 6 October near 30N 160E, 1,350 km north-northwest of Wake Island.

Typhoon Seth (9432)

Seth developed from Tropical Depression 32W which formed near 9N 157E, 590 km east-northeast of Chuuk on 2 October. Seth moved westward on 3 October as it reached tropical storm intensity. Seth followed a general west-northwest track through 6 October as it passed south of Guam. However, it passed far enough south of the island that there were no reports of significant winds or pressures. Typhoon intensity was achieved on 5 October. Seth took on a northwest track on 7 October as it reached a peak intensity of 220 km h^{-1}. Seth turned north-northwest on 8 October and passed through the southern Ryukyu Islands on 9 October, entering the East China Sea west of the Ryukyus with 160 km h^{-1} winds. At this time Seth affected the southern Ryukyu Islands and Taiwan. Pengia Yu, Taiwan reported 143 km h^{-1} sustained winds with a pressure of 96.98 kPa at 2100 UTC 9 October. Yonagunijima Island, Japan reported a minimum pressure of 96.16 kPa at 1200 UTC, while Ishigakijima Island, Japan reported 113 km h^{-1} sustained winds at 1500 UTC both on the same day. Heavy rain and high winds associated with the outer circulation of Seth affected Taiwan with 8 people reported killed, 15 injured and 6 others missing. Electricity supply to over 600,000 households was disrupted. About 100 house were damaged and a total of 2,200 hectares of farmland flooded. Agricultural losses were put at NT$ 60 million. The typhoon turned north-northeast on 10 October, then it accelerated northeast and weakened to a tropical storm before moving into South Korea late on 11 October. Seth produced tropical storm conditions over South Korea and the adjacent islands. Molsulpu reported 93 km h^{-1} sustained winds with the exact time unknown. Pusan reported 69 km h^{-1} sustained winds with gusts to 91 km h^{-1} at 2000 UTC 11 October. Cheju International Airport reported a minimum pressure of 98.2 kPa at 1700 UTC the same day, and numerous other stations reported pressures below 99 kPa. In Korea one person was killed and 550 people left homeless. Seth then moved into the Sea of Japan and became extratropical some 350 km east of Seoul, near 38N 131E, on 12 October.

Typhoon Verne (9433)

Shortly after the dissipation of Seth, Tropical Depression 33W formed about 400 km east of Bikini Atoll, near 11N 169E, on 15 October. The system moved west at about 30 km h^{-1} to the east of the Mariana Islands with 55 km h^{-1} winds. Verne assumed a west to west-northwest track on 17 October as it reached tropical storm strength some 600 km east of Guam. This motion continued through 20 October, with the storm passing through the southern Marianas on 18 October. Verne reached typhoon strength on 20 October. Verne affected the Mariana Islands from Tinian south. Rota reported 65 km h^{-1} sustained winds with gusts to 124 km h^{-1} at 2100 UTC 18 October, along with a minimum pressure of 99.26 kPa. Ship KIRH reported 50 kt sustained winds at 0000 UTC 23 October with a minimum pressure of 99.7 kPa six hours later. There are no reports of damage or casualties. Verne turned northwest on 21 October, then the cyclone stalled near 18N 131E, about 1,000 km south-southeastof Okinawa, the next day drifting erratically near 18N 130E with 175 km h^{-1} winds. Verne drifted south on 24 October as it reached a peak intensity of 215 km h^{-1}, and this motion continued through 26 October when the storm became stationary some 860 km east of Manila near 15N 129E. Verne turned north-east on 27 October as it weakened to a minimal typhoon, then it turned north the next day while weakening to a tropical storm. Verne turned northeast on 29 October and then east-northeast on 30 October with 95 km h^{-1} winds. Verne continued east-northeast until it became extratropical near 29N 154E, about 1,500 km east-southeast of Tokyo, on 1 November. While Verne did not affect any land areas during this period, it did cause problems for shipping. Ship JPEX reported 93 km h^{-1} winds and a pressure of 99.8 kPa at 0000 UTC 27 October, with ship JGAC reporting 89 km h^{-1} sustained winds and a pressure of 99.74 kPa at 1200 UTC 29 October. A drifting buoy reported a 98.09 kPa pressure at 1000 UTC 29 October. Verne passed through the Volcano Islands on 31 October. Iwo Jima reported 70 km h^{-1} sustained winds at 0600 UTC, with a gust to 109 km h^{-1} at 1200 UTC. Chichi-jima reported a minimum pressure of 99.35 kPa at 1800 UTC. There are no reports of damage or casualties from the Volcano Islands, or from the Mariana Islands that Verne affected early in its life.

Typhoon Teresa (9434)

Tropical Depression 34W formed around 200 km west-northwest of Saipan in the Mariana Islands, near 16N 144E, on 16 October. The system initially moved west, and this motion continued through 19 October. Tropical storm strength was reached on 17 October, with Teresa reaching typhoon strength on 19 October. Teresa became a typhoon about 600 km east of Manila early on 20 October and turned west-southwest as it reached a peak intensity of 150 km h^{-1}. This motion continued as the cyclone tracked across Luzon in the Philippine Islands on 21 October. Teresa affected the central and

northern Philippine Islands. Infanta on Luzon reported 109 km h^{-1} sustained winds and a pressure of 98.28 kPa at 0200 UTC 21 October. Sangley Point also reported 109 km h^{-1} sustained winds at 0600 UTC the same day. Manila reported 74 km h^{-1} sustained winds with gusts to 109 km h^{-1} and a pressure of 98.9 kPa at 0500 UTC 21 October. Ship JNBO reported 93 km h^{-1} sustained winds at 1200 UTC 23 October, and a pressure of 99.6 kPa at 2100 UTC the same day. During its passage across the Philippines Teresa caused 11 deaths, four people were reported missing and 100,000 had to be evacuated. There was heavy damage to rice paddy and coconut plantations and electricity supply to Manila and the surrounding areas was interrupted. Two crew were found dead and another fourteen were reported missing out of a total of 36 on board a tanker, Thanassis A, which capsized and sank in the South China Sea about 600 km southeast of Hong Kong. Teresa weakened to a tropical storm as it passed over the Philippines, but it regained typhoon intensity over the South China Sea on 22 October as it moved west-southwest to west with 120 km h^{-1} winds. Teresa continued to drift west on 24 October as its winds increased to 140 km h^{-1}, before it drifted west-northwest to the Vietnam coast on 25 October. The typhoon weakened to a tropical storm before making landfall over southern Vietnam about 200 km east of Ho Chi Minh City early on 26 October. Teresa continued west-northwest over land and dissipated later on 26 October. There are no significant meteorological reports from the landfall region in Vietnam, and no reports of damage or casualties. However, ship DVPZ reported 76 km h^{-1} sustained winds at 0000 UTC 25 October.

Typhoon Wilda (9435)

Tropical Depression 35W formed about 300 km west-northwest of Enewetak in the Mrashall Islands, near 14N 161E, on 20 October. The system moved west-northwest at about 13 km h^{-1} as it reached tropical storm strength later the same day. Wilda then followed a general west-northwest track through 22 October, before turning west on 23 October. Wilda reached typhoon intensity about 1,100 km west-southwest of Wake Island on 22 October, as it moved west toward the Mariana Islands with 185 km h^{-1} winds. Wilda moved to a southwest track on 24 October, then it briefly stalled about 220 km northeast of Saipan on 25 October. It reached a peak intensity of 250 km h^{-1} at this time. Wilda then recurved and moved northeast and weakened later on 25 October. Wilda was a large system that affected most of the Mariana Islands. Saipan reported a minimum pressure of 98.72 kPa at 0000 UTC 25 October, along with 56 km h^{-1} sustained winds gusting to 83 km h^{-1}. Higher winds probably occurred, as no further reports were received until after the peak effects on the island. The Joint Typhoon Warning Center on Guam recorded a gust to 133 km h^{-1} at 1547 UTC 24 October. Ship VMBD reported 113 km h^{-1} sustained winds at 0600 UTC 25 October and a minimum pressure of 99.1 kPa 12 hours earlier. There are no reports of damage or casualties. Wilda moved generally north-northeast on 26-27 October. The storm turned north-northwest on 28 October and then northwest the next day while maintaining 160-165 km h^{-1} winds. Wilda again turned north-northeast on 30 October with 160 km h^{-1} winds before turning northeast and accelerating on 31 October as it weakened to a tropical storm. The system became extratropical the next day near 39N 165E, about 2,250 km east-northeast of Tokyo.

Tropical Storm Yuri (9436)

Tropical Depression 36W formed near 24N 176E, some 1,100 km east-northeast of Wake Island, on 23 October from a non-tropical low pressure system which had moved west across the International Dateline. The cyclone reached tropical storm strength later that day as it moved rapidly westward at about 50 km h^{-1} with 65 km h^{-1} winds. Yuri reached a peak intensity of 85 km h^{-1} on 24 October, then it weakened to a depression the next day as it continued a general westward motion. Yuri turned northwest on 26 October and dissipated over water near 30N 154E, about 1,750 km northwest of Wake Island, on 27 October.

Tropical Storm Zelda (9437)

Tropical Depression 37W formed 150 km south of Wake Island, near 18N 167E, on 28 October from a disturbance that moved in a southwest direction past Wake Island. The system tracked generally west-southwestward reaching tropical storm strength on 29 October. This track continued the next day, then Zelda turned west-northwest on 1 November as it reached typhoon intensity. Zelda moved north-northwest on 2 November and northwest on 3 November while passing through the northern Mariana Islands. Saipan reported 83 km h^{-1} sustained winds with gusts to 102 km h^{-1} at 0355 UTC 3 November, with a minimum pressure of 98.91 kPa at 0250 UTC. An automated weather station on Pagan reported 69 km h^{-1} sustained winds at 1600 UTC the same day. There are no reports of damage or casualties. Zelda then turned west on 4 November, and northwest on 5 November as it reached a peak intensity of 260 km h^{-1}. The

following day Zelda turned north-northeast through the open Pacific with 215 km h^{-1} winds. It accelerated on 7 November, then turned east-northeast later that day. Rapid weakening occurred during this time, and Zelda deteriorated to tropical storm status before becoming extra-tropical around 565 km southeast of Tokyo, near 32N 144E, on 8 November.

Typhoon Axel (9438)

In the Caroline Islands Tropical Depression 38W formed near 7N 152E, 50 km south-southeast of Chuuk, on 13 December. Initially moving west, Axel turned west-southwest the next day. The system turned west on 15 December, and this general track continued the following day as it reached tropical storm strength. Axel turned west-north-west on 17 December and continued this motion as it slowly intensified. Axel passed through the Caroline Islands as it developed. Yap reported a minimum pressure of 99.43 kPa at 2100 UTC 17 December. There are no reports of damage or casualties. Axel was packing 110 km h^{-1} winds on 18 December and reached typhoon strength the next day as it took on a westerly track. The typhoon continued to move west at 16 km h^{-1} on 20 December as it reached a peak intensity of 185 km h^{-1}. This track continued the next day as it moved into the central Philippine Islands affecting, in particular, Leyte, Samar, Cebu, and Panay. Guiuan on Samar reported 120 km h^{-1} sustained winds and a pressure of 97.82 kPa at 0700 UTC 21 December. Press reports indicate that 5 people were killed in the city of Bacolod with 4 others missing. Elsewhere in the Philippines another 11 people were killed and 45 injured. There was also major power disruption on the island of Luzon. Axel then turned west-northwest and weakened to a tropical storm as it moved into the South China Sea on 22 December. The storm turned north-northwest and briefly regained typhoon strength on 23 December. It then turned northwest on 24 December with 110 km h^{-1} winds. Axel weakened rapidly on 25 December to a 55 km h^{-1} tropical depression although continuing to move northwest over the South China Sea. The system stalled near 19N 116E, some 410 km east-southeast of Hong Kong on 26 December, then it turned south and dissipated the next day near 16N 115E, 700 km to the south of Hong Kong.

Tropical Storm Bobbie (9439)

The last tropical storm of 1994, Tropical Depression 39W, formed in the Marshall Islands near 5N 171E, about 230 km south of Majuro, on 17 December. The system followed a general westward track through the Marshall Islands with maximum winds of 55 km h^{-1}. Kosrae in the Marshalls reported a minimum pressure of 99.91 kPa at 2000 UTC 18 December. The system turned west-northwest on 19 December as it reached tropical storm strength. Bobbie continued west-northwest through 21 December, then it briefly turned west while approaching the Mariana Islands on 22 December. Bobbie reached a peak intensity of 95 km h^{-1} while moving west-northwest through the central Mariana Islands on 22-23 December. Saipan reported pressures of 100.3-100.4 kPa for several hours on those days, but maximum winds remained below tropical storm force. Bobbie continued west-northwest on 24 December, then turned northwest while weakening to a depression with 45 km h^{-1} winds on 25 December. The system turned northeast and dissipated near 24N 138E, 1,000 km east-southeast of Okinawa, on 26 December.

Acknowledgements

The satellite images used in this report are GMS-4 Visible images of the Japanese Meteorological Agency, Tokyo processed at the Royal Observatory, Hong Kong. All sources are gratefully acknowledged.

B.Y. Lee, O. Wong, C.M. Cheng, S.C. Tai and Y.S. Hung

Royal Observatory

Hong Kong

Hong Kong's New Doppler Weather Radar

ABSTRACT

The Royal Observatory installed a Doppler Weather Radar in Hong Kong in 1994. This paper provides an introduction to the principle of operation and the various features of the radar. Illustrative examples of useful products and diagnostic tools are also presented.

Introduction

Weather radars are used in Hong Kong to monitor the location, movement and development of rain areas. They are particularly useful in locating tropical cyclones when they come within radar range. The Royal Observatory, Hong Kong (RO) implemented a Doppler Weather Radar at Tates's Cairn in 1994. In addition to rain detection, the radar features the capability to measure the speed of approach of weather. The following sections describe the radar's various features and products as well as the utilities for testing, calibration and fault diagnosis.

Principles of Radar Operations

A weather radar detects rain in the atmosphere by sending out pulses of microwave energy from its scanning antenna. The antenna acts as both a transmitter and receiver. When a radar pulse encounters rain drops or ice particles, part of its energy is reflected back to the antenna. The time taken by the pulse to make the round trip provides quantitative information on the distance of the rain area from the radar. Rain intensity is then determined from this distance and the received signal strength (Battan, 1973; Rinehart, 1991).

In addition to rain intensity, a Doppler Weather Radar also measures the velocity of approach and departure of the rain areas. Its principle of operation may be likened to a train blowing its whistle while passing in front of an observer, who will notice that the pitch of the whistle decreases as the train passes by. In the case of radar, it is a stationary radar observing moving targets such as raindrops. Each moving target will shift the frequency of the radar signal an amount that depends on its speed of motion. One particularly useful application of this Doppler capability in a radar is in estimation of wind strength in tropical cyclones (Rinehart, 1991).

Radar Measurements

The Doppler Weather Radar measures three basic parameters; reflectivity, radial velocity (*i.e.* along the line joining the radar and the target), and the velocity spectrum width.

Reflectivity (**Z**, in $mm^6\ m^{-3}$) is a measure of the strength of the radar echo from an area of rain. Rain intensity (**R**, in $mm\ h^{-1}$) is obtained from reflectivity using the Marshall-Palmer relationship: $\mathbf{Z} = a\ \mathbf{R}^b$. The constants, a and b, have default values of 200 and 1.6 respectively and are modifiable by the user.

The **radial velocity** ($\mathbf{V}_r$, in $m\ s^{-1}$) is obtained from the frequency shift (**f**, in Hz) in radar echoes from a moving target, using the following relationship: $\mathbf{V}_r = \mathbf{f}.\ \lambda/2$ where λ is the radar wavelength in metres. The principle of radial velocity measurement is shown in Figure 1. The radar system obtains the frequency shift in terms of *phase change* in the waveform (*i.e.* an angular measure) between successive radar pulses reflected back from the moving target. Because the largest angle that can be determined unambiguously is radians, there is a limit to the maximum velocity that can be measured.

The **velocity spectrum width** (σ_v, in $m\ s^{-1}$) is

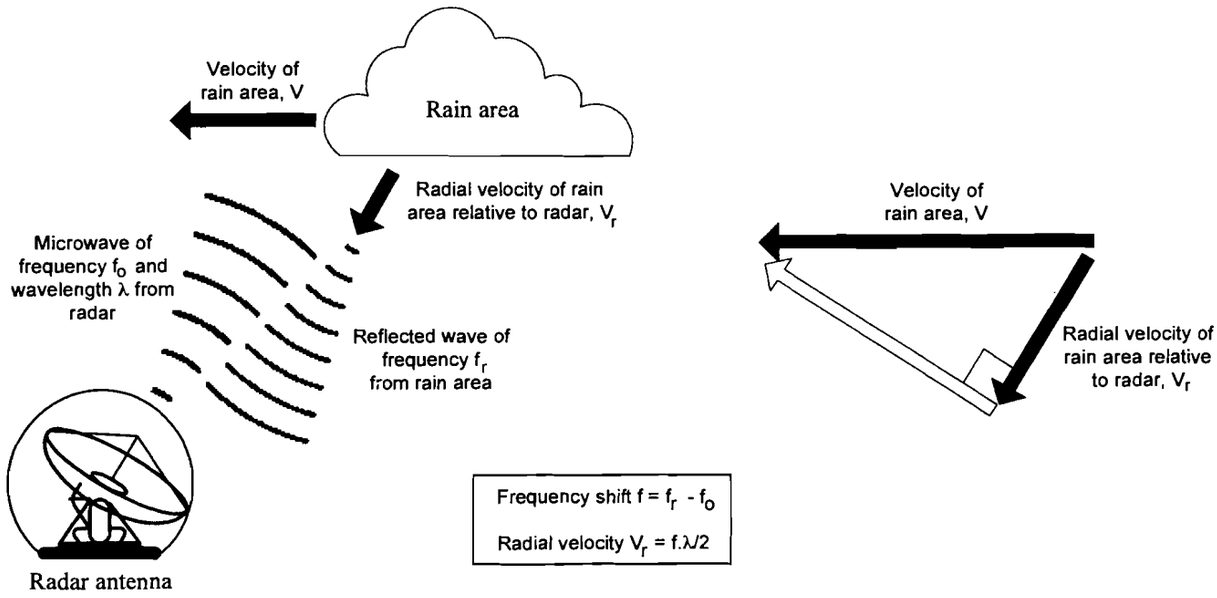

Figure 1 Principles of radial velocity measurement.

a measure of the variability of wind speeds within a volume of atmosphere sampled by the radar. This parameter is useful in the monitoring of turbulence and wind shift.

The Doppler Dilemma

Since the radar sends out microwave energy in pulses, there is a maximum range beyond which the location of rain echoes cannot be detected unambiguously. This maximum unambiguous range ($\mathbf{r}_{max}$, in km) corresponds to the distance a radar pulse travels and returns before the next pulse is sent out. Ideally, the longer the separation between successive pulses, the larger will be the maximum unambiguous range $\mathbf{r}_{max}$.

However, for a given radar the maximum unambiguous velocity decreases with the separation between pulses as discussed earlier. Thus, the maximum unambiguous range and the maximum unambiguous velocity represent two constraints that combine to form what is called the ***Doppler Dilemma***: $\mathbf{v}_{max} \cdot \mathbf{r}_{max} = \mathbf{c}\ \lambda\ /\mathbf{8}$, where **c** is the velocity of propagation of electromagnetic energy. A large $\mathbf{v}_{max}$ would therefore mean a small $\mathbf{r}_{max}$ and vice versa.

For the Doppler radar at Tate's Cairn, operating parameters have been chosen to give an $\mathbf{r}_{max}$ of 256 km and thus a $\mathbf{v}_{max}$ of 15 m s^{-1}.

Velocity Folding

Velocity folding occurs when the radial velocity of rain echoes exceeds the maximum unambiguous velocity of the set. Under these circumstances the velocities will be displayed as ***folded***. This means that $\mathbf{v}_{display} = \mathbf{v}_{true} - \mathbf{n} \cdot \mathbf{v}_{max}$, **n** being an integer. The velocity finally displayed is thus always within the range $-\mathbf{v}_{max}$ to $+\mathbf{v}_{max}$. When folding occurs, this is seen on the display as an abrupt discontinuity in the velocity, *e.g.* a switch from - 15 m s^{-1} to +15 m s^{-1}.

It is normally easy to identify ***folding*** on the radar display. Figure 2 shows an example of velocity folding during the approach of Severe Tropical Storm Harry on the morning of 26 August 1994. Within the rainband of Harry, the region in white colour to the south-southeast of Hong Kong has near zero radial velocity relative to the territory. To the left of that region, echoes are yellow to red in colour indicating they are moving away from Hong Kong. To the right, however, the colour changes from green to blue, representing echoes moving towards the territory, and then rather suddenly back to red and orange. This ***velocity folding*** occurring to the east-southeast of Hong Kong actually represents an approach

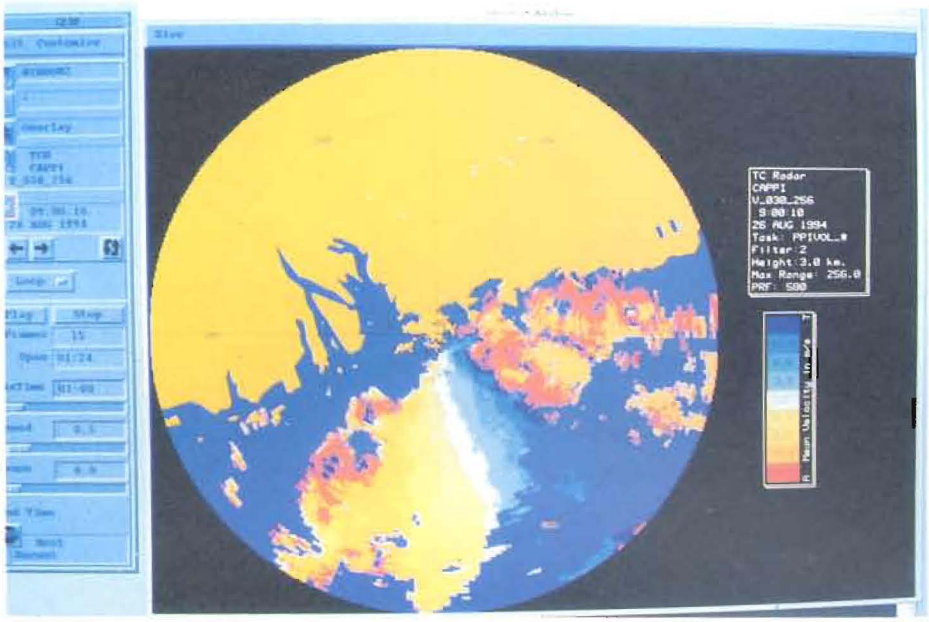

Figure 2 Radar velocity map showing the approach of Severe Tropical Storm Harry on 26 August 1994 as an illustrative example of velocity folding.

speed, not a departure, of about 25 m s^{-1} (*i.e.* 90 km h^{-1}). It suggests that Harry at that time might have reached the intensity of a Severe Tropical Storm which is defined as having a maximum sustained wind speed of 88-117 km h^{-1} near the centre.

Clutter Supression

Clutter is non-meteorological echo that interferes with the observation of rain. Examples of clutter are high mountains, towers, buildings, trees and even a flock of birds near the radar station. Ground clutter, which includes all but the last of these, either does not move or barely moves relative to the radar. Thus the radial velocity associated with ground clutter is close to zero.

There are two basic methods of eliminating ground clutter. The first involves the production of a ***clutter map*** which is obtained by scanning the atmosphere on a perfectly fine day. The echoes that show up on the scan should be non-meteorological in origin and thus represent ground clutter. During normal operation of the radar, this clutter map is subtracted from the raw data to produce the final display products.

The second method of eliminating ground clutter makes use of a ***clutter filter***. The function of the clutter filter is to identify radar echoes with near zero radial velocity, which are then filtered from the display.

Set-up of the Doppler Weather Radar

The Doppler Weather Radar was installed at Tate's Cairn radar station in 1994. For a brief history of weather radar measurement at that site the reader is referred to Wong and Ho (1994). An aerial photograph of the site is presented in Figure 3.

A schematic diagram of the set-up of the Doppler Weather Radar system is shown as Figure 4. Located at the Tate's Cairn site are an antenna, a pedestal, a radar transmitter and receiver, a Radar Control Processor (RCP), a Radar signal Processor (RSP), and a Data Processing Work-station (DPW).

The antenna of the Doppler radar measures 4.3 m in diameter, giving a beamwidth of 1.8 degrees. The operating frequency is 2.92 GHz, *i.e.* in the

Figure 3 Aerial view of Tate's Cairn radar station overlooking Kowloon to the southwest. The Doppler Weather Radar (right) is enclosed within a protective radome and is located alongside a Digital Weather Radar (left) installed in 1983 (photo courtesy HK Government Flying Services).

microwave region, corresponding to a wavelength of 10.3 cm. The peak power is 500 kW while the typical average power is 500 W. For reflectivity the sensitivity attainable is 0.15 mm^{-1} rainfall rate at 200 km. For Doppler measurements the maximum velocity that can be determined is 45 m s^{-1}.

The data processing workstation at Tate's Cairn is used to control the operation of the radar and to pre-process the radar signals. The pre-processed data is transmitted via a dedicated telephone line to a Data Analysis Workstation (DAW) in the Central Forecasting Office (CFO) at the Royal Observatory Headquarters (ROHq).

The Data Analysis Workstation in CFO further processes the radar data to generate various products ready for display and also archives the pre-processed data on magnetic tapes. A Radar Display Terminal (RDT), also in CFO, provides additional display space. There is full automatic control so that the forecaster or operator can select the appropriate scanning mode of the radar through keyboard entries at ROHq.

Radar pictures are also disseminated to the Data Display Terminal (DDT) at the Airport Meteorological Office at Hong Kong International Airport and to other users via dedicated telephone lines.

Radar Products

The following common forms of radar display are available with the system.

a) **Plan Position Indicator (PPI)**, a top view, map display of a horizontal surface scanned by the radar beam.

b) **Constant Altitude Plan Position Indicator (CAPPI)**, a PPI at constant height. Figure 5 shows an example of a 3-km CAPPI taken on 3 January 1995 of a rainband affected the northwest part of Hong Kong.

c) **Range Height Indicator (RHI)**, a vertical cross section scanned by the radar in an upward-downward manner. A sample RHI is presented in Figure 6 showing thunderstorms to the west of Hong Kong on 19 April 1995.

d) **Cross Section**, a vertical cross section of the atmosphere along any line. A sample is also included in Figure 6. Although resolution is

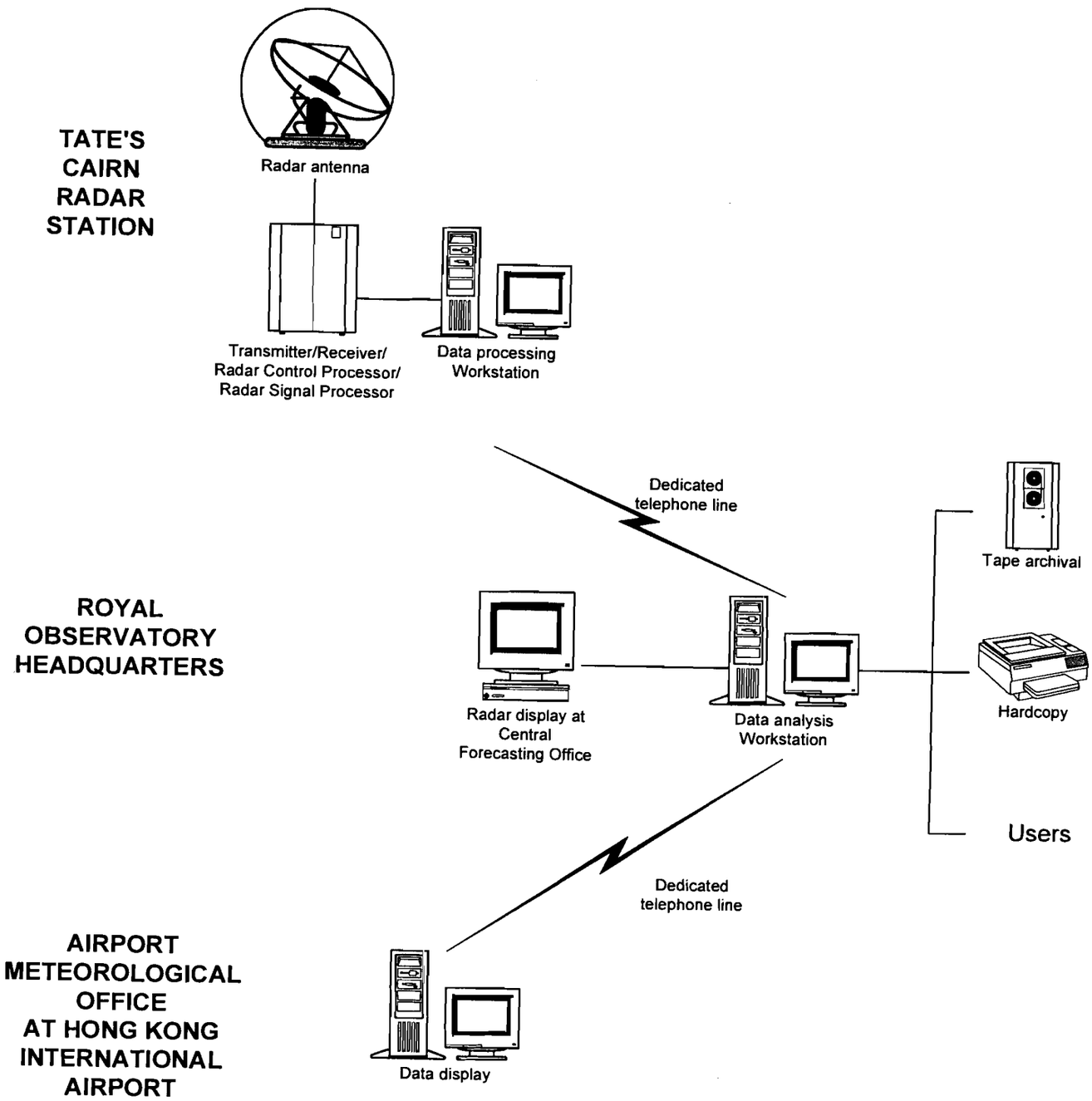

Figure 4 Set-up of Tates's Cairn Doppler Weather Radar system.

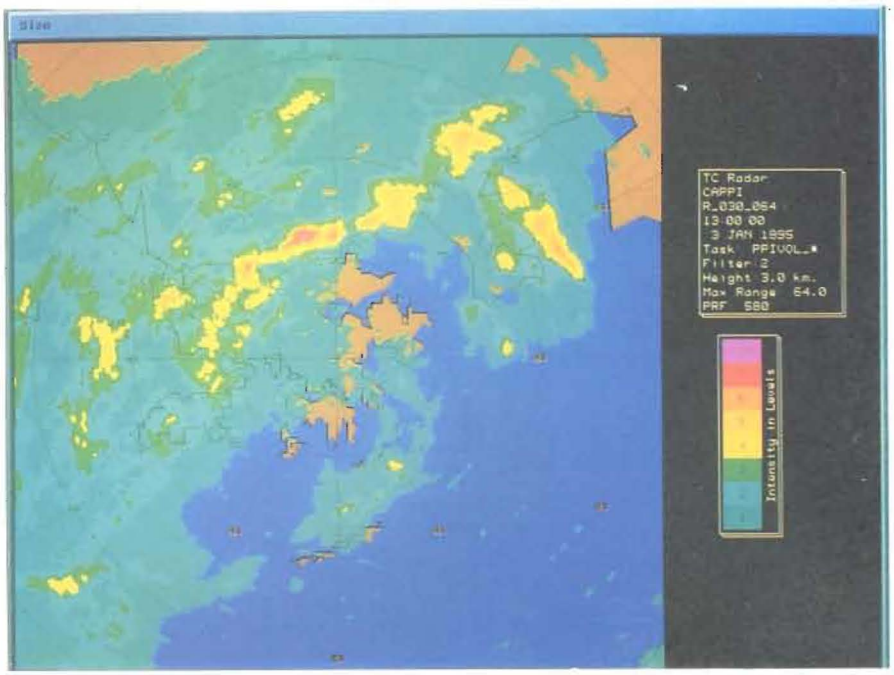

Figure 5 *A 3-km CAPPI picture taken at 1300 HKT on 3 January 1995 showing a rainband that began to affect Hong Kong.*

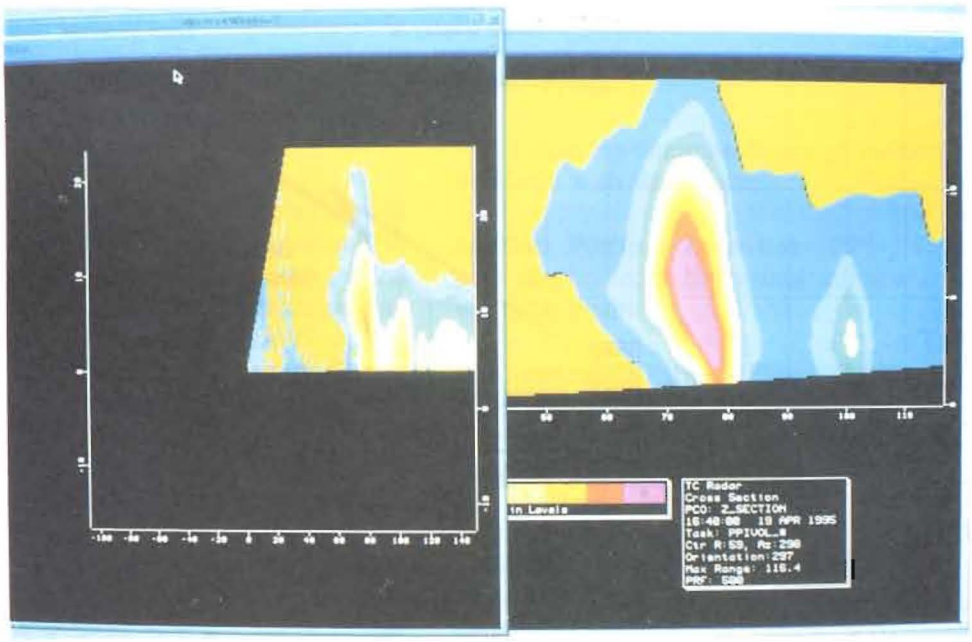

Figure 6 *Left: RHI scan showing thunderstorms to the west of Hong Kong on 19 April 1995. Right: vertical cross section of the same area of severe weather a few minutes after the RHI scan.*

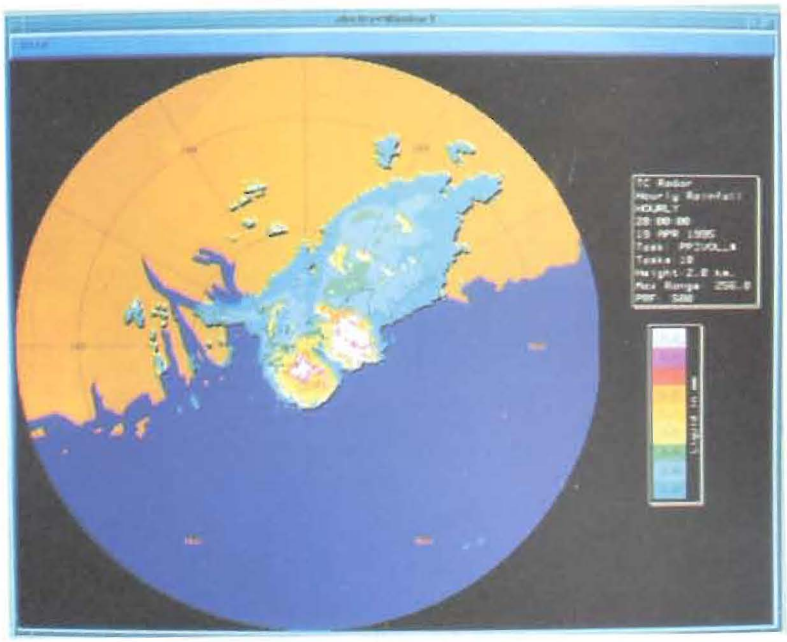

Figure 7 Radar picture showing cumulative rainfall over a period of one hour ending at 2000 HKT on 19 April 1995.

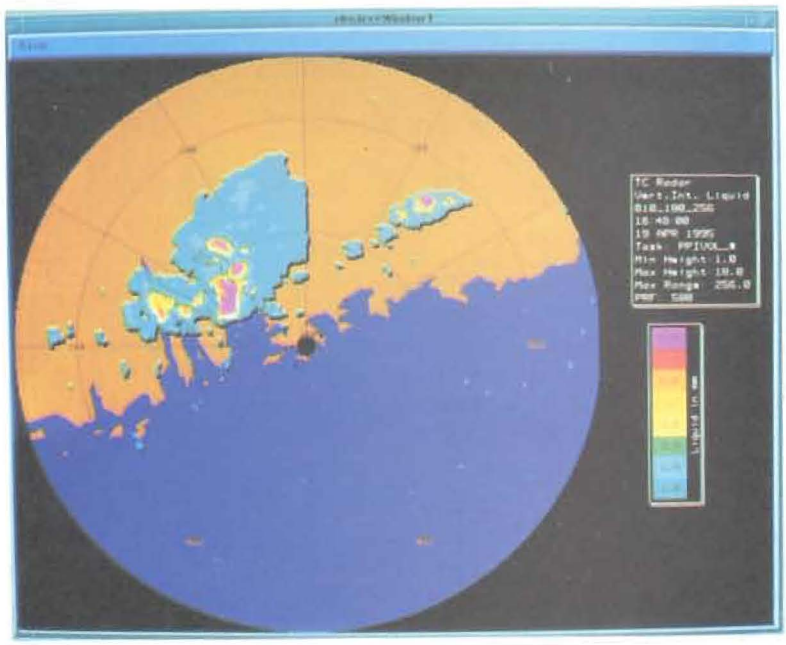

Figure 8 Radar picture showing the vertically integrated liquid water (VILW) for a rainband over the coast of Guangdong at 1648 HKT on 19 April 1995.

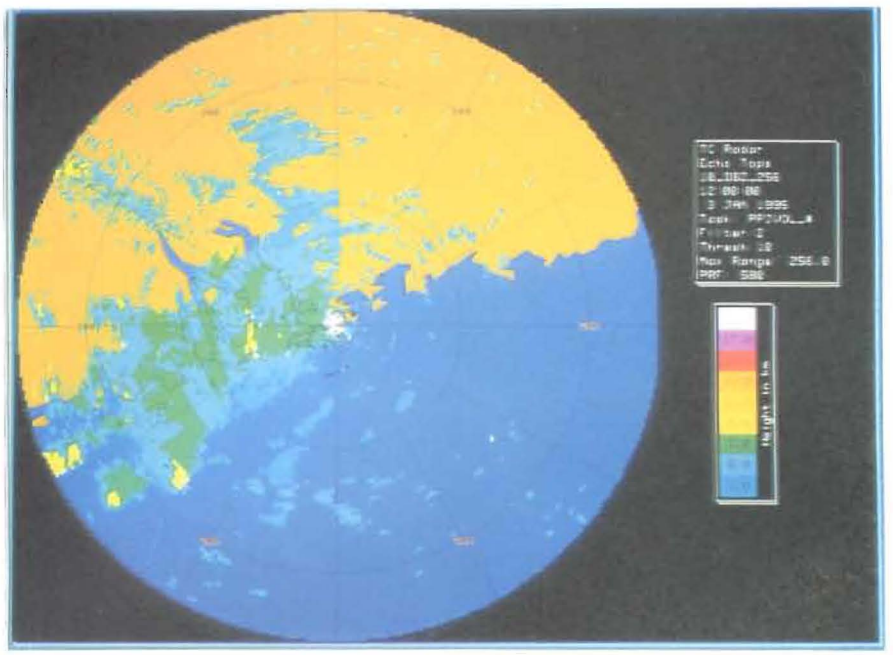

Figure 9 Radar picture taken at 1200 HKT on 3 January 1995 showing the height of the echo top within 256 km of Hong Kong.

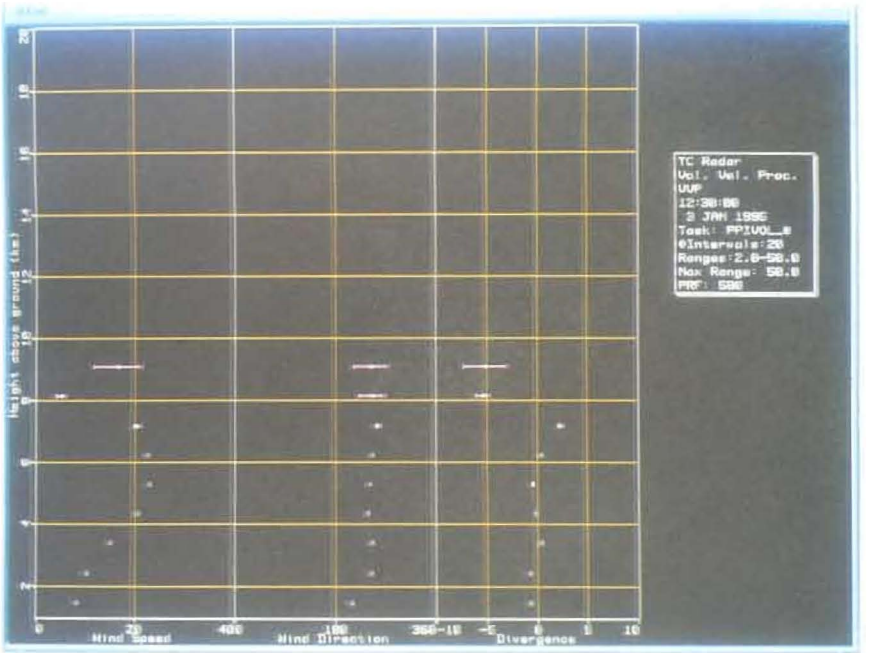

Figure 10 Radar picture of velocity volume processing (VVP) showing the vertical variation of wind speed on the left, wind direction in the middle, and divergence on the right, directly above Hong Kong at 1230 HKT on 3 January 1995.

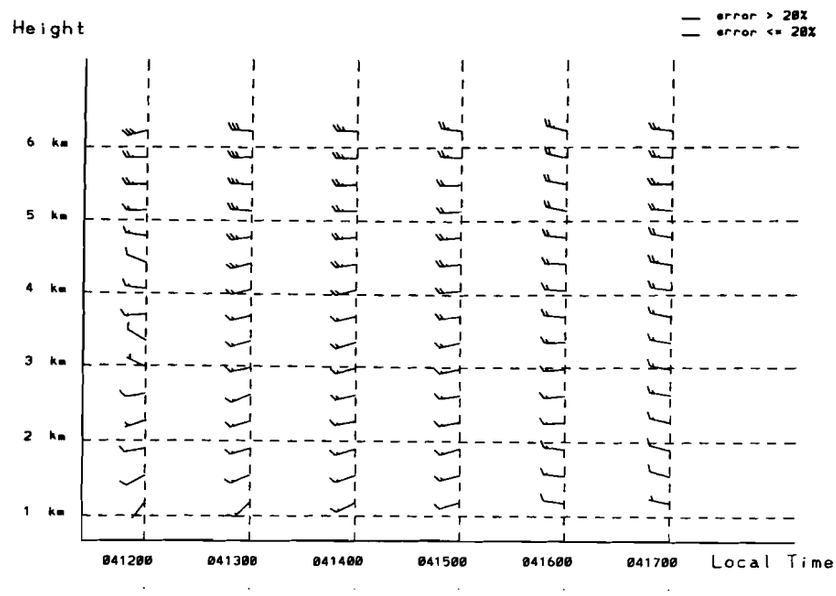

Figure 11 Time series of upper winds extracted from VVP radar pictures for the afternoon of 4 May 1995.

generally lower than for an RHI, there is the advantage that because it does not require a separate scan as RHI does, a cross section can be generated much faster. Another advantage is that a cross section can be obtained along any line marked out by the cursor on the screen.

e) **Automated Warning**, a warning message produced when a certain preset criterion is met (*e.g.* rainfall rate). This is particularly useful during severe weather situations, such as thunderstorms, floods and rainstorms.

f) **Maximum Rain Intensity**, indicated for each pixel in the radar picture, together with east-west and north-south projections on side panels.

g) **Rainfall Accumulation**, a map of cumulative rainfall over a specified time period. Figure 7 presents a sample obtained for a one-hour period ending at 2000 HKT on 19 April 1995.

h) **Vertically Integrated Liquid Water**, (**VILW**), a map of estimated depth of water contained in the atmosphere aloft. A sample for a rainband over the coast of Guangdong at 1648 HKT on 19 April 1995 is presented in Figure 8. The water depth for a particular spot is obtained by integrating over a column of atmosphere scanned by the radar over that spot.

i) **Echo Top**, a contour of the tops of the rain areas. An example for the region within 256 km of Hong Kong at 1200 HKT on 3 January 1995 is shown in Figure 9.

j) **Forecast**, interactive tropical storm tracking and prediction.

k) **Velocity Volume Processing** (**VVP**), display produces graphs of wind speed, direction and divergence against height. Figure 10 presents an example for the region directly above Hong Kong at 1210 HKT on 3 January 1995. Based on the VVP products a time series of upper winds measured by the radar can be constructed. An example for the afternoon of 4 May 1995 above Hong Kong is given in Figure 11.

Modes of Operation

In routine operation the Doppler radar performs two scans of the atmosphere every six minutes. The first is a PPI scan of reflectivity data out to a maximum range of 512 km at an elevation of 0.5°. This scan is useful for monitoring the approach of rain areas from a distance. The second scan is a volume scan of the atmosphere, which consists of twelve PPI scans with angles of elevation between 0.5° and 34.7°. This scan collects both reflectivity data as well as radial

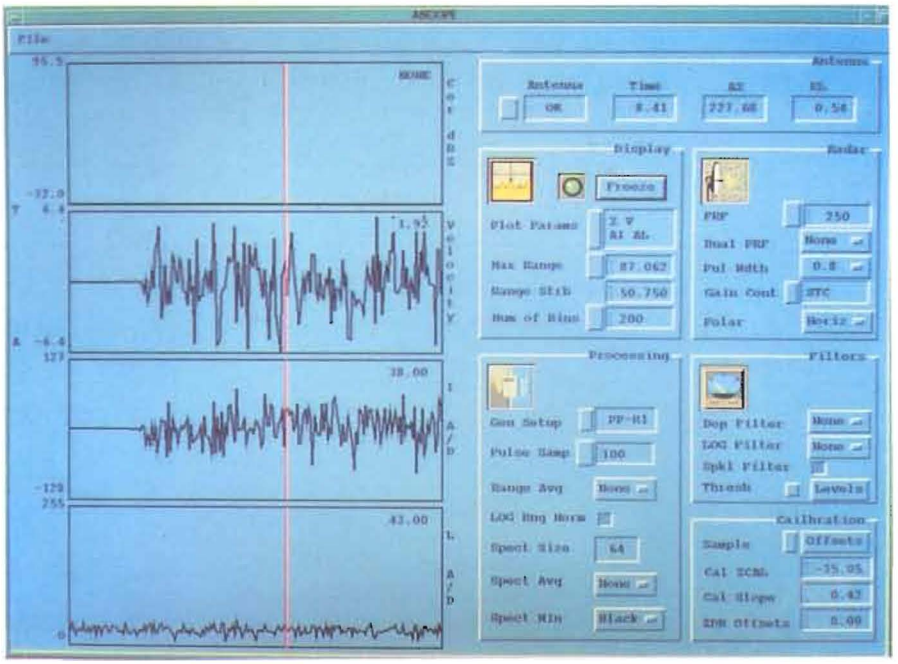

Figure 12 Sample display of the ASCOPE utility for diagnostic purposes.

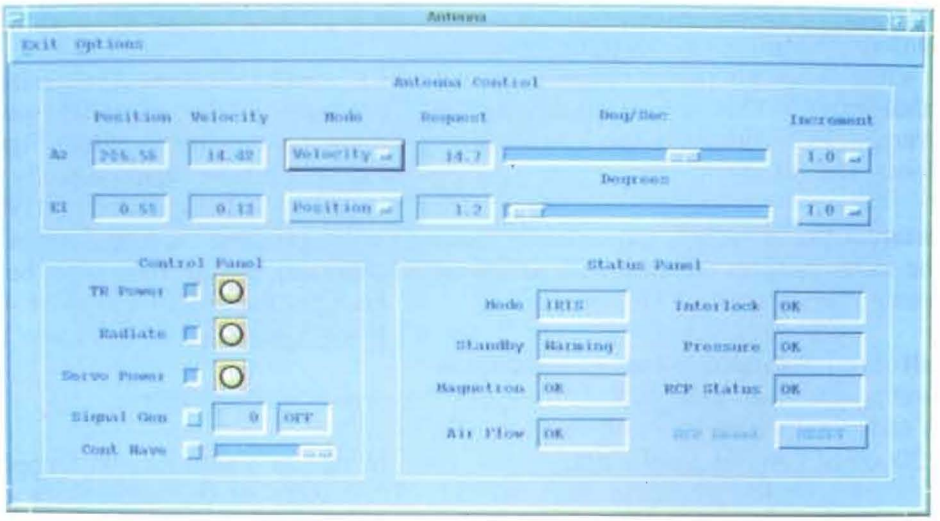

Figure 13 Sample display of the ANTENNA utility available at the Royal Observatory Headquarters for controlling radar operations at Tate's Cairn.

velocity data of the atmosphere out to a range of 256 km. This allows users to visualize both the rain intensity and the wind field associated with the weather systems. The radar can also perform an RHI when it is so scheduled.

Diagnostic and Calibration Tools

Apart from collecting and displaying radar information, the Doppler Weather Radar system is equipped with a number of utilities for monitoring and maintaining the operation of the system, particularly the radar equipment at the Tate's Cairn radar station. Because of the dedicated telephone line information on the operational status of the radar equipment at Tate's Cairn is continually available at the Data Analysis Workstation at ROHq. Maintenance staff can perform preliminary diagnosis and carry out simple adjustments at ROHq without having to physically travel to the radar station.

A number of utilities are provided with the Doppler Weather Radar system. These utilities are all software driven and fall into three main categories according to their primary function. These include: (1) **configuration** utilities for setting up the mode of operation of the radar; (ii) **calibration** utilities for the radar hardware; and (iii) **monitoring** and **testing** utilities for routine maintenance purposes. Two examples of the utilities available are now presented.

ASCOPE is a calibration utility for testing and aligning the signal processor of the radar. It operates like an oscilloscope and can show the plot of reflectivity against range, velocity against range, spectrum width against range among a selection of plots. Users can display up to five plots simultaneously. Figure 12 presents a sample display of the ASCOPE utility.

ASCOPE is a monitoring and testing utility for controlling the radar antenna. Users are allowed to control the position, the scanning velocity and the radiation status of the antenna via the keyboard. A sample of the ANTENNA utility is depicted in Figure 13.

Archives and Supply of Radar Data

All radar data are stored on magnetic tape and floppy diskettes. Time sequences of CAPPI rain intensity are video-taped and are regularly shown on local television weather programmes. Radar images are also routinely exchanged with the Guangdong Meteorological Bureau via a Beijing-Hong Kong data circuit. In addition they are disseminated to various aviation and air traffic control users.

Discussion

The Doppler Weather Radar system has been running smoothly without major breakdown since it started operating last year. Through extensive use of software control the system features a high degree of user-friendliness. Different types of radar pictures are readily available at the user's fingertips. Changing the operation of the system requires only a click of the mouse or a few keystrokes on the keyboard. Furthermore, preliminary trouble-shooting of the radar equipment at Tate's Cairn can be done remotely from the Royal Observatory Headquarters.

The usefulness of the Doppler feature was demonstrated during the approach of Severe Tropical Storm Harry on 26 August 1994. Originally estimated to be of tropical storm strength (*definition:* maximum sustained wind speed of 63-87 km h^{-1} near the centre), Harry's Doppler pattern (presented in Figure 2), made it apparent that the wind strength could be higher. This piece of evidence contributed to the storms subsequent upgrading to a severe tropical storm (*definition:* maximum sustained wind speed of 88-117 km h^{-1} near the centre).

We have yet to be exposed to the radar images associated with the full range of weather systems that can affect the South China Coast each year. There is a learning curve to ride, particularly in the interpretation of the Doppler patterns. It is hoped that, in time, the full potential of the radar in observing the various weather systems can be realized.

References

BATTAN, L.J., 1973: Radar Observations of the Atmosphere. University of Chicago Press, Chicago.

RINEHART, R.E., 1991: Radar for Meteorologists. P.O. Box 6124, Grand Forks, ND.

WONG, S.K. and K.L. HO, 1994: A brief history of the Royal Observatory weather radars. *HKMetS Bull.*, **4(2)**, 7-11.

Issue 6, 1st Quarter, 1995

United Nations Climate Change Bulletin

Published quarterly by the interim secretariat for the UN Climate Change Convention, the Secretariat of the UNEP/WMO Intergovernmental Panel on Climate Change (IPCC), and the UNEP/WMO Information Unit on Climate Change (IUCC). This newsletter provides general information only and does not represent the official views of the United Nations or any of its specialized agencies. Readers are welcome to reprint the contents giving appropriate credit. For a free subscription please contact IUCC, UNEP, Geneva Executive Center, CP 356, 1219 Chatelaine, Switzerland.

Contents

****

Germany Welcomes First Session of the Conference of the Parties

-- Angela Merkel,
Minister for the Environment,
Germany

Climate protection is one of the greatest challenges for present and future environmental policy. If no measures are taken, it is estimated that the average temperature of the Earth's lower atmosphere will rise by 3°C (plus or minus 1.5°C) by the end of the next century. The repercussions of such a rise would be dramatic -- a shift in climatic and vegetation zones, a change in rainfall distribution, and a worsening of the global food situation.

The United Nations Framework Convention on Climate Change can serve as a basis for combating this risk. The Convention was signed by the international community in Rio de Janeiro in June 1992 on the occasion of the United Nations Conference on Environment and Development. Around 120 states, plus the European Union, have since ratified the Convention, which entered into force on 21 March 1994.

During the Rio "Earth Summit", the German Chancellor Helmut Kohl extended an invitation to hold the first session of the Conference of the Parties (COP-1) in Berlin. The United Nations General Assembly accepted this invitation, and the session will take place from 28 March to 7 April 1995. As well as expressing our commitment to a global environmental policy, particularly for climate change, the invitation to host the COP expresses Germany's increased commitment to the United Nations.

What happens after 2000?

The first session of the COP will set the direction for the long-term follow-up to the Framework Convention.

The ultimate objective of the Convention is to stabilize atmospheric concentrations of greenhouse gases at a level that would avoid dangerous anthropogenic (human-induced) interference with the climate system. In view of this, one of the central purposes of the Berlin COP will be to review the adequacy of Article 4.2(a) and (b) of the Convention. This Article commits industrialized countries to take measures aimed at returning their greenhouse gas emissions to 1990 levels by the year 2000. It does not state that these countries should remain at or below 1990 levels after the year 2000.

Current commitments, then, leave the steps to be taken after 2000 completely open. What's more, according to current scientific knowledge they

will not achieve the Convention's ultimate objective. Because of this, Annex I parties (developed countries and countries with economies in transition) broadly agree that the present commitments are inadequate and need to be strengthened and further elaborated. Germany therefore believes that the COP should at its very first session seek consensus on a commitment by developed countries to stabilize their carbon dioxide emissions at 1990 levels beyond the year 2000.

We know that if we are to reach agreement in Berlin on the post-2000 period, a large number of negotiating partners will still have to be convinced of the urgency of taking such a step. Moreover, if we are to be successful in protecting our climate, it is essential that efforts be made by all countries. Because of their contribution to global emissions, and their financial and technological capabilities, it is first and foremost a matter for the industrialized countries to lead the way in meeting the challenge of climate change. They have expressly acknowledged this obligation as a principle of the Framework Convention on Climate Change.

However, in the long run, this in itself will be insufficient to prevent the serious disturbance of the climate system, as the greenhouse gas emissions of developing countries will continue to rise considerably. In the foreseeable future, then, the developing countries, too, should make appropriate commitments and limit the increase in their emissions according to the principle of common but differentiated responsibilities. Only through a global partnership for environment and development can we give our climate effective and sustainable protection.

Protocol negotiations should begin

Acceptance by the industrialized countries of responsibility for stabilizing emissions beyond the year 2000 would be a step in the right direction. But further measures need to be taken urgently, and it is Germany's view that the Convention should be swiftly followed up by a protocol containing concrete goals and measures for all greenhouse gases.

We believe that a comprehensive protocol for greenhouse gases, involving sources and sinks as well as all relevant economic sectors, should be negotiated without delay. This protocol should be flexible enough to allow other relevant gases to be gradually incorporated if called for by new scientific knowledge. It should also combine targets and timetables for limiting and reducing emissions with agreements on coordinated policies and measures for such areas as energy and transport, agriculture and forestry, and fluorocarbons.

Numerous proposals for concrete action are already on the table. Improving the energy efficiency of combustion technologies, heating systems and domestic appliances is vitally important, as is reducing unnecessary traffic and developing more environmentally friendly vehicles. If possible, by the year 2005 the average petrol efficiency of new cars should have been steadily reduced to five litres per 100 kilometres.

In setting such new and far-reaching commitments, due regard must be paid to the principles set out in Article 3 of the Convention, including the principles of balanced burden sharing and of the common but differentiated responsibilities and respective capabilities of Parties.

We are aware that adopting such a protocol at COP-1 is extremely unlikely. The majority of our international negotiating partners first see a need for intensive negotiations on the various aspects of a protocol. We cannot expect miracles from the Berlin Conference.

However, what I do consider possible in Berlin is agreement on a mandate for opening negotiations on a protocol. The mandate should give directions for the content of the Protocol, as well as a time-frame for completing negotiations by the Third Session of the Conference of the Parties in 1997. This, together with an agreement to stabilize carbon dioxide emissions beyond the year 2000, would be considerable progress.

****

Berlin 1995:

A Brief Guide to COP-1

Five years ago, international action to reduce the risk of climate change was no more than an idea, a possibility. Since then, the IPCC has published its First Assessment Report confirming the scientific basis for climate change (1990), a treaty was negotiated (1991 to 1992) and signed by over 150 countries at the Rio Earth Summit (1992), the treaty entered into force (1994), and its framework was filled in (1992 to 1995).

Now action under the Climate Change Convention can begin in earnest. An important new phase of the international response to climate change will be launched at the First Session of the

Conference of the Parties (COP-1). What follows is a brief round-up of the meeting and what to expect.

When is the meeting being held?

COP-1 will open on Tuesday, 28 March, and close on Friday, 7 April. The final three days (5-7 April) will be held at the ministerial level and will be inaugurated by Chancellor Helmut Kohl.

Where will it take place?

The meeting is being hosted by the Government of Germany at the International Congress Centre in Berlin.

Who will be there?

The Convention specifies that a country becomes a Party to the Convention three months after ratifying it. This means that the 116 Parties (115 governments plus the European Union) that ratified by 28 December 1994 are eligible to participate fully on the opening day. Two other countries that ratified shortly after this date will become Parties during the meeting, so there will be a total of 118 Parties when decisions are formally adopted at the end of the meeting (*see Ratifications Update in Section 6*).

Other governments can attend the meeting as observers. Many hundreds of intergovernmental organizations (IGOs), non-governmental organizations (NGOs), and journalists will also attend. Some of these organizations will be sponsoring special events during the meeting.

What is on the agenda?

When the Intergovernmental Negotiating Committee (INC) concludes its eleventh and final session in New York on 17 February, it will adopt a series of recommendations to be forwarded to the COP. At a minimum, however, the Convention requires COP-1 to address the following issues:

* First review of national communications. By October 1994, 15 Annex I countries (developed countries and countries with economies in transition) had submitted their first national communications describing their efforts to implement the Convention (*see the next article, Section 3*). The Parties will assess this information and what it reveals about "the extent to which progress towards the objective of the Convention is being achieved". They will also need to agree on the process for future reviews.

* Adequacy of commitments. Article 4 of the Convention requires Annex I Parties to take measures aimed at returning their greenhouse gas emissions to 1990 levels by the year 2000. In Berlin the Parties must review whether this commitment is an "adequate" step towards the Convention's ultimate objective of stabilizing "greenhouse gas concentrations in the atmosphere at a level that would prevent dangerous anthropogenic interference with the climate system." Based on this review, the COP "shall take appropriate action". Some Parties are expected to propose that COP-1 launch a new round of negotiations on additional commitments. (*see the articles, Sections 4 and 5*).

* Institutional arrangements. The Parties must "designate a permanent secretariat and make arrangements for its functioning"; give guidance for the work of two subsidiary bodies (one for implementation of the treaty, the other for scientific and technological advice); and consider whether to extend or make permanent the "interim arrangements" for the Convention's financial mechanism, currently operated by the Global Environment Facility (GEF).

* Rules of procedure. The COP must specify what kind of voting majorities will be needed to adopt particular decisions (e.g. to adopt protocols).

What is the Berlin meeting likely to achieve?

COP-1 is the first global climate change meeting attended by ministers since the 1992 Rio Earth Summit. This makes it an important conference -- but Berlin should be seen primarily as the first step in a long and difficult process. Responding to global climate change is a massive and complex undertaking, with enormous economic, social, and political implications. It will require developed and developing countries to pursue new avenues of cooperation. Therefore COP-1 can be considered a success if it creates a solid foundation of institutions and procedures and strengthens the existing political consensus. With these essential building blocks in place, the Convention process will gain the momentum it needs to mobilize national and international action up to and through the early 21st century.

****

Governments Act on Treaty Commitments: A First Review

-- Richard Kinley, Special Advisor to the, Executive Secretariat, Convention Secretariat.

The Climate Change Convention has taken a major step forward into its operational phase. The "national communications" from developed countries have started to arrive and the process of reviewing them has begun. These communications describe how governments are carrying out their treaty commitments. Their regular review is a key feature of the Convention, and one that should become a driving force in the international response to climate change. The review process that has been agreed promises to be the most intensive global-level review of environment-related policies ever attempted.

The initial phase of the first review was completed in late 1994 on the basis of information received from 15 developed countries. The results offer both governments and the public a general picture of where action under the Convention is heading. They will also help the Parties take decisions at the upcoming Berlin Conference of the Parties (COP) on whether the current commitments are adequate to achieving the Convention's ultimate objective.

The synthesis

Developed countries that ratified the treaty by the end of 1993 were required to submit their national communications by 21 September 1994. The Convention gives the others nine months from the date they ratify (developing countries have over three years). Each national communication includes an inventory of 1990 greenhouse gas (GHG) emissions by sources and removals by sinks, a description of policies and measures to limit greenhouse gas emissions, a projection of how these measures will affect future emissions, a section on the provision of financial support to developing country Parties, and a description of educational, research, and other activities.

Communications from 15 countries, averaging 120 pages each, were received in time for the first synthesis report. (Five more have since been received, and several others remain overdue.) The communications were analyzed and synthesized by an international team of 20 experts assembled by the Convention's secretariat. The team worked night and day for ten weeks to transform the mass of national information into a coherent cross-national synthesis. The result, a 70-page report, was presented to the final session of the Intergovernmental Negotiating Committee (INC) in February 1995.

This synthesis document is neither a summary nor a country-by-country analysis. Instead, it provides an overview of the implementation of the Convention across Parties, noting trends and providing indications of the progress achieved.

In general, it reveals that Parties have provided extensive information on a wide range of activities. It also shows that carbon dioxide emissions continue to rise and that further measures to limit emissions appear to be necessary.

Policy goals and instruments

The Parties reviewed account for 41% of 1990 global carbon dioxide emissions from fossil fuel combustion. All are implementing policies and measures to limit their emissions, and the majority reported actions to enhance sinks. Most of their efforts are focused on controlling carbon dioxide emissions, particularly in the residential, commercial and institutional, transport, and industry end-use sectors. A number of main policy goals emerge from the review:

* Increasing competition and improving efficiency and fuel switching in power generation;

* Improving the efficiency of industrial equipment and industrial processes;

* Improving automobile fuel efficiency, controlling vehicle emissions, and encouraging public transportation;

* Improving energy efficiency in buildings, mechanical systems, and appliances;

* Reducing emissions from animals and the use of nitrogen fertilizer;

* Preserving forest biomass and encouraging afforestation;

and

* Reducing waste and emissions from landfills.

To achieve these goals, the Parties reported using a wide array of policy instruments. Regulatory efforts are focusing on preserving forests and on new standards for appliances, industrial equipment, GHG precursors from vehicle emissions, and building codes.

Economic instruments are being widely applied. Subsidies, rebates, and incentives predominate and are used to encourage power generation efficiency, renewable energy and alternative fuels, the use of public transport, and afforestation. Taxes are less common, and mostly applied to the transport and waste sectors, although

broad-based taxes are being used by some Parties.

Voluntary agreements are being used, particularly where large industries are involved. Information and education programmes are being established, notably in the agriculture and waste sectors and to influence consumer choices in most sectors. Most Parties also reported on research and development programmes aimed at developing technologies or practices to reduce emissions, particularly from the energy sector.

Future emissions and transfers

The emissions projections have proved to be of great interest, despite the limitations inherent in developing them. The projections are summarized as follows.

For carbon dioxide emissions (excluding land-use change and forestry), five Parties project that they will stabilize or even decrease emissions in the year 2000. Nine Parties project an increase by the year 2000 in the absence of additional measures. Of these, however, several stated that they do intend to develop and implement further measures. Their projections may therefore change. (The remaining Party did not provide a projection for 2000, but projected decreased emissions in 2005.)

For methane, the picture is more encouraging. All but two Parties project decreasing emissions by the year 2000.

No clear picture emerges for nitrous oxide.

As for financial and technological transfers, the communications reveal that developed country Parties are transferring resources to developing countries through the Global Environment Facility (GEF). It was not possible, however, to assess the extent to which resources meet the Convention's provision that they be "new and additional". Bilateral and other multi-lateral channels are also being used, with some emphasis on capacity-building activities.

What's next?

In addition to producing valuable information on the international response to climate change, the first review also offers lessons in how to improve the process for next time. One problem that will be difficult to resolve is comparability. National circumstances do vary, making it difficult to present information that is comparable from country to country. In addition, three Parties "adjusted" their data to take account of climatic or other variations when projecting emissions, while others did not. Some refinement of the guidelines for the preparation of the communications may be needed.

The in-depth phase of the review process is now being launched. A small team of national experts will examine each communication and report to the Convention's subsidiary bodies. Like the first synthesis review, these in-depth reviews will not be designed as compliance exercises, but rather as fruitful exchanges of national experiences and lessons learned.

Other Annex I Parties continue to submit national communications. This growing reservoir of information will be important for the work of the COP and will assist Parties in advancing the Convention's implementation.

Comments

All communications gave projections for CO_2 emissions, although some of them addressed only emissions from energy use of fossil fuels and one of them did not give figures for 2000. Nine Parties projected an increase from 1990 levels in 2000, according to the starting points of their projections, while five Parties projected either stabilization or a reduction from that level. The Party that did not provide 2000 figures projected a 5 per cent decrease from 1990 to 2005. The projected growth in emissions is above 10 per cent for five Parties. Among the Parties that projected declines, all but one projected reduction of less than 8 per cent. The exception was an economy in transition whose projected emissions reached the lowest level in 1994 and then started to rise. If projected 2000 emissions are compared with 1990 inventory figures for the three Parties that made adjustments, the results change from projected decreases for all of them to stabilization, a 0.5 per cent increase and a 3.2 per cent increase.

****

The Adequacy Debate I: Make the Toronto Target the Next Commitment

-- Susan Subak, Centre for Social & Economic Research for the Global Environment (CSERGE) and Jacob Werksman, Foundation for International Environmental Law and Development (FIELD)

The Parties attending the Berlin COP must decide

whether or not the Convention's present commitments are adequate for achieving its ultimate objective -- the "stabilization of greenhouse gas concentrations in the atmosphere at a level that would prevent dangerous anthropogenic interference with the climate system". The following two articles offer differing perspectives on how the Parties should handle this question.

Five years after the Intergovernmental Panel on Climate Change (IPCC) adopted its First Assessment Report, four years after the first session of the Intergovernmental Negotiating Committee (INC), three years after the Convention was adopted, and a year after it entered into force, the international scientific consensus on the likely dangers of global warming remains fundamentally unchanged. The intervening years have also confirmed how difficult it is to forge an international consensus on how and when countries should respond to this challenge.

In Berlin, the Parties to the Convention will, for the first time, be both bound and empowered to review the adequacy of Annex I (developed) Parties' commitments. This should be done, says the Convention, "in the light of the best available scientific information and assessment on climate change and its impacts". Based on this review, the Parties "shall take appropriate action, which may include the adoption of amendments to the commitments . . ."

At present, Annex I Parties are committed to taking measures aimed at stabilizing their emissions by returning to 1990 levels in the year 2000. Adopting in Berlin a protocol or other legally binding instrument containing specific targets and timetables for reducing greenhouse gas emissions would offer an appropriate next step towards matching the compelling demands of scientific evidence with concerted action.

A number of developed country Parties have begun to take the lead in achieving the Convention's objective by publicly pledging to reduce their emissions of carbon dioxide (CO_2). At least six Annex I countries have already unilaterally adopted targets equivalent to, or more ambitious than, the Toronto Target, which calls for reducing carbon dioxide emissions to 20% of 1990 levels (originally 1988) by the year 2005. A protocol would help to strengthen and broaden these early pledges by providing a legal framework holding all Annex I Parties to such a commitment. It would also help these Parties to coordinate their efforts.

A closer look at the climatic implications of various possible outcomes of the Berlin summit suggests that these new commitments should be undertaken as the next step in the long-term process of slowing global warming.

Stabilizing concentrations *vs* emissions

The Convention's objective calls on countries to stabilize greenhouse gas concentrations in the atmosphere at safe levels. In principle, the Parties could convert this objective into a commitment linked directly to atmospheric concentrations, rather than emissions. If we accept that current concentrations, though higher than the pre-industrial level, are safe enough, then governments could stabilize atmospheric concentrations of CO_2 at today's level.

This would require reducing global CO_2 emissions by more than 60% by the end of the next century. Our current understanding of the climate system and the global carbon cycle suggests that such a programme of reductions would limit global warming to an estimated 0.3°C global-average increase by the year 2100. However, while many of the predicted adverse effects of accelerated climate change would be avoided by this effort, it is widely accepted that political and economic constraints, in both the North and the South, make an agreement to stabilize concentrations highly unlikely.

Alternatively, should Annex I Parties choose in Berlin merely to bind themselves to the Convention's current "quasi-target" of stabilizing their greenhouse gas emissions at 1990 levels, the effect on the future predicted rise of global temperature is expected to be minor. Even if all the Annex I countries were to achieve this emissions stabilization target (which looks increasingly unlikely), the IPCC's best-guess temperature projection may be only slightly lower than the projected temperature rise based on "business as usual" assumptions. Current commitments may lead to a global-average temperature rise by 2100 of about 2.2°C, which is only about 0.2°C less than expected in the absence of a climate agreement.

Although the precise implications of a 2.2°C rise in temperature are not known, such an increase appears to present intolerable risks. As part of its forthcoming Second Assessment Report, the IPCC is now assessing numerous examples of possible adverse impacts and maladaptations to global warming. Possible impacts include declining crop yields; forest die-back; the extension of disease vectors; the loss of important species; reduction in fresh-water supplies; and increased beach erosion, flooding, and salt water intrusion due to sea-level rise.

The Toronto Target

Given the Convention's objective, an adequate commitment undertaken at Berlin should lie somewhere between the extremes of merely stabilizing industrialized country emissions (leading to a predicted rise of 2.2°C by 2100) and reducing global emissions by 60% or more in order to stabilize current atmospheric concentrations by the end of the next century (leading to a predicted rise of 0.3°C).

A protocol adopted at Berlin and based on the Toronto Target, requiring Annex I Parties to reduce their emissions of greenhouse gases by 20% by the year 2005, would be a sound next step.

This target must be part of a longer term strategy, however. Achieving the Toronto Target alone, without taking further steps after 2005, would still lead to an expected global temperature rise of 2.0°C by the end of the next century. This warming would come with many of the risks associated with the "business as usual" scenario. Further steps in the longer term should take the form of deeper cuts in developed country emissions. They should also include arrangements to assist developing countries to constrain their future emissions growth through energy efficiency, renewable energy, and long-term incentives for improved land-use management.

The authors can be contacted at FIELD, SOAS, University of London, 46-47 Russell Square, London WC1B 4JP, United Kingdom, and CSERGE, University of East Anglia, Norwich, Norfolk NR4 7TJ, United Kingdom.

****

Adequacy Debate II: Precautionary Approach Also Applies to Economy

-- Juhani Santaholma, Chairman,
Working Party on Climate Change,
International Chamber of Commerce

The implementation of the Climate Change Convention is still at an early stage. Ratifications continue to come in, and the first national action plans are only now being put into action. Soon these plans will be subjected to a first review. This review will start generating valuable information on the world-wide progress we are making. Despite this promising start, some people are already calling for new initiatives with the objective of undertaking additional commitments. In our view, however, it is premature to judge or abandon existing commitments. It is still too early for governments to make a realistic commitment to new treaty obligations.

Missing information

Article 4.2(d) of the Convention requires the first session of the Conference of the Parties to review the adequacy of commitments. The Convention specifies that this must be done again no later than 31 December 1998, and then again in future years.

Given this agreed series of opportunities for reviewing existing commitments, there is no reason to set an arbitrary target date by which to complete discussions of new commitments. Such a date can best be determined after the Parties have considered what further information and experience they will require given the commitments already in place.

Some of this information will relate to the many areas of great uncertainty that have been identified by the Intergovernmental Panel on Climate Change (IPCC). The IPCC stresses that we need further research into climate science, economic impacts, and the effects of various mitigation and adaptation strategies. The Parties should take full account of these uncertainties when assessing the risks and potential benefits of actions they may take under the Convention.

Another consideration is that an appropriate and effective long-term response to climate change should also include developing countries and those with economies in transition. The efforts of these countries will be more effective if they can benefit from the experience of the developed countries in implementing national action plans. The experience thus far is limited.

Economic growth

Along with precautionary measures to protect the environment, we must also be cautious about unduly harming the world economy. It is here that industry can bring an important perspective to the policy deliberations on the type of commitments we need under the Convention.

Industry and the private financial community marshals most of the financial resources that drive the world's economic growth. Industry develops, finances, and manages most of the investments that will enhance and protect the environment. It will also carry out a substantial part of the national action plans for responding to

climate change.

Governments can strike an effective balance between protecting the environment and promoting economic growth by favouring flexible, market-driven, and cost-effective initiatives. These initiatives should reflect the unique objectives, resources, and economic circumstances of each state. In general, though, they should include voluntary programmes that are designed with industry participation, energy efficiency and conservation initiatives, and the removal of competitive distortions.

The concept of joint implementation (JI) also has much to commend it as a policy initiative. It has as its driving force the principles of cost-benefit analysis. It could give industry and government the opportunity to work together in developing, financing, and implementing projects that support the Convention while providing economic opportunities for developing countries. A pilot phase would allow participants to evaluate JI's economic feasibility and to identify possible political problems.

It should be recognized, however, that joint implementation will represent only a portion of industry's ongoing joint and cooperative ventures. Investments bring technologies which address basic environmental priorities of water, air, and waste, contributing to the objective of the Climate Change Convention.

A role for business

At the August 1994 session of the Intergovernmental Negotiating Committee (INC), a number of governments called for greater industry participation in the Convention process. This reflects a recognition that industry is a critical player in the policy deliberations relating to climate change. Fortunately, consultations with business have been an integral part of most national policy processes.

The most appropriate and effective consultative mechanisms will function at the national level, since policy initiatives are the responsibility of national governments. However, if decisions by the Conference of the Parties (COP) suggest the need for industry consultation at the international level, industry will respond positively, and should clearly be part of the process for defining a mechanism for such consultation.

The world community faces great challenges in striving to maintain economic growth, social development, and environmental protection. Effective responses to these challenges will depend heavily on the decisions of policy-makers; the efforts and innovations of business; and not least the actions of consumers -- for we are living in a world of increasing demand for the services and products that industry provides.

Founded in 1919, the International Chamber of Commerce (ICC) is a non-governmental organization of thousands of companies and business associations in 137 countries. Sixty-four national committees world-wide present ICC views.

****

*Ratification Update: The Berlin COP**

	State	Date
1)	Mauritius	(4/9/92)
2)	Seychelles	(22/9/92)
3)	Marshall Islands	(8/10/92)
4)	United States	(15/10/92)
5)	Zimbabwe	(3/11/92)
6)	Maldives	(9/11/92)
7)	Monaco	(24/11/92)
8)	Canada	(4/12/92)
9)	Australia	(30/12/92)
10)	China	(5/1/93)
11)	Saint Kitts and Nevis	(7/1/93)
12)	Antigua and Barbuda	(2/2/93)
13)	Ecuador	(23/2/93)
14)	Fiji	(25/2/93)
15)	Mexico	(11/3/93)
16)	Papua New Guinea	(16/3/93)
17)	Vanuatu	(25/3/93)
18)	Cook Islands	(20/4/93)
19)	Guinea	(7/5/93)
20)	Armenia	(14/5/93)
21)	Japan	(28/5/93)
22)	Zambia	(28/5/93)
23)	Peru	(7/6/93)
24)	Algeria	(9/6/93)
25)	Saint Lucia	(14/6/93)
26)	Iceland	(16/6/93)
27)	Uzbekistan**	(20/6/93)
28)	Dominica**	(21/6/93)
29)	Sweden	(23/6/93)
30)	Norway	(9/7/93)
31)	Tunisia	(15/7/93)
32)	Burkina Faso	(2/9/93)
33)	Uganda	(8/9/93)
34)	New Zealand	(16/9/93)
35)	Mongolia	(30/9/93)
36)	Czech Republic	(7/10/93)
37)	Tuvalu	(26/10/93)
38)	India	(1/11/93)
39)	Nauru	(11/11/93)
40)	Jordan	(12/11/93)

41)	Micronesia	(18/11/93)
42)	Sudan	(19/11/93)
43)	Sri Lanka	(23/11/93)
44)	United Kingdom	(8/12/93)
45)	Germany	(9/12/93)
46)	Switzerland	(10/12/93)
47)	Republic of Korea	(14/12/93)
48)	Netherlands	(20/12/93)
49)	Denmark	(21/12/93)
50)	Portugal	(21/12/93)
51)	Spain	(21/12/93)
52)	E.U. (formerly E.E.C)	(21/12/93)
53)	Cuba	(5/1/94)
54)	Mauritania	(20/1/94)
55)	Botswana	(27/1/94)
56)	Hungary	(24/2/94)
57)	Paraguay	(24/2/94)
58)	Austria	(28/2/94)
59)	Brazil	(28/2/94)
60)	Argentina	(11/3/94)
61)	Malta	(17/3/94)
62)	Barbados	(23/3/94)
63)	France	(25/3/94)
64)	Bahamas	(29/3/94)
65)	Ethiopia	(5/4/94)
66)	Italy	(15/4/94)
67)	Bangladesh	(15/4/94)
68)	Ireland	(20/4/94)
69)	Malawi	(21/4/94)
70)	Nepal	(2/5/94)
71)	Finland	(3/5/94)
72)	Luxembourg	(9/5/94)
73)	Pakistan	(1/6/94)
74)	Chad	(7/6/94)
75)	Romania	(8/6/94)
76)	Gambia	(10/6/94)
77)	Liechtenstein	(22/6/94)
78)	Trinidad and Tobago	(24/6/94)
79)	Benin	(30/6/94)
80)	Malaysia	(13/7/94)
81)	Estonia	(27/7/94)
82)	Poland	(28/7/94)
83)	Georgia**	(29/7/94)
84)	Philippines	(2/8/94)
85)	Greece	(04/8/94)
86)	Grenada	(11/8/94)
87)	Uruguay	(18/8/94)
88)	Indonesia	(23/8/94)
89)	Slovakia	(25/8/94)
90)	Costa Rica	(26/8/94)
91)	Nigeria	(29/8/94)
92)	Guyana	(29/8/94)
93)	Kenya	(30/8/94)
94)	Bolivia	(3/10/94)
95)	Albania**	(3/10/94)
96)	Senegal	(17/10/94)
97)	Cameroon	(19/10/94)
98)	San Marino	(28/10/94)
99)	Belize	(31/10/94)
100)	Comoros	(31/10/94)
101)	Viet Nam	(16/11/94)
102)	Myanmar	(25/11/94)
103)	Cote d'Ivoire	(29/11/94)
104)	Samoa	(29/11/94)
105)	D.P.R. of Korea	(05/12/94)
106)	Egypt	(05/12/94)
107)	Lebanon	(15/12/94)
108)	Chile	(22/12/94)
109)	Bahrain	(28/12/94)
110)	Kuwait**	(28/12/94)
111)	Mali	(28/12/94)
112)	Russian Federation	(28/12/94)
113)	Saudi Arabia**	(28/12/94)
114)	Solomon Islands	(28/12/94)
115)	Thailand	(28/12/94)
116)	Venezuela	(28/12/94)
117)	Lao People's D.R.**	(4/1/95)
118)	Jamaica	(6/1/95)

* To become a Party in time for the opening of the Berlin Conference, countries had to ratify the Convention by 28 December 1994. Two countries will become Parties during the meeting and thus able to vote in the final days.)

** Accession

News and Announcements

This section is intended for dissemination of news and announcements by the Society or any of its members. If members wish to relay any news or make any announcement of interest to members which is related to the aims of the Society they should mail or fax such information to the Editor-in-chief along with their name(s) and membership number(s).

RECORD LOW OZONE LEVELS OVER NORTHERN HEMISPHERE - WHAT'S GOING ON?

Hugh Easton posted the following article to newsgroup sci.geo.meteorology *on Tue, 3 Jan 1995*

According to the United Nation's 1994 Scientific Assessment of Ozone Depletion, tropospheric levels of manmade ozone depleting gases (CFCs and other compounds containing chlorine/bromine) were expected to peak in late 1994. Peak stratospheric levels are expected to lag behind by 3-5 years, reaching their maximum around 1998. Although CFC levels have only now reached their peak the rate of increase slowed greatly in 1989, and the annual percentage increase has been fairly minimal since then.

Although unusually low ozone levels during the Antarctic spring can be seen in data going back as far as the late seventies, the worst ozone losses by far have taken place since this decade began. A less well known fact is that since 1990 substantial ozone losses have been taking place outside the Antarctic ozone hole as well. Prior to 1990, these mid-latitude ozone losses were always under 5 percent. In the winter-spring months of 1990-1991, ozone losses of up to 8 percent were measured over Europe and North America. The following year losses as high as 12 percent were measured. The worst losses occurred in 1992-3, when losses of up to 17 percent were measured.

These extraordinary rates of ozone depletion for 1991-3 have so far been attributed to dust and sulphate aerosol injected into the stratosphere by the Mt. Pinatubo eruption in June 1991. It is thought that the presence of volcanic debris provided a surface for ozone-destroying chemical reactions to take place on, thereby increasing the rate of CFC-induced ozone destruction.

Volcanic debris has a lifetime of about 3 years in the stratosphere, suggesting that the amplified ozone destruction should have largely ended by 1994. In fact, ozone losses in the Northern hemisphere for the winter-spring of 1994 were around 10 percent, a substantial improvement on the previous two years. This year the losses should be similar or perhaps even lower as the last traces of volcanic debris fall out of the stratosphere.

It is not difficult to estimate roughly what percentage ozone losses should be taking place in the absence of volcanic debris. Prior to 1990 the ozone losses were always less than 5 percent, and the CFC level measured now is only about 10 percent higher than it was in 1990. However the stratospheric CFC level is thought to lag the tropospheric CFC level by 3-5 years, and CFCs were increasing rapidly prior to 1989. It is therefore possible that stratospheric CFCs have increased by substantially more than 10 percent since 1990, perhaps even as much as 20 percent.

Applying a 20 percent increase to the 1990 ozone losses of 5 percent gives a figure of 6 percent. So the winter/spring ozone levels being measured now should be somewhere between the 10 percent measured last year and the 6 percent to be expected when the last remnants of aerosol from Mt. Pinatubo have settled out of the stratosphere. Barring any further major volcanic eruptions,

there is no chance of us again experiencing ozone depletion comparable to that measured between 1991 and 1993 which makes a recent news item in *New Scientist* difficult to understand.

"Levels of ozone hit record lows last month in parts of North America, and even lower levels in Europe. However, the lows, 214 Dobson units at a ground station in North America and 205 at one in Europe, are not dramatically below previous records.

"*We're going through a trend of decreasing ozone, and must be expected to break records periodically*", says Joe Farman, the British scientist who found the hole in the ozone layer over Antarctica, where ozone can drop to about 100 Dobson units. Background ozone in the northern hemisphere has dropped by 15 per cent over the past two decades.

Forrest Mims, an independent researcher, measured 214 Dobson units in Seguin, Texas in mid-November. Bill Barnard, who monitors ultraviolet radiation for the US Environmental Protection agency, says his network recorded 215 Dobson units in Georgia." - **Ozone Lowest Yet**, *New Scientist* 3 December, 1994 *p* 12.

These really are exceptionally low ozone levels. Compare them with some figures from Robert Parson's ozone depletion FAQ on the Internet:

> The ozone layer is thinnest in the tropics, about 260 DU, almost independent of season. Away from the tropics seasonal variations become important, but in no case (outside the Antarctic ozone hole) does the layer become appreciably thinner than in the tropics. For example:

Location	Column thickness, Dobson Units			
	Jan	Apr	Jul	Oct
Huancayo, Peru (12°S)	255	255	260	260
Aspendale, Australia (38°S)	300	280	335	360
Arosa, Switzerland (47°N)	335	375	320	280
St. Petersburg, Russia (60°N)	360	425	345	300

(*further on*)

> Recent NOAA measurements (Elkins *et al.*) show that the *rate of increase* of halocarbon concentrations in the atmosphere has decreased markedly since 1987, by a factor of 4 for CFC-11 and a factor of 2 for CFC-12. It appears that the Protocols are being observed. Under these conditions total stratospheric chlorine is predicted to peak at 3.8 ppbv in the year 1998, 0.2 ppbv above current levels, and to slowly decline thereafter (WMO 1994). Extrapolation of current trends suggests that the maximum ozone losses will be (WMO 1994):
>
> Northern Mid-latitudes in winter/spring:
> 12-13% below late 1960's levels,
> ~2.5% below current levels.
>
> Northern mid-latitudes in summer/fall:
> 6-7% below late 1960's levels,
> ~1.5% below current levels.
>
> Southern mid-latitudes, year-round:
> ~ 11% below late 1960's levels,
> ~2.5% below current levels.

Assuming that ozone levels are typically around 280-300 DU in late autumn for mid to high latitudes in the Northern Hemisphere, the "*record low ozone levels*" reported in New Scientist represent a depletion of around 25 percent. This is far worse than any of the figures quoted above for maximum ozone losses (which are not, in any case, expected until 1998). These latest results provide support for a theory I have been promoting since early last year: that ozone losses are linked to tropical sea surface temperatures, and that the very large losses reported in recent years are at least in part due to a continuing warming trend in tropical oceans.

"Conventional wisdom blames chlorine compounds and other chemicals that destroy ozone. But Walter Komhyr and his colleagues at NOAA in Boulder, Colorado, say that sea surface temperatures in the eastern equatorial Pacific ocean may affect levels of ozone over the Antarctic and elsewhere. The researchers studied sea surface temperatures in the eastern Pacific for 25 years. They found that the eastern equatorial Pacific cooled between 1962 and 1975 and, during that time, global ozone increased. When these waters warmed, between 1976 and 1988, global ozone decreased. Another factor was a sudden drop in the region's sea surface temperature in June 1988. The following October, after several years of decreasing ozone over Antarctica, ozone levels stayed comparatively high. In fact, Komhyr has observed the correlation of cold sea surface temperatures from June through August followed by high levels of ozone in the Antarctic spring in 21 of the 27 years between 1962 and 1989." - **Ozone Hole Linked to Sea Temperatures**, *New Scientist*, 13 July 1991, *p* 22.

Komhyr and his team found a strong correlation between low sea surface temperatures and small ozone losses in the years prior to 1990; events since then suggest that there is also a link between high SST's and unusually large ozone losses. The warming and cooling of the eastern equatorial Pacific is strongly associated with the waxing and waning of El Nino - indeed, one of the criteria for determining what constitutes an ENSO event is the temperature in the eastern Pacific. Since 1990, ozone losses have closely followed the pattern of ENSO events. 1990 (not an ENSO year) was also the last year of near-normal ozone levels over the northern hemisphere. ENSO conditions persisted from 1991 to 1993, and during this time ozone losses over the northern hemisphere steadily worsened. Meanwhile, the ozone hole over Antarctica grew steadily deeper, although CFC levels by this time were showing very little increase. On 6 October 1993, an ozone level of only 88 Dobson units was measured at the South Pole - the lowest level of total column ozone ever measured on Earth.

For the first few months of 1994 it looked as though the ENSO had ended: the trade winds and associated upwelling of cold, deep water off the coast of Peru, and SSTs had all returned to something close to normal. Ozone levels over Europe and North America made a dramatic recovery, returning to levels similar to those measured in 1991. Then something occurred which is completely without precedent - the trade winds slackened, the cold water upwelling ceased and SSTs began to increase once more. By September the forecasts saying that El Nino had ended were revised. Over Antarctica, the ozone hole showed no signs of the recovery that northern hemisphere ozone levels had earlier in the year; apparently it was similar in size and depth to that of 1993. Now, as ENSO conditions intensify, we have reports of record low levels of ozone measured over Europe and North America, when no more records should be broken.

According to the December advisory, ENSO conditions look set to persist for at least the next six months *i.e.*. through spring and well into the northern hemisphere's summer. If the link between ENSO and ozone depletion is real then ozone levels this year will fall as low or even lower than they did in 1993, so take care in the sun this summer!

in response to the above Marc Allaart of KNMI The Netherlands posted the following reply on Mon, 9 Jan 1995

The values quoted in the table are monthly average values. Day to day changes are quite big in the mid-latitudes, and they are closely related to the weather. Here are for example the daily average (Brewer) total ozone values for De Bilt (52.10 N, 5.18 E) from 12 to 18 November 1994: 239 222 208 248 274 273 235 Dobson Units.

208 is the lowest value for 1994. The previous low record was probably 210 DU at 2 December 1992 (we did not have our Brewer at that time....) So I agree with the conclusion "*not dramatically below previous records.*" (The difference of two Dobson Units is well below the typical error in these measurements.)

The problem is that in mid November the stratospheric temperatures are not low enough to have fast ozone destruction. It is more likely that a very strong transport of sub-tropical air to more northern latitudes played an important role. November 1994 was the hottest on record in Holland, with an average temperature of 10.2°C compared to 5.9°C normally.

A total ozone map for 14 November 1994 compiled from the NOAA-12 TOVS measurements is available as:
http://infosrv.knmi.nl/allaart/low.ozone.gif

HISTORICAL SOVIET DAILY SNOW DEPTH CD-ROM

The U.S. National Snow and Ice Data Center (NSIDC) announces the Historical Soviet Daily Snow Depth CD-ROM. Production of this CD-ROM was funded by the NOAA Earth Science Data and Information (ESDIM) Initiative through the National Geophysical Data Center (NGDC).

Historical Soviet Daily Snow Depth is based on observations at a series of 284 World Meteorological Organization (WMO) stations throughout the Former Soviet Union. The earliest operational stations began recording snow depth in 1881 and the data continues until 1985. Geographic distribution of stations is primarily in the mid latitudes of Eurasia and correspond to inhabited areas. Stations range from 35 to 75 degrees north latitude and from 20 to 180 degrees west longitude. Stations range in altitude from -15 meters to 2100 meters.

Daily data, as well as NSIDC-generated monthly means, are available on a single CD-ROM containing ASCII data files, extraction software, and data documentation. The source of the data used is the State Hydrometeorological Service in

Obninsk, Russia. Data were provided to NSIDC via the Bilateral US-USSR WG-8 Exchange.

The cost of the CD-ROM is US$ 50.

For further information please contact NSIDC User Services at:

Internet: nsidc@kryos.colorado.edu.
Telephone: (303) 492-6199

Mailing address:
National Snow and Ice Data Center
Cooperative Institute for Research in Environmental Sciences (CIRES)
Campus Box 449, University of Colorado
Boulder, Colorado 80309-0449, USA

NEW ADDITIONS TO NSSL WWW HOMEPAGE

from: Harold Brooks, National Severe Storms Laboratory (10 Jan 1995)

Several new additions of possible interest have been made to the NSSL WWW page (http://www.nssl.uoknor.edu) have been made over the past month to which I'd like to call your attention.

1. A page on the future of operational forecasting (http://www.nssl.uoknor.edu/special/future/), concentrating on the role of humans and the use of numerical weather prediction systems.

2. A conceptual model of the supercell thunderstorm spectrum, written by Erik Rasmussen of NSSL/CIMMS, in collaboration with Jerry Straka of the University of Oklahoma. The link for it is:
http://www.nssl.uoknor.edu/personal/Rasmussen/Trilogy.html

3. An animation of mesoscale model output from a simulation of the 21-22 November 1992 southeastern US severe weather outbreak illustrates an approach to using mesoscale and cloud-scale models in operational forecasting. The animation is at:
http://www.nssl.uoknor.edu/images/stensrud.mpg

As always, general information on the laboratory and the work of its scientists (including electronic versions of some publications) can be accessed from the NSSL home page. We welcome your responses on any of the items included there.

METEOR-3 TOMS (GLOBAL OZONE MAPPER) FAILS

from: U.S. National Center for Atmospheric Research, Chemistry Division, Boulder, Colorado (24 Jan 1995)

TOMS = Total Ozone Mapping Spectrometer

TOMS instruments have been mapping global total column ozone on a regular basis for many years. The venerable TOMS on Nimbus-7, launched in 1978, failed in early 1993, leaving the instrument on the Russian Meteor-3 spacecraft, launched in August of 1991, to carry on the work.

The Meteor-3 TOMS has suffered from intermittent problems with its chopper motor, a key component of the instrument, for some time. According to the TOMS group at NASA/GSFC, the instrument finally succumbed to this problem altogether and ceased operating on December 27, 1994. Recovery efforts through 20 January 1995 have been unsuccessful despite excellent cooperation reported between the TOMS team and Russian controllers. A final recovery effort may be made in April when the instrument will be at its maximum temperature. No operating TOMS is therefore currently on orbit. Global ozone mapping is still possible, however, using SBUV/2 and UARS, among others.

A new TOMS instrument is scheduled for launch on an Earth-Probe mission in April of this year, and would be expected to be producing ozone data by June. A further TOMS will be installed on the Japanese ADEOS spacecraft due to be launched in early 1996.

EL NINO FALSE ALARM?

The following press release from NASA highlights the dangers of trying to second guess El Nino!

TOPEX Confirms El Nino is Back and Stronger Than in 1993

RELEASE: 95-7 January 24, 1995

The El Nino phenomenon is back and is getting stronger, according to scientists studying data from the ocean-observing TOPEX/POSEIDON satellite. El Nino is a climatic event that can bring devastating weather to several parts of the

world, including the recent heavy rains and flooding in California, and the warmer than normal winter in the eastern United States.

"*The satellite has observed high sea-surface elevation, which reflects an excessive amount of unusually warm water in the upper ocean,*" said Dr. Lee-Leung Fu, JPL TOPEX/POSEIDON project scientist at NASA's Jet Propulsion Laboratory, Pasadena, CA. "*The associated excess of heat creates high sea-surface temperatures, which affect the weather world-wide by heating the atmosphere and altering the atmospheric jet streams.*"

Jet streams are high-level winds, five to ten miles above the Earth's surface, created when warm and cold air masses meet. Shifts in the location of jet streams change temperatures and precipitation zones at the surface.

El Nino begins when the westward trade winds weaken and a large warm water mass, called a Kelvin wave, is allowed to move eastward along the equator in the Pacific Ocean. Data from the radar altimeter onboard TOPEX/POSEIDON, recorded from October through December 1994, reveal a new Kelvin wave moving toward the western coast of South America.

"*This wave is currently occupying most of the tropical Pacific Ocean. It will take another month or two before the wave disperses. Compared to the El Nino condition of the winter of 1992-93, the present one appears somewhat stronger and might have stronger and longer lasting effects,*" Fu said.

TOPEX/POSEIDON, a joint program of NASA and the Centre Nationale d'Etudes Spatiales, the French space agency, uses a radar altimeter to precisely measure sea-surface height. Scientists use the TOPEX/POSEIDON data to produce global maps of ocean circulation. Launched Aug. 10, 1992, the satellite has completed two and a half years of its three-year prime mission and has provided oceanographers with unprecedented global sea level measurements that are accurate to better than 2 inches (5 centimeters).

"*The global sea-surface elevation information provided by TOPEX/POSEIDON is unique because it is related to the amount of heat stored in the upper ocean, which is important for long-range weather forecasting. The speed and direction of ocean currents also can be determined from the elevation information, providing another piece of critical information about the ocean, which is the key to climate change,*" Fu continued.

TOPEX/POSEIDON is part of NASA's Mission to Planet Earth, a coordinated, long-term research program to study the Earth's global environment. TOPEX/POSEIDON's sea-surface height data are essential to understanding the role oceans play in regulating global climate, one of the least understood areas of climate research. TOPEX/POSEIDON will provide the first comprehensive, consistent measurements of the circulations of the ocean.

The Jet Propulsion Laboratory manages the TOPEX/POSEIDON mission for NASA.

GOES-8 REALTIME IMAGES AVAILABLE

from: Chad Johnson and Tom Whittaker, Space Science and Engineering Center, University of Wisconsin (13 Feb. 1995)

The Space Science and Engineering Center at the University of Wisconsin, Madison, in cooperation with NOAA/NESDIS, is pleased to announce the availability of real-time, gridded GOES-8 imagery over North America in gif format.

We will be uploading the images every half hour unless our network loading is too stressed, in which case we'll back off to once per hour.

The URLs are:
gopher://gopher.ssec.wisc.edu/
gsdc.d/realtime-8.d/
ftp://ftp.ssec.wisc.edu/gopher/
gsdc.d/realtime-8.d/

The filenames are:
G8VIS.GIF for the visible data
G8IR.GIF for the infrared (IR2 - window)
G8WV.GIF for the water vapor channel

The image resolution is nominally 4km; the image sizes are 900 x 1024. The data from h+15 to h+45 are used, and are normally available on line ten minutes later. After the satellite has reached its fixed longitude, we may shift the image a little eastward to avoid viewing too much space.

In addition, we are providing a once-per-day globe visible and IR from GOES-8.

The URLS are:

gopher://gopher.ssec.wisc.edu/
gsdc.d/browse-8.d/

ftp://ftp.ssec.wisc.edu/gopher/
gsdc.d/browse-8.d/

The filenames are:
G8VISHEM.GIF for the visible data
G8IRHEM.GIF for infrared (IR2 - window)

The image resolution is nominally 32km; the image sizes are about 452 x 480. The data from 1745 are used, and the images are normally posted by 1820Z each day.

NOAA/NASA AVHRR OCEANS PATHFINDER DATA PROCESSING UPDATE

from: Sue Digby, Jet Propulsion Laboratory, Pasadena, CA (27 Mar. 1995)

The following is an update on processing and production of NOAA/NASA AVHRR Oceans Pathfinder Sea Surface Temperature Data Set Products.

PRODUCT OVERVIEW

This data consists of global sea surface temperature (SST) from January 1981-present as derived from the five-channel AVHRR instruments onboard the NOAA 7/9/11 polar orbiting satellites. The SST fields form a high quality data set suitable for global change studies. This data product is improved over previously available satellite derived SST data sets in that the data has been produced using improved data processing including incorporation of new cloud detection algorithms applied at the University of Miami, inter calibration among the satellites, and quality analysis procedures implemented through the AVHRR Pathfinder Ocean group at the Jet Propulsion Laboratory. In addition the data are more complete because they are derived from the original AVHRR data rather than from a subset as provided by NOAA for operational purposes.

SUBSETTING

We (actually Andy Tran) have developed a subsetting capability for Pathfinder data that is accessible via the homepage through
http://sst-www.jpl.nasa.gov.
Mosaic should be used as the Web browser. The subsetting routine only pertains to best SST data from '87 - '90.

Through an order form format a user specified temporal and spatial subset can be obtained. The order automatically spawns a subsetting routine at JPL and the subset is produced and staged for pick-up via ftp. The requester is notified of the completion of the subset and is given the file name(s) and their location via an e-mail message.

UPDATE

Three product lines are now available:

Product 51:

Title: AVHRR Oceans Pathfinder global equal-angle best SST (NOAA, NASA) Years: '87 - '90 (*see below for missing files*)

Extent: Daily data at 9 and 18 km resolution; 54km resolution available as product 53.

Data format: HDF and raw binary. Available on tape or via ftp from (podaac.jpl.nasa.gov) Subsets can be obtained via Mosaic (http://sst-www.jpl.nasa.gov)

Product 50:

Title: AVHRR Oceans Pathfinder global equal-angle all SST (NOAA, NASA) Years: '87 - '90 (*see below for missing files*)

Extent: Daily data at 9 and 18 km resolution; 54km resolution available as product 53.

Data format: HDF Available on tape only

Product 53:

Title: AVHRR Oceans Pathfinder 0.5-degree spatial resolution global SST (NOAA, NASA) Years: '87 - '90 (*see below for missing files*)

Extent: Daily data at 54 km resolution.

Data format: HDF

Data: both best SST and All Pixel available

Available: Best pixel and all pixel available via ftp and on tape.

Best SST data can be accessed as subsets via Mosaic (http://sst-www.jpl.nasa.gov)

NEWLY PROCESSED DATA VIA FTP

Newly processed data (1991) can be accessed via ftp or Mosaic.

FTP site: sst-www.jpl.nasa.gov
WWW URL : http://sst-www.jpl.nasa.gov

'87 - '90 DATA VIA FTP

Data that used to reside on the ftp site sst-www.jpl.nasa.gov has been moved to the main PO.DAAC site;

FTP site: podaac.jpl.nasa.gov

QUALITY REPORTS

For each daily file there is a quality report, it is recommended that you consider reading these first to determine the value of the data to you prior to taking the time to download the large data files. Please refer any questions that you have about the quality reports to Mike Hamilton (mkh@pacific.jpl.nasa.gov)

MISSING FILES

Missing files for years 1987 - 1990

Years: 1987 - (days 001-365) complete
1988 - (days 001-366)
Missing day: 88314 ascending and descending; no data due to change of satellites NOAA-9 to NOAA-11
1989 - (days 001-364) complete
1990 - (days 001-364)
Missing days: 90027 ascending
90125 descending
90132 descending
90139 descending
90146 descending
90153 descending
90160 descending
90161 ascending
90162 ascending
90178 ascending
90186 ascending
90336-90364 asc & desc
1991 - Currently processing.

New data will be made available via FTP or WWW site.

Note: Missing days are currently being reprocessed. They will be made available via the FTP site or the WWW site:
sst-www.jpl.nasa.gov.

JPL INSTRUMENT WILL MEASURE EARTH'S ATMOSPHERIC TEMPERATURE

PUBLIC INFORMATION OFFICE
JET PROPULSION LABORATORY
CALIFORNIA INSTITUTE OF TECHNOLOGY
NASA, PASADENA, CA. 91109.

Contact: Mary A. Hardin

FOR IMMEDIATE RELEASE *April 3, 1995*

An experimental instrument, launched today from Vandenberg Air Force Base in Lompoc, Calif., could alter the way scientists monitor global atmospheric temperatures and climate change by using the worldwide array of Global Positioning System satellites.

The Global Positioning System Meteorology instrument -- or GPS Met -- was launched aboard an Orbital Sciences Corporation Microlab satellite on a Pegasus launch vehicle. The instrument, developed by the Jet Propulsion Laboratory, was successfully placed into orbit at 6:48 a.m. Pacific Daylight Time.

From its vantage point in low-Earth orbit, GPS Met will receive and track the radio signals broadcast by 24 high-orbiting satellites of the U.S. military's GPS network. Just before each GPS satellite passes out of view of the Earth, its signal, as seen by GPS Met, will slice through the atmosphere from the top of the stratosphere down to the Earth's surface. This process is known as atmospheric occultation or radio occultation.

"*As the signal descends, the atmosphere acts as a lens, causing the signal's path to bend and its travel time to increase by a small, but perceptible amount*," said JPL engineer Dr. Thomas Yunck, one of a team of experts who proposed the GPS technique in the late 1980s. "*By precisely measuring the signal's increasing travel time and the fluctuating signal strength, we can recover highly accurate profiles of atmospheric density, pressure, temperature and, to some degree, turbulence and winds*."

"*The most obvious scientific application of this technique will be monitoring changes in climate by providing precise, stable and high-resolution profiles of atmospheric temperatures across the globe*," added Rob Kursinski, a JPL scientist on the GPS Met team. "*The GPS Met data represent the first, hopefully, in a long-term observation*

program, which will provide us with much needed, long-term information about how trace greenhouse gases may be modifying Earth's atmosphere and climate".

GPS Met will also be used to study the amount of water vapor in the lower atmosphere, the JPL science team said.

"*Water vapor is extremely important to Earth's weather and climate system*," Kursinski explained. "*It is crucial to the operation of the Earth's atmospheric heat engine, which redistributes absorbed solar energy to higher latitudes. Water vapor is also the primary greenhouse gas in our atmosphere.*"

Using the technique of radio occultation to explore planetary atmospheres dates back to 1965, when scientists studied the signal sent back by Mariner 4 as it passed behind Mars. In the years since, this technique has been used to study other planets in the solar system and their moons.

"*Studying Earth with this technique has been difficult because the observations require both a radio source and a suitable receiver located off the planet, outside the atmosphere*," Yunck said. "*Until now, we have not had such matched pairs in Earth orbit. Additionally, to be of use in studying Earth's atmosphere, whose nature we know quite well, such measurements must be continuous and comprehensive*," he said. "*We therefore need many transmitters and receivers aloft at once, densely sampling the global atmosphere every few hours. The cost of such an enterprise has generally made it impractical within Earth science programs.*

The advent of microsatellites and small launcher technologies is changing all of that. GPS Met is the first "proof-of-concept" *demonstration of the GPS occultation technique. If successful, it could lead to a future constellation of tiny microsatellites, each no larger than a small paperback book and weighing less than 2 kilograms (4.4 pounds), that would continuously survey the global atmosphere with unprecedented accuracy and spatial resolution*," Yunck said.

"*The GPS observations from a constellation of tens or hundreds of receivers in low-Earth orbit may have a dramatic impact on weather forecasting because they would provide a number of unique and fundamental features which would complement the present suite of worldwide weather monitoring measurements*," Kursinski explained.

Another important application of the GPS Met technology will be its ability to map the ionosphere -- the area of the upper atmosphere consisting of free electrons. Low frequency radio waves broadcast from Earth interact strongly with the ionosphere. This interaction allows the radio signals to be sent great distances as they are reflected off the ionosphere. Ionospheric disturbances have been known to cause violent solar flares, for example, which can disrupt radio communications worldwide.

"*With a large array of orbiting GPS receivers, it will be possible to create three-dimensional images of the ionosphere that will help scientists map its structure and could give them a near real-time picture of the ionosphere's often erratic behavior*," Yunck said.

The GPS Met experiment is sponsored jointly by NASA's Office of Mission to Planet Earth, the National Science Foundation, the National Oceanographic and Atmospheric Administration and the Federal Aviation Administration.

The instrument was developed by NASA's Jet Propulsion Laboratory and is being managed by the University Corp. for Atmospheric Research in Boulder, Colo.

ROYAL METEOROLOGICAL SOCIETY ON WORLDWIDE WEB

The Royal Meteorological Society is pleased to announce the existence of its World Wide Web pages. These can be accessed by connecting to:

http://typhoon.rdg.ac.uk/rms/rms.html

Information contained in these pages includes details of Society meetings and other activities Specialist Groups and Local (Regional) Centres Journals, including titles of papers for 1994 and 1995 published in:

Quarterly Journal
International Journal of Meteorology
Meteorological Applications
Weather

together with general information about the Society (including how to join), the Society's Chartered Meteorologist scheme, policy statements, useful email addresses, and pointers to other national servers across the globe.

The Society is grateful to the help and support provided by the Department of Meteorology,

University of Reading in the running of this server.

Comments and suggestions may be sent to the maintainer:

(Roger Brugge,: brugge@met.rdg.ac.uk).

DOES CLOUD COVER AFFECT TEMPERATURES?

Fri, 28 Apr 1995

Scientists trying to take the world's rising temperature have discovered a data dilemma: It is warming more at night in some places and more in the daytime elsewhere.

American researchers reported last year that nighttime temperatures in much of the world were rising three times faster than daytime readings. But there have been conflicting studies. And some wonder whether divergent cloud-cover patterns mostly account for the phenomenon.

Researchers in fact have found, unmistakably, a general increase in the Earth's temperature in recent years. But they generally agree that it's too soon to declare a trend because the amount of temperature change is small enough to be considered part of normal climate variation.

Meteorologists in India have found daytime temperatures going up faster than those at night in some areas. Researchers in Switzerland found that day and night readings were up by about the same amount for mountain communities, though the valleys warmed more at night than in the daytime. And a Washington climate conference last fall heard reports that no significant nighttime warming has occurred in polar regions, while some Pacific Islands have experienced equal day and night increases.

In general, studies of global temperatures suggest that nighttime minimum readings are rising faster than daytime maxima. But that doesn't imply everyone is in the same category.

"*There are important reasons for differences from one place to another and many seem to be related to changes in cloud cover*," said Thomas Karl of the U.S. National Climatic Data Center in Asheville, N.C.

The findings are part of research into the threat of global warming. Scientists have voiced concern in recent years that chemicals released into the atmosphere by industry will turn the Earth into a sort of giant greenhouse, raising temperatures everywhere. Indeed, scientists gathered in Berlin in April considered the possibility that there may even be a threat of global cooling developing -- at least in industrialized nations where cloud cover is increased by pollutants.

The British magazine *New Scientist* reports that an unpublished study by Guy Brasseur and Mai Pham of the U.S. National Center for Atmospheric Research found that cooling is exceeding warming over Europe, the eastern United States and parts of Russia, China and the Far East. "*Increased cloudiness may be the reason that some areas have experienced more warming at night than in the daytime*," Karl wrote in a recent paper in the *Bulletin of the American Meteorological Society.*

Warmer temperatures can cause more water to evaporate, leading to more clouds. Clouds can act as a blanket to prevent nighttime radiation cooling. They may also shade the Earth from the sun, cooling the daytimes.

"*One of the problems is, we tend to say: 'What's the single cause of this?' In truth there very rarely is a single cause,*'" Karl said.

If warming is concentrated at night, some researchers see possible benefits, such as a longer growing season and fewer killing frosts. And they say water evaporation, a threat in a warmer world, would be less likely if higher temperatures occurred at night. On the other hand, nighttime warming might encourage crop pests. Also, there could be a shorter dormancy period, adversely affecting plant growth. And people might suffer more from heat waves with less nighttime cooling.

James Hansen of the National Aeronautics and Space Administration's Goddard Institute for Space Studies, a pioneer in global warming research, cautioned against accepting claims that global warming is a "*benign*" nighttime trend. "*In the long run global warming will continue despite increased cloudiness or other factors that appear to be reducing its effect*", he predicted in a paper presented to associates last year.

The uneven warming trend was first detailed by Karl and a team including George Kukla of Columbia University and Philip D. Jones of England's University of East Anglia. They reported that between 1951 and 1990, average nighttime lows increased by 1.5 degrees Fahrenheit, while average daytime highs rose 0.5 degrees. In other words, nighttime warmed up more than daytime. They studied the United

States, Canada, the former Soviet Union, China, Japan, eastern Australia, Sudan and South Africa.

However, at 121 weather stations in India, average nighttime lows were unchanged between 1901 and 1987, while daytime highs rose about 1 degree, according to a report in the journal *Geophysical Research Letters* by meteorologists at the Indian Institute of Tropical Meteorology in Pune.

Kukla said that, too, is related to cloud cover. "*While clouds at middle and high latitudes lead to cooling in the daytime, it's a different situation close to the equator. We, by no means were claiming that changes are uniform all over the world, no way*," Kulka said.

A separate study of the period 1951-87, done for comparison with Karl's report, could detect no overall temperature trend in India, researchers K. Rupta Kumar, K. Krishna Kumar and G. B. Pant reported in *Geophysical Research Letters*. They didn't try to explain why Indian findings differ from studies of other areas.

"*No one has done an analysis of cloud changes in India since about 1960, it would be very interesting to look at what's happening to clouds there*", said Karl. "*Cloud cover there might have decreased ... From 1960 to 1990 precipitation is less, and normally when you find precipitation going down you find cloudiness going down as well*," he commented.

The geophysical journal also carried a report from the Paul Scherrer Institute in Villigen, Switzerland, that had mixed results. That study of several Swiss, German and Austrian weather stations from 1901 to 1990 was similar to Karl's findings for valley locations, but up on the mountains, daytime highs and nighttime lows both rose more than 1 degree. The reason for this may be low-level clouds that keep the valleys warm at night, while the mountains poke through the layer and experience equal day and night changes, suggested researchers Rudolf O. Webber, Peter Talkner and Gerard Stefanicki. But Karl said that similar studies of mountain stations in the Pyrenees failed to confirm the Swiss results.

WILL GLOBAL WARMING AFFECT THE TROPICS?

Hugh Easton posted the following article to newsgroup sci.geo.meteorology *on Wed, 17 May 1995*

Until very recently, climatologists thought that global warming will mainly affect polar regions, while the tropics will be largely unaffected. That perception is now changing, according to David Rind, a climate research scientist at NASA's Goddard Institute for Space Studies in New York. In "**Drying Out the Tropics**" (*New Scientist*, 6 May, 1995) he explains why.

Summarizing the first part of his article:

Most climate researchers were predicting that the tropics would escape almost all of the effects of global warming. There was fossil evidence, including the CLIMAP assessment published in 1981, which indicated that tropical ocean temperatures hardly changed even at the peak of the last ice age. There was also more limited evidence from around 3 million years ago that temperatures in equatorial regions were much the same as they are today, while the high latitudes were up to 10°C hotter than they are now. A method of modelling past CO_2 levels developed in the 1980s by Bob Berner of Yale University, suggested that atmospheric CO_2 levels were higher 3 million years ago. This would explain the warmer climate back then. There was even an explanation for the stability of tropical temperatures - a thermostat mechanism based on increased cloudiness, developed by V. Ramanathan and colleagues at NCAR.

He then goes on to make a rather surprising statement:

"*But while observational studies were coming up with reassurance for the tropics, computer models were telling a different story. In particular, the computer number-crunchers suggested that as the climate started to warm, the oceans would release more water vapour into all levels of the atmosphere. Rather than acting to thicken clouds and so reflect sunlight, this additional vapour would spread itself widely and act predominantly as a greenhouse gas. This would further accentuate the warming at all latitudes, including the tropics. When the level of carbon dioxide in the model atmosphere was doubled, numerical models of the climate showed a significant tropical warming - anything from 1°C to 4°C. Because these models were built on rather shaky foundations - no one could be sure of the precise mechanisms associated with water vapour transport and cloud generation, for example - many researchers assumed that they must be wrong. Those scientists already convinced by the observational data that the tropics would not warm, suspected that the models were flawed and were coming up with the wrong answer.*"

He then mentions the large temperature rise in the tropics in recent years, and summarizes some recent research which has overturned many of the earlier assumptions about a stable tropical climate. The article ends with a description of some of the possible consequences of a substantial tropical warming, such as droughts and more severe tropical storms.

I have in front of me the predictions from one model for a CO_2-doubled world (the book gives *IPCC Scientific Assessment*, Cambridge University Press, 1990 as the source). It shows almost no warming over tropical oceans and only slight warming over Africa and South America, while the largest temperature increases occur at high latitudes in the northern hemisphere.

A question: How did the climate models change from giving the "*wrong*" answer (a large amount of tropical warming) to giving the "*right*" answer (plenty of warming at mid and high latitudes and almost no tropical warming)? It seems as if you can make a climate model show more or less anything you like. A great way of "*proving*" that the currently fashionable theory is correct, but hardly a good way of accurately predicting what the future pattern of climate change will be.

In their 1990 assessment, the IPCC used climate models to predict a 1.5°C to 4.5°C global temperature rise when CO_2 levels have doubled. How much reliance can we place on those predictions if the models they are based on are now openly admitted to be wrong? Perhaps it might be time to pay a little more attention to the growing indications of climate change.

FORECAST OF ATLANTIC SEASONAL HURRICANE ACTIVITY FOR 1995

from: W.M. Gray, C.W. Landsea,
P.W. Mielke, Jr. and K.J. Berry,
Department of Atmospheric Sciences
and Department of Statistics,
Colorado State University
(7 June 1995)

Internet: landsea@downdry.atmos.colostate.edu

This forecast is based on ongoing research by the authors at Colorado State University, together with recent April-May 1995 meteorological information.

****

ABSTRACT

This paper presents details of the authors' forecast for the amount of tropical cyclone activity expected to occur in the Atlantic Ocean region including the Caribbean Sea and the Gulf of Mexico during 1995. This forecast is based on the authors' ongoing research relating the amount of seasonal Atlantic tropical cyclone activity to five basic physical parameters. These are:

1) the Quasi-Biennial Oscillation (QBO) of equatorial stratospheric winds;
2) the El Nino-Southern Oscillation (ENSO);
3) West African Rainfall (AR) anomalies during the previous year;
4) anomalous west to east gradients of surface pressure and surface temperature (Delta PT) in West Africa during February through May; *and*
5) Caribbean Basin Sea Level Pressure and Upper Level Zonal Wind Anomalies (SLPA and ZWA, respectively).

Information received by the authors up to 6 June 1995 indicates that the overall 1995 hurricane season should be an above average season with about 8 hurricanes (average is 5.7), 12 named storms (average is 9.3) of at least tropical storm intensity, a total of about 35 hurricane days (average is 23), 65 named storm days (average is 46) and total Hurricane Destruction Potential (HDP) of 110 (average is 68). It is also expected that there should be 3 intense or major hurricanes of Saffir/Simpson intensity category 3, 4 or 5 this season (average is 2.1) and about 6 major hurricane days (average is 4.5).

These parameters represent an overall measure of total hurricane and tropical cyclone activity which is about 140 percent of the last 45-year average. The amount of hurricane activity in this forecast has been increased somewhat from that in the first author's 30 November 1994 forecast and is above the 13 April 1995 assessment given at the Atlantic City National Hurricane Conference.

This early June enhancement of the hurricane forecast is due to the dissipation of the long running El Nino event and the observed return of cold water conditions in the equatorial East Pacific, to new estimates of African Western Sahel rainfall (+0.27 S.D.), and to warm eastern Atlantic sea surface temperature conditions which have become established the last two months. This is favorable for hurricane activity.

This forecast will again be updated on 4 August 1995, at the beginning of what is climatologically the most active part of the hurricane season. The updated August forecast will make use of June and July data and should provide a more reliable forecast, particularly with regard to the African rainfall as it relates to prospects for intense hurricane activity during the most active part of the season. The updated August forecast will also provide a much better gauge on the extent of expected development of a (cold water) La Nina event in the equatorial east Pacific.

INTRODUCTION

The Atlantic basin, including the Atlantic Ocean, Caribbean Sea and Gulf of Mexico, experiences more season-to-season variability of hurricane activity than any other global hurricane basin. The number of hurricanes per season in recent years has ranged as high as 12 (as in 1969), 11 (as in 1950) and 9 (as in 1980, 1955), and as low as 2 (as in 1982) and 3 (1994, 1987, 1983, 1972, 1962, 1957). Until recently there has been no objective method for determining whether a forthcoming hurricane season was likely to be active, inactive, or near normal. Recent and ongoing research by the author and colleagues indicates that there are surprisingly skillful 3 to 11 month (in advance) predictive signals for Atlantic basin seasonal hurricane activity.

FACTORS KNOWN TO BE ASSOCIATED WITH ATLANTIC SEASONAL HURRICANE VARIABILITY

This early June Atlantic seasonal hurricane forecast is based on the current values of indices derived from various global and regional scale predictive factors which the author and his colleagues have previously shown to be statistically related to seasonal variations of hurricane activity. Successive sets of values for these predictive factors are obtained by late November of the previous year, by early June of the concurrent year, the official start of the hurricane season and by early August (at the start of the most active portion of the hurricane season). These predictive factors include the following:

(a) The stratospheric Quasi-Biennial Oscillation (QBO) influence. The QBO refers to variable east-west oscillating stratospheric winds which circle the globe near the equator. On average, there is nearly twice as much intense Atlantic basin hurricane activity during seasons when equatorial stratospheric winds at 30 hPa and 50 hPa (23 and 20 km altitude, respectively) are more westerly as compared to when they are more easterly directed. During the 1995 season, these QBO winds will be from an westerly direction and are expected to be an enhancing influence for this season's hurricane activity.

(b) El Nino - Southern Oscillation (ENSO) influence: ENSO characterizes the presence of either warm or cold sea surface temperature anomalies in the eastern equatorial Pacific. The effects of a moderate or strong El Nino (warm water) event in the eastern equatorial Pacific act to reduce Atlantic basin hurricane activity. By contrast, seasons with cold sea surface temperatures, or La Nina years, have enhanced hurricane activity. These differences are related to alterations of upper tropospheric (200 hPa or 12 km) westerly winds over the Caribbean Basin and western Atlantic. These westerly winds are enhanced during El Nino seasons. This condition creates strong vertical wind shear over the Atlantic which inhibits hurricane activity. During La Nina (or cold) years, these westerly winds and the associated vertical wind shear are reduced and hurricane activity is typically greater. It is expected that the unusually long lasting 1991-94 El Nino has finally run its course and cold water conditions are settling in. This, in turn, should be a factor enhancing this year's Atlantic basin hurricane activity. New April-May data indicates that distinctly cold conditions are developing for this year.

(c) African Rainfall (AR) influence: The incidence of intense Atlantic hurricane activity is typically enhanced during those seasons when the Western Sahel and Gulf of Guinea regions of West Africa had above average late summer and fall precipitation during the previous year (in this case during the fall of 1994). Hurricane activity is typically suppressed if the prior fall rainfall in these two regions was below average. Rainfall amounts in the Western Sahel in August-September 1994 was +0.08 S.D.; Gulf of Guinea rainfall was +0.24 S.D. during August through November 1994. From these slightly wetter than average rainfall amounts we anticipate that Western Sahel rainfall will be slightly above normal in 1995 and distinctly above the very low rainfall which has occurred in the recent years of 1990-1993 and also greater than the drought years of the 1970s and 1980s. This Western Sahel rainfall forecast is based upon our early June forecast of rainfall.

(d) West Africa west-to-east surface pressure and surface temperature gradients (Delta PT)

influence. Recent project research has shown that anomalous west-to-east surface pressure and surface temperature gradients across West Africa during February through May are strongly correlated with the hurricane activity which follows later in the year. We find that Atlantic hurricane activity is enhanced when the February to May east minus west pressure gradient is higher than normal and/or when the east minus west temperature gradient anomaly is below average. These pressure and temperature gradients during February through May 1995 indicate an about average West African monsoon and an about average amount of seasonal hurricane activity.

(e) Caribbean Basin Sea Level Pressure Anomaly (SLPA) and upper tropospheric (12 km) Zonal Wind Anomaly (ZWA) influence. April and May values of SLPA and ZWA have a modest predictive potential for hurricane activity during the following season. Negative anomalies (low pressure and easterly anomalies) imply enhanced seasonal hurricane activity while positive values imply suppressed hurricane activity. April-May 1994 values of SLPA and ZWA were both slightly below average, indicating a slight enhancing influence on this season's hurricane activity.

Our seasonal forecast scheme has the following general form:

Predicted Amount of TC Activity per Season = Average Season + (QBO + EN + AR + PT + SLPA + ZWA)

where

QBO = 30 hPa and 50 hPa Quasi-Biennial Oscillation zonal wind influence. (Increased hurricane activity for westerly (or positive) zonal wind anomalies; reduced hurricane activity for easterly or negative zonal wind anomalies);

EN = El Nino influence. (Warm surface water in the equatorial East Pacific reduces hurricane activity, cold water enhances it);

AR = Western Sahel rainfall. (Increase activity if wet; reduce activity if dry);

PT = West Africa west-to-east gradients of surface pressure and surface temperature during February through May. (High values of west-to-east pressure gradient and high values of east-to-west temperature gradient indicate more hurricane activity; less hurricane activity with opposite gradients);

SLPA = Average Caribbean Sea Level Pressure Anomaly (SLPA) for Spring and early Summer. (Reduce hurricane activity if SLPA is significantly above average; add activity if SLPA is significantly below average);

ZWA = Zonal Wind Anomaly at 200 hPa (12 km) for five low latitude upper air stations in the Caribbean. (Reduce hurricane activity if positive; increase hurricane activity if negative).

SEASONAL FORECAST

Based on data through the end of May 1995, the 1 June predictors in our forecast equations indicate an above average hurricane season for 1995. Table 1 shows our objective forecast from our forecast equations and our qualitative adjustment of our actual forecast. Observe that our prediction equations indicate an extremely active hurricane season for this year. We have added a downward adjustment to many of the values here shown. Last year our adjustment to our forecast equation actually gave a poorer forecast.

Table 1: The 1995 seasonal forecasts obtained by substitution of the parameter values in Table 2 into Equation (1). The authors' qualitative adjustments and actual forecast are shown on the right column.

Forecast Parameter	Objective Forecast	Qualitative Adjustment and Actual Forecast
named storms (N)	12.6	12
named storm days (NS)	77.9	65
hurricanes (H)	10.4	8
hurricane days (HD)	49.5	35
intense hurricanes (IH)	2.3	3
intense hurricane days (IHD)	5.7	6
hurricane destruction potential (HDP)	135.4	110
net tropical cyclone activity (NTC)	153.5%	140%
Western Sahel rainfall forecast	+0.27 S.D.	+0.27 S.D.

Table 2 expresses each parameter in this adjusted forecast as a percentage of the last 45-year average. Note that all forecast parameters are well above the long period average. Table 3 compares this early June forecast to the first author's late November 1994 forecast of last year. The November 1994 forecast anticipated cold ENSO conditions to be in place during the height of the 1995 hurricane season. As of early June, this late November, 1994 assessment appears to be on target. Table 4 gives a

Table 2: 1995 Atlantic basin seasonal forecast values as a percent of the long term (1950-1994) average.

named storms (N)	129%
named storm days (NS)	141
hurricanes (H)	140
hurricane days (HD)	152
intense hurricanes (IH)	136
intense hurricane days (IHD)	133
hurricane destruction potential (HDP)	162
net tropical cyclone activity (NTC)	140

Table 3: Comparison of current, early June 1995, seasonal predictions with the 1995 seasonal predictions made in late November 1994.

Forecast Parameter	30 Nov. 1994 Fcst.	Qualitative Adjustment 13 Apr. 1995	Current 1995 Early June Fcst.	Changes in 7 June 1995 Fcst. from 30 Nov. 1994 Fcst.
N	12	10	12	0
NS	65	50	65	0
H	8	6	8	0
HD	35	25	35	0
IH	3	2	3	0
IHD	8	5	6	-2
HDP	110	75	110	+10
NTC	140%	100%	140%	0

Table 4: Comparison of early June 1995 seasonal predictions with activity in previous years.

	7 June 1995 Fcst.	..... Observed 1994	1993	1992	Average Season 1970-87	Average Season 1950-69	45-Year Average 1950-94
N	12	7	8	6	8.3	9.8	9.3
NS	65	28	30	38	37.3	53.4	46.1
H	8	3	4	4	4.9	6.5	5.7
HD	35	7	10	16	15.5	30.7	23.0
IH	3	0	1	1	1.6	3.4	2.1
IHD	8	0	0.75	3.25	2.1	8.8	4.5
HDP	110	15	23	51	42.7	100.0	68.1
NTC	140%	37%	55%	62%	73%	123%	100%

comparison of this year's seasonal activity forecast with the amount of hurricane activity which has occurred during past years. Note that the 1995 season is expected to be much more active than have the last four hurricane seasons and more active than most of the hurricane seasons since the late 1960's.

US East Coast and Florida Hurricane Landfall.

Hurricane Andrew and Bob have been the only US landfalling hurricanes of the last five years (Emily, 1993 only skimmed the outer banks as a minimal category 3 hurricane). All of these cyclones did not become of hurricane intensity until they were poleward of 25N. It is unusual to go five consecutive years without any low latitude origin hurricanes threatening upon the US coastline. These inhibiting influences are not expected to be present during the 1995 hurricane season, however.

Gulf of Mexico.

During the last five years (1990-94), there was only one hurricane (Andrew, 1992) to make landfall on the US Gulf Coast. This is much below the long term average. This reduction of hurricane activity in the Gulf was primarily a response to the long lasting El Nino event of 1991-94. Historical records show that Gulf hurricane activity is usually suppressed during El Nino years and enhanced during La Nina (cold SST) years. The probability of hurricane activity within the Gulf of Mexico will be higher during 1995 than it has been since 1989.

Caribbean Basin.

There has been no hurricane activity at all within the Caribbean during the last five years. This is a consequence of the long lasting El Nino event of 1991-94, Western Sahel drought conditions during 1990-93 and higher than average Caribbean basin surface pressures during the last five years. These inhibiting influences are not expected to be present during the 1995 season. Consequently, the probability of Caribbean basin hurricane activity will be greater this year than any of the last five years.

DISCUSSION

It is well known that Atlantic Basin seasonal hurricane activity is quite variable. Past records indicate that it is typical to have a number of suppressed or somewhat below normal years in a row which are then followed by a year of greatly increased hurricane activity. It appears that 1995 will be one of those seasons wherein a large

upsurge in hurricane activity occurs. The El Nino, stratospheric QBO, West African rainfall, and Atlantic sea surface temperature anomalies are all coming together to promote the large-scale wind and thermal-moisture conditions which are associated with an active season. The first author now regrets his qualitative downward adjustment of the forecast in early April. The sea surface temperature pattern in both the Atlantic and Pacific have been more favorable for hurricane activity in the last two months.

It is important to keep in mind that the early season hurricane activity has *no* bearing on the entire season. Early June Hurricane Allison means nothing with regards to the hurricane activity to follow later in the season. The number of named storms (hurricanes) occurring in June and July correlates at an insignificant r = +0.13 (+0.02) versus the whole season activity. Actually, there is a slight *negative* association of early season storms (hurricanes) versus late season, August through November, r = -0.28 (-0.35). Thus, early season activity, be it very active or quite calm, has little or no bearing on the season as a whole.

SCHEDULE OF UPDATED SEASONAL HURRICANE FORECAST OF 1995

An updated forecast, to be made at the start of the most active part of the hurricane season, will be issued on Friday August 4, 1995. A verification report on the 1995 hurricane season and a forecast for the 1996 hurricane season will be issued in late November of this year. In addition, seasonal forecasts for 1996 ENSO conditions and 1996 Sahel rainfall will also be issued at that time.

CAUTIONARY NOTE

It is important that the reader realize that this seasonal forecast is based on a statistical scheme which will fail in some years. This forecast also does not specifically predict where within the Atlantic basin storms will strike. Even if 1995 should prove to be an active hurricane season, there are no assurances that hurricanes will necessarily strike along the US or Caribbean Basin coastline and do much damage. Or, if 1995 should prove to be an inactive season there is no assurance that no storms will come ashore.

LIKELY INCREASE OF LANDFALLING MAJOR HURRICANES IN COMING DECADES

There has been a great lull in the incidence of intense (category 3-4-5) landfalling hurricanes on US East Coast, Florida and Caribbean Basin during the last 25 years. We see this as a natural consequence of the slowdown in the Atlantic Ocean (thermohaline) Conveyor Belt circulation which has set off a variety of global circulation and rainfall pattern changes such as the Sahel drought, increased El Nino activity, Pacific and Atlantic middle latitude zonal wind increases.

Historical and geological records indicate that this lull in major landfalling hurricane activity will not continue indefinitely. A return of increased major landfalling hurricane activity should be expected within the next decade or two. When this happens, (because of the large coastal development during the last 25-30 years), the US will see hurricane destruction as never before experienced. More research on the causes and the likely timing of this change-over to increased intense hurricane activity is desperately needed. This is a more assured and immediate threat to the US than that of greenhouse gas warming and other environmental problems which are receiving much greater attention in comparison to the hurricane threat.

Changes in the North Atlantic.

We may be seeing the early stages of the beginning speed-up of the Atlantic thermohaline (Conveyor Belt) circulation from its three decades long slow down. Dr. Aagaard has recently reported on a large decrease in ice flow through the Fram Strait (the North Atlantic passage between Greenland and Spitzbergen). This decreased ice flow reduces the introduction of fresh water and low salinity values into the North Atlantic. This ice flow reduction is leading to salinity increases in the North Atlantic. Other researchers have also recently reported recent salinity increases in the North Atlantic. Saline water weighs more than fresh water and is able to sink more readily to the bottom of the North Atlantic.

These salinity increases that are now being measured in the North Atlantic may result in a speed-up of the Atlantic Ocean thermohaline circulation in the next few years. If this does occur, then we should see a general increase in West African Sahel rainfall, a decrease in Atlantic summertime upper tropospheric westerly winds and an increase of Atlantic basin intense hurricane activity. These new regional Atlantic measurements may be an ominous sign of future increases in US and Caribbean basin landfalling hurricane activity. The quarter century lull which we have enjoyed cannot be expected to continue indefinitely into the future.

VERIFICATION OF PAST SEASONAL FORECASTS

The first author has now issued seasonal hurricane forecasts for the last eleven years. In most of the prior forecasts, predictions have been superior to climatology, which was previously the only way to estimate future hurricane activity (see Table 5). The seven late May and early June seasonal forecasts for 1985, 1986, 1987, 1988, 1991, 1992 and 1994 were more accurate than climatology. The forecasts for 1984 and 1990 were only marginally successful and the two seasonal forecasts for 1989 and 1993 were failures. The 1989 forecast was a failure because of processes associated with the excessive amounts of rainfall which fell in the Western Sahel that year. Prior to 1990, our seasonal forecast did not include African rainfall as a predictor. We have corrected this important omission and forecasts since 1990 have incorporated Western Sahel rainfall estimates. The failure of the 1993 seasonal forecast is attributed to our failure to anticipate the resurgence and continuation of El Nino conditions through the whole of the 1993 hurricane season. In particular, the first author failed to anticipate the re-emergence of stronger El Nino conditions after the middle of August 1993. It is very unusual to have an El Nino last as long as the recent 1991-94 event has. This failure motivated us to develop a new extended range ENSO prediction scheme.

Table 5: Verification of the author's previous seasonal predictions of Atlantic tropical cyclone activity for 1984-1994.

Year and Category Forecasted	Late Nov. Forecast	Late May/ early June Forecast	Late July/ early Aug. Forecast	Observed
1984 & NS	-	10	10	12
1984 & NSD	-	45	45	51
1984 & H	-	7	7	5
1984 & HD	-	30	30	18
1985 & NS	-	11	10	11
1985 & NSD	-	55	50	51
1985 & H	-	8	7	7
1985 & HD	-	35	30	21
1986 & NS	-	8	7	6
1986 & NSD	-	35	25	23
1986 & H	-	4	4	4
1986 & HD	-	15	10	10
1987 & NS	-	8	7	7
1987 & NSD	-	40	35	37
1987 & H	-	5	4	3
1987 & HD	-	20	15	5
1988 & NS	-	11	11	12
1988 & NSD	-	50	50	47
1988 & H	-	7	7	5
1988 & HD	-	30	30	24
1988 & HDP	-	75	75	81
1989 & NS	-	7	9	11
1989 & NSD	-	30	35	66
1989 & H	-	4	4	7
1989 & HD	-	15	15	32
1989 & HDP	-	40	40	108
1990 & NS	-	11	11	14
1990 & NSD	-	55	50	68
1990 & H	-	7	6	8
1990 & HD	-	30	25	27
1990 & IH	-	3	2	1
1990 & IHD	-	-	5	1
1990 & HDP	-	90	75	57
1991 & NS	-	8	7	8
1991 & NSD	-	35	30	22
1991 & H	-	4	3	4
1991 & HD	-	15	10	8
1991 & IH	-	1	0	2
1991 & IHD	-	2	0	1.2
1991 & HDP	-	40	25	23
1992 & NS	8	8	8	6
1992 & NSD	35	35	35	38
1992 & H	4	4	4	4
1992 & HD	15	15	15	16
1992 & IH	1	1	1	1
1992 & IHD	2	2	2	3.2
1992 & HDP	35	35	35	51
1993 & NS	11	11	10	8
1993 & NSD	55	55	50	30
1993 & H	6	7	6	4
1993 & HD	25	25	25	10
1993 & IH	3	2	2	1
1993 & IHD	7	3	2	0.8
1993 & HDP	75	65	55	23
1994 & NS	10	9	7	7
1994 & NSD	60	35	30	28
1994 & H	6	5	4	3
1994 & IH	2	1	1	0
1994 & IHD	7	1	1	0
1994 & HDP	85	40	35	15
1994 & NTC	110	70	55	37

DEFINITIONS

Atlantic basin - The area including the entire Atlantic Ocean, the Caribbean Sea, and the Gulf of Mexico.

Hurricane (H) - A tropical cyclone with sustained low level winds of 74 miles per hour (33 ms^{-1} or 64 knots) or greater.

Hurricane Day (HD) - Four six-hour periods during which a tropical cyclone is observed or estimated to have hurricane intensity winds.

Tropical Cyclone (TC) - A large-scale circular flow occurring within the tropics and subtropics which has its strongest winds at low levels including hurricanes, tropical storms, and other weaker rotating vortices.

Tropical Storm (TS) - A tropical cyclone with maximum sustained winds between 39 (18 ms^{-1} or 34 knots) and 73 (32 ms^{-1} or 63 knots) miles per hour.

Named Storm (NS) - A hurricane or tropical storm.

Named Storm Day (NSD) - Four consecutive six--hour periods during which a tropical cyclone is observed or estimated to have attained tropical storm or hurricane intensity winds.

Hurricane Destruction Potential (HDP) - A measure of a hurricane's potential for wind and storm surge destruction defined as the sum of the square of a hurricane's maximum wind speed (IN 10,000 knots*knots) for each six-hour period of its existence.

Intense Hurricane (IH) - A hurricane reaching at some point in its lifetime a sustained low level wind of at least 111 mph (96 kt or 50 ms^{-1}). This constitutes a category three or higher storm intensity rating on the Saffir/Simpson scale (a "major" hurricane).

Intense Hurricane Day (IHD) - Four six-hour periods during which a hurricane has Saffir/Simpson category three intensity or higher.

Hectopascal (hPa) - A measure of atmospheric pressure often used as a vertical height designator. Average surface values are about 1000 hPa; the 200 hPa level is about 12 km and the 50 hPa is about 20 km altitude. Monthly averages of surface values in the tropics show maximum summertime variations of about +/-2 hPa which are associated with variations in seasonal hurricane activity.

El Nino (EN) - A 12-18 month period during which anomalously warm sea surface temperatures occur in the eastern half of the equatorial Pacific. Moderate or strong El Nino events occur irregularly, about once every 5-6 years or so on average.

Delta PT - A parameter which measures the anomalous west to east surface pressure (Del-P) and surface temperature (Del-T) gradient across West Africa.

SOI - Southern Oscillation Index - A normalized measure of the surface pressure difference between Tahiti and Darwin.

QBO - Quasi-Biennial Oscillation - A stratospheric (16 to 35 km altitude) oscillation of equatorial east-west winds which vary with a period of about 26 to 30 months or roughly 2 years; typically blowing for 12-16 months from the east, then reverse and blowing 12-16 months from the west, then back to easterly again.

Saffir/Simpson (S-S) Category - A measurement scale ranging from 1 to 5 of hurricane wind and ocean surge intensity. One is a weak hurricane whereas 5 is the most intense hurricane.

SLPA - Sea Level Pressure Anomaly - A deviation of Caribbean and Gulf of Mexico sea level pressure from observed long term average conditions.

SST(s) - Sea Surface Temperature(s).

ZWA - Zonal Wind Anomaly - A measure of upper level (200 hPa) west to east wind strength. Positive anomaly values mean winds are stronger from the west or weaker from the east than normal.

Net Tropical Cyclone Activity (NTC) - Average seasonal percentage sum of NS, NSD, H, HD, IH, IHD. Gives overall indication of Atlantic basin seasonal hurricane activity.

1 knot = 1.15 miles per hour = .515 meters per second

JUNE TO SEPTEMBER RAINFALL IN THE AFRICAN SAHEL: A SEASONAL FORECAST FOR 1995

from: C.W. Landsea, W.M. Gray,
P.W. Mielke, Jr. and K.J. Berry,
Department of Atmospheric Sciences
and Department of Statistics,
Colorado State University
(6 June 1995)

The rainy season in North Africa's Sahel occurs almost exclusively during the months of June through September when the ITCZ reaches its farthest northward extension. The Sahel is defined here as the North African region between 10 and 20N. It is this area that has experienced numerous devastating droughts within the last three decades. This report provides a forecast for this year's June to September seasonal rainfall for the Sahel based upon data available through early June.

Because of rainfall variability within the region, a homogeneous index of precipitation should not be utilized for the entire Sahel. Instead, three west to east subregions are organized where precipitation shows similar fluctuations. These regions are the West, Central, and East Sahel. The West Sahel extends from the Atlantic coast to 6W including portions of the countries of Mauritania, Senegal, Gambia, Guinea-Bissau, Guinea, and Mali. The Central Sahel is the region from 6W to 26E and includes parts of Mali, Burkina Faso, Ghana, Togo, Benin, Niger, Nigeria, Cameroon, Chad, Central African Republic, and Sudan. The East Sahel reaches from 26E to the Red Sea and is composed of parts of Sudan, Ethiopia, Eritrea, and Djibouti. Note that the Central Sahel is by far the largest of the three regions, comprising well over one half of the entire Sahel.

STATISTICAL METHODOLOGY AND 1995 FORECAST

The forecasting techniques are detailed in full in Landsea *et al.* (1993) and Gray *et al.* (1992, 1993, 1994). We use a Least Absolute Deviations (LAD) regression instead of the traditional Ordinary Least Squares (OLS) multiple regression based upon the years 1950 to 1991. LAD is selected over OLS in that LAD is based upon minimizing the absolute differences between predicted and observed instead of the square of that value. Thus outliers do not overly influence the prediction equations. The amount of skill is estimated by the regression applied to the whole data set with a standard degradation applied (as detailed in Mielke *et al.*, 1995). In general, degradation increases with the number of predictors and decreases with the number of years under consideration. Thirteen predictors based upon the phase and magnitude of the stratospheric Quasi-Biennial Oscillation (QBO), North African surface data, and Caribbean and El Nino-Southern Oscillation (ENSO) information are utilized for the early June forecast.

The individual predictors and their values to be used as input for the 1995 forecast are the following:

QBO Predictors:

Zonal U winds at 50 hPa at 10N (extrapolated for Sep 1995) = -1 m s^{-1}

Zonal U winds at 30 hPa at 10N (extrapolated for Sep 1995) = -5 m s^{-1}

|U50hPa-U30hPa| (extrapolated for Sep 1995) = 4 m s^{-1}

North African Predictors:

Aug-Sep 1994 West Sahel rainfall	= +0.08 S.D.
Aug-Nov 1994 Gulf of Guinea rainfall	= +0.24 S.D.
Feb-May 1995 Sea level pressure anomaly gradient	= -1.0 S.D.
Feb-May 1995 Surface temperature anomaly gradient	= +0.75 S.D.

Caribbean and ENSO Predictors:

Apr-May 1995 Sea level pressure anomalies (Caribbean)	= -0.2 hPa
Apr-May 1995 200 hPa zonal wind anomalies (Caribbean)	= -1.5 ms^{-1}
Apr-May 1995 SOI	= -1.0 S.D.
Apr-May minus Jan-Feb 1995 SOI	= -0.35 S.D
Apr-May 1995 "Nino 3" Central Pacific SST anomalies	= -0.35 °C
Apr-May minus Jan-Feb 1995 "Nino 3" SST anomalies	= -1.2 °C

Given these values for the predictors based upon information available to us at CSU by the end of May, the statistical model predicts values of:

West Sahel	.... +0.27 S.D. (NEUTRAL QUINTILE)
Central Sahel	..... +0.30 S.D. (WET QUINTILE)
East Sahel	... +1.05 S.D. (VERY WET QUINTILE)

These various values of rainfall are due to: 1) slightly favorable conditions for rainfall throughout the Sahel due to strong west phase of the QBO and the small vertical shear between 30 and 50 hPa; 2) near average rainfall amounts in the West Sahel indicating for near average rainfall based on persistence; 3) slightly above average rainfall occurring during last fall along the Gulf of Guinea suggests that the evaporation/evapotranspiration moisture source will be slightly above average contributing to a wet Sahel; 4) North African sea level pressure

and surface temperature gradients show a mixed signal with the temperature gradients being favorable and the pressure gradients being unfavorable - overall a neutral factor primarily effective for the West and Central Sahel; 5) Caribbean and ENSO factors suggest a return to near neutral or cool ENSO conditions during the following few months and thus wetter than average conditions especially in the West and East Sahel regions.

In combination the West Sahel is expected to be near average (conditions in the middle quintile "NEUTRAL", 40-60% of rainfall years), the Central Sahel moderately wet (conditions in the second quintile "WET", 20-40% of rainfall years), and the East Sahel very wet (conditions in the wettest quintile "VERY WET", in the top 20% of occurrences). Note that the West Sahel that has been previously shown (Landsea and Gray 1992) to be most strongly correlated with concurrent Atlantic seasonal hurricane activity; a near average West Sahel should correspond to having two or three major hurricanes this year.

The forecast that was issued in early December (Landsea et al 1994) was similar to what is described here:

	Early December forecast	Early June forecast
West Sahel	+0.34 S.D. (WET)	+0.27 S.D. (NEUTRAL)
Central Sahel	+0.17 S.D. (WET)	+0.30 S.D. (WET)
East Sahel ..	+0.02 S.D. (NEUTRAL)	+1.05 S.D. (VERY WET)

The increases in the East Sahel are primarily due to the ENSO cool event that is occurring, while the slight decrease in the West Sahel is due to having a mixed signal in the North African pressure and temperature gradients.

The amount of skill indicated in the hindcast testing of the five predictors during the years 1950 to 1991 is 56% of the variability in the West Sahel, 56% in the Central, and 40% in the East. Note that simple use of only persistence provides just 25%, 32%, and 14% for the three regions, respectively. Recent tests (Mielke *et al.*, 1995), however, have suggested that the true skill that would be found in independent data would be lower.

A verification of this forecast as well as an accompanying extended range outlook for 1996 Sahelian rainfall will be made by early December of this year.

REFERENCES

Gray, W.M. C.W. Landsea, P. Mielke, Jr. and K. Berry, 1992: Predicting Atlantic basin seasonal hurricane activity 6-11 months in advance. *Weather and Forecasting*, **7**, 440-455.

Gray, W.M. C.W. Landsea, P. Mielke, Jr. and K. Berry, 1993: Predicting Atlantic basin seasonal tropical cyclone activity by 1 August. *Weather and Forecasting*, **8**, 73-86.

Gray, W.M. C.W. Landsea, P. Mielke, Jr. and K. Berry, 1994: Predicting Atlantic basin seasonal tropical cyclone activity by 1 June. *Weather and Forecasting*, **9**, 103-115.

Landsea, C.W. and W.M. Gray, 1992: The strong association between western Sahel monsoon rainfall and intense Atlantic hurricanes. *J. Climate*, **5**, 435-453.

Landsea, C.W., W.M. Gray, P.W. Mielke, Jr. and K. Berry, 1993: Predictability of seasonal Sahelian rainfall by 1 December of the previous year and 1 June of the current year. *Preprints of* 20th Conference on Hurricanes and Tropical Meteorology, San Antonio, Amer. Meteor. Soc., 473-476.

Landsea, C.W., W.M. Gray, P.W. Mielke, Jr. and K.J. Berry, 1994: June to September rainfall in the African Sahel - Verification of our 1994 forecasts and an extended range forecast for 1995. CSU Dept. of Atmospheric Science report released on 1 December, 1994, 5 pp.

Mielke, Jr., P.W., K.J. Berry, C.W. Landsea and W.M. Gray, 1995: Artificial skill and validation in weather forecasting. Accepted to *Weather and Forecasting*, 38 pp.

Bill Kyle

Department of Geography & Geology

The University of Hong Kong

Hong Kong Weather Reviews

Climatological information employed in the compilation of this section is derived from published weather data of the Royal Observatory, Hong Kong and is used with the prior permission of the Director.

Review of autumn 1994

Important climatological events

In contrast to the cooler and very much wetter months of July and August, autumn 1994 was generally characterized by somewhat above normal temperatures and considerably drier conditions. The season started off with the continuation of the mainly cooler conditions that characterized the previous two months. However, September posted a rainfall amount of 298.9 mm, less than a millimetre under the 1961-90 normal value. The month was also cloudier and more humid than normal, the mean relative humidity being the tenth highest and total bright sunshine the second lowest on record for the month respectively. The generally cooler temperatures continued through October although that month was generally fine and dry as a consequence of the influence of a persistent northeast monsoon. Rainfall was only 2.2 mm (2 percent of the 1961-90 normal) making it the eighth driest October since records began in 1884. In marked contrast, the absence of significant monsoon surges resulted in a considerably warmer than normal November. The monthly mean minimum temperature of 21.1°C set a new record as the highest measured since 1884 at the Royal Observatory. The mean monthly temperature of 22.9°C was the second highest on record, exceeded only by the figure of 23.1°C recorded in November 1966. Although the humidity was high, the mean dewpoint temperature of 17.8°C being the fourth highest on record for the month, the weather remained fine and rainfall was rare. The total of 0.2 mm was the sixth lowest for November.

Mean daily temperature	**25.0°C**	**(+0.3°C)**
Rainfall (provisional)	**301.3 mm**	**(63 %)**

September

September 1994 continued the cooler conditions characteristic of the previous two months, the mean monthly temperature of 27.1°C being 0.5°C below the 1961-90 normal for the month. A mean relative humidity of 83 percent, the tenth highest on record for September, also meant that the month was more humid than normal. High cloudiness (10 percent above normal) and low sunshine were also a common feature. The total bright sunshine totalled only 124.8 hours, 69 percent of normal, making the value the second lowest for September. Rainfall, however, was only 0.8 mm below the normal value of 299.7 mm.

The first two days of the month were fine and hot. As a result of the long periods of sunshine temperatures reached the month's high of 31.9°C during the afternoon of 2nd. Conditions began to change with the arrival of an easterly airstream the following morning which brought showery weather. The influence of the outer rainbands of tropical cyclone Joel which developed over the northern part of the South China Sea affected the territory during the following two days and brought unsettled weather. Improvements took place on 6th and weather remained generally fine with isolated showers for the next three days. The night of 10th brought the return of unsettled conditions with heavy rain and thunderstorms. Over 50 mm of rain were recorded in Kowl

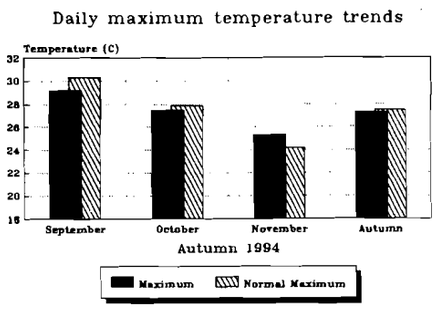

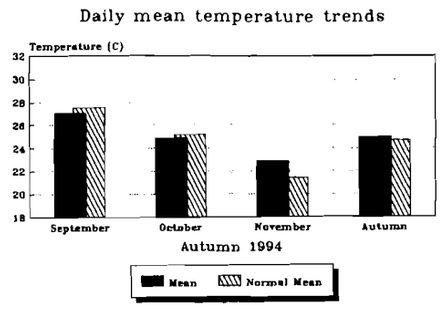

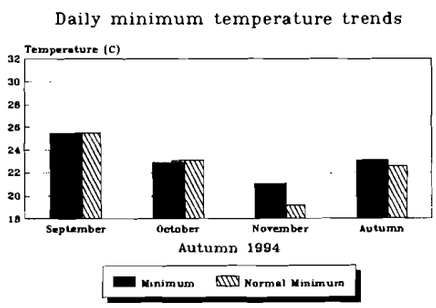

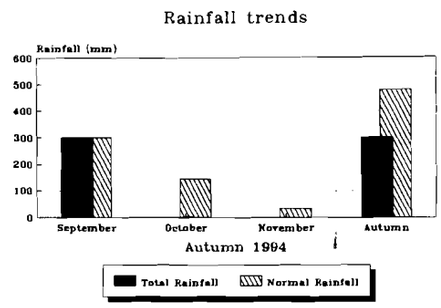

between 8 and 9 pm in one of the heaviest downpours. During this time several people were injured and there were extensive reports of flooding. The following day Tropical Storm Luke crossed the Luzon Strait and entered the South China Sea moving closer to Hong Kong. That night winds strengthened from the east and strong winds and squally showers affected the territory on 12th with 50 mm of rainfall being recorded on Hong Kong Island. Rain eased off the following day with the arrival of a continental northeast monsoon although winds offshore remained strong. Windy and cloudy conditions continued on 14th but weather improved the next day. Under the influence of a cool northeast monsoon a spell of mainly fine weather began and continued until 22nd. During this period temperatures dropped to the minimum value for the month of 23.1°C on 18th. Heavy thundery showers in the early morning and again later in the night of 23rd marked the return of disturbed weather. On that day rainfall amounts exceeding 100 mm were reported in Tsuen Wan and Shatin. Cloudy conditions continued on 24th but generally fine weather returned on the following two days. Cloud and rain reappeared for the next two days before the arrival of a dry continental airstream from the north. This change resulted in the weather becoming sunny and dry for the remainder of the month.

Mean daily temperature 27.1°C (-0.5°C)
Rainfall (provisional) 298.9 mm (100 %)

October

The month of October was generally fine and dry due to the influence of a persistent northeast monsoon. The mean cloud amount for the month was only 36 percent, 20 percent below the October normal. The monthly rainfall of only 2.2 mm made it the eighth driest October on record.

During the first five days of the month the weather was fine and warm as a broad ridge of high pressure dominated the South China region. This spell of fine weather was interrupted with the arrival of a fresh easterly airstream on the morning of 6th which brought cloudy weather with some rain. However, fine conditions and rising temperatures returned for the next few days and as Typhoon Seth traversed the East China Sea its peripheral northerly flow brought hot, dry continental air to the territory on 10th and 11th.

Consequently the mean relative humidity dropped to 63 percent on those two days. During the next five days there was generally sunny weather with moderate to fresh easterly winds which brought the temperature to the month's high of 31.1°C on a fine afternoon on 17th. The next day a cold front over Guangdong began to advance south and reached the south China coast on 19th. Locally winds strengthened from the north that night. Advection of cool, dry continental air behind the front led to a significant drop in both temperature and relative humidity. On 21st mean relative humidity dropped to 37 percent and the month's minimum temperature of 16.5°C was recorded on 22nd. The northeast monsoon flow continued to be sustained by the persistence of a high pressure system over China so the remainder of the month was cool, fine and dry.

Mean daily temperature	**24.9°C**	**(-0.3°C)**
Rainfall (provisional)	**2.2 mm**	**(2 %)**

November

Like the preceding month November 1994 was fine and rain was rare. However, with no significant surges of the winter monsoon it was also much warmer than usual. The monthly mean minimum and monthly mean temperature of 21.1°C and 22.9°C were the highest and second highest values respectively since records began. The monthly rainfall of only 0.2 mm was the sixth lowest on record. Even though rainfall was low the month was relatively humid with the mean dewpoint temperature of 17.8°C the fourth highest for November.

The fine weather of the last week in October extended into the first half of November. During the first ten days the weather was fine with long periods of sunshine during the day and clear skies at night. The consequential high levels of outgoing longwave radiation resulted in the lowest temperature for the month of 19.9°C being recorded on the early mornings of both 1st and 2nd. Although cloud increased from 11th to 13th the weather remained generally fine and dry creating problems with hillfires in the grassland of the New Territories. The 13th saw the arrival of a continental airstream over the coastal areas of Guangdong which led to a strengthening of easterly winds offshore on the morning of 14th which lasted until the next day. Despite the windy conditions the month's high temperature of 27.1°C was recorded on the sunny afternoon of 15th. Winds moderated on 16th and fine, warm conditions continued for the next three days until a weak replenishment of the northeast monsoon arrived early on 20th. This brought with it cloudy weather with light rain although the clouds dispersed the next day as the monsoon moderated. Weather remained generally fine apart from occasional light rain in the early morning for the following week. A moist, easterly airstream returned on 29th to bring cloudy weather for the remainder of the month.

Mean daily temperature	**22.9°C**	**(+1.9°C)**
Rainfall (provisional)	**0.2. mm**	**(1 %)**

Review of winter 1994-95

Important climatological events

Overall winter 1994-95 was characterized by warmer and wetter conditions than usual although a change did take place in the latter half of the season. The month of December was warm, cloudy and unusually wet. The monthly mean temperature of 19.8°C and the monthly mean minimum temperature of 18.2°C were both second highest on record for December. The high cloud amount (33 percent above normal) was also reflected in a record low for the month of only 70.2 hours of bright sunshine. The rainfall of 122.6 mm was almost four and a half time the normal and the fourth highest ever recorded for the month. Unusually heavy rain on 8th resulted in the issuance of the first ever flood warning in December. Overall January was cloudier and slightly warmer than normal with only two days with minimum temperatures below 10°C. However, towards the end of the month a strengthening winter monsoon heralded a change to cooler conditions. February on the whole was slightly cooler and drier with a monthly mean temperature 0.8°C below the 1961-90 normal value.

Mean daily temperature	**17.1°C**	**(+0.6°C)**
Rainfall (provisional)	**176.8 mm**	**(179 %)**

December

The month of December was characterized by warmer than usual temperatures, considerable cloudiness and wet conditions. The monthly mean temperature of 19.8°C and the monthly mean minimum temperature of 18.2°C were both the second highest recorded at the Royal Observatory since the start of measurements in 1884. It was also cloudier than usual with a

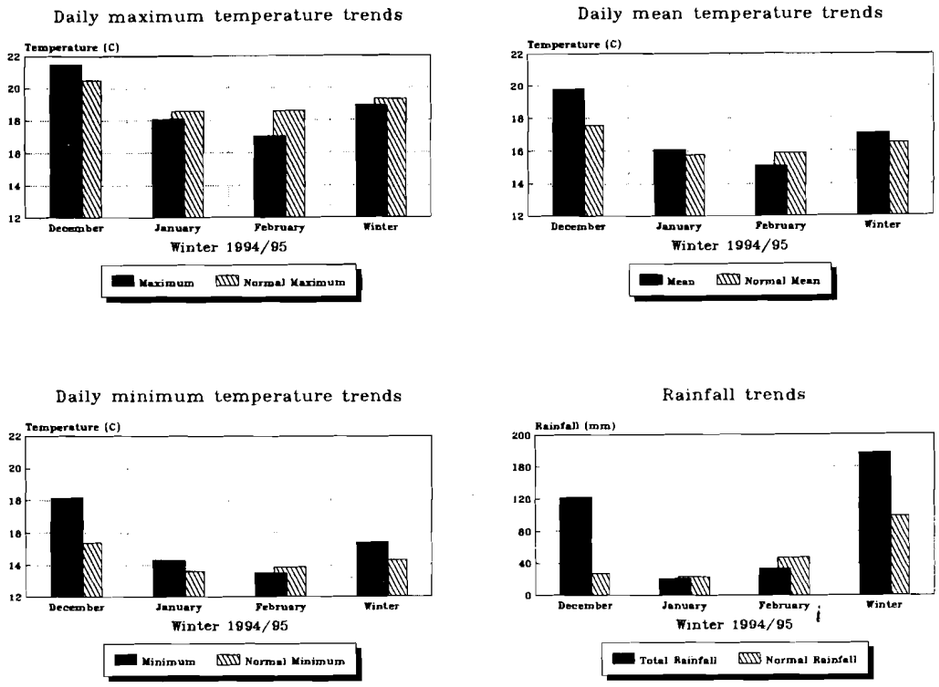

mean cloud amount of 82 percent compared to the 1961-90 normal of 49 percent. As a result a new low sunshine duration for the month of 70.2 hours, 111.3 hours less than normal, was recorded for the month. Rainfall was also unusually high with the total of 122.6 mm, nearly four and a half times normal, being the fourth highest for December. Heavy rain on 8th also created a precedent in being responsible for the first ever flood warning issued in the month of December in the territory.

The month started with warm, generally cloudy conditions associated with the easterly airstream that affected the weather at the end of November. A surge of the northeast monsoon reached the coast of South China early on 3rd bringing with it strong winds which affected areas offshore for most of that day. In the evening winds turned northerly resulting in a lowering of temperatures and a clearing of the clouds to give cool and dry conditions for the next two days. However, clouds returned on 6th and 7th before a moist easterly airstream brought periods of heavy rain on 8th. The Royal Observatory recorded 58.9 mm on that day although over 160 mm were measured over the Sai Kung area. The event led to the first ever issuance, from 1330 to 1730, of a flood warning in December. Cloud and light rain continued on 9th before humid conditions with morning mist associated with a change to a southeasterly airstream set in. During this time temperatures began to rise steadily culminating in the month's maximum of 25.7°C being reached on the afternoon of 12th. That evening saw the arrival of a cold front from the north at the south China coast and temperatures fell nearly ten degrees overnight. Continued replenishment of the winter monsoon produced cool and mainly fine weather for the following ten days with temperatures dropping steadily during that time. The month's minimum temperature of 13.7°C was attained early on the morning of 22nd. Two days later the presence of Severe Tropical Storm Axel over the South China Sea brought a moist easterly airstream over the territory. As a result overcast conditions with rain dominated the weather over the Christmas period. A total of 48.6 mm was recorded at the Royal Observatory on 24th and 25th. The rain eased the next day and some bright periods returned. This pattern of cloudy weather with some bright spells continued from 27th to the end of the month.

Mean daily temperature	**19.8°C**	**(+2.2°C)**
Rainfall (provisional)	**122.6 mm**	**(449 %)**

January

The year 1995 began with a slightly warmer and more cloudy January than usual. The mean temperature of the month, 16.1°C, was 0.3°C higher than the 1961-90 normal and the duration of bright sunshine posted a shortfall of 34.5 hours at a total of 117.9 hours for the month. The minimum temperature fell below 10 on only two days. Rainfall too, was below 10 percent below normal at 21.1 mm.

Mild conditions with windy conditions offshore characterized the first two days of the month. The arrival of a cool northerly airstream brought disturbed weather with rain on 3rd and produced the first thunderstorm of the year that afternoon. Early on 4th rain eased and clouds dissipated as a dry winter monsoon reached the territory. During the next three days fine, dry and cold conditions prevailed as this influence continued to dominate the weather. As the monsoon subsided on 8th temperatures began to climb giving fine though hazy conditions. With the winds turning to the east on 10th cloud and mist returned. A cold front advanced south over Guangdong on 11th and reached the coast early the next day bringing about a fall of local temperatures of about 3°C. The weather then remained cool but generally fine from 13th to 17th before the return of milder weather for a period of five days. This mild spell culminated in a sunny afternoon on 22nd when the month's high temperature of 23.0°C was recorded. Another cold front crossed the south China coast the next day bring cool and cloudy weather until 26th. As the winter monsoon continued to dominate the remainder of the month was cold and rainy with the month's minimum temperature of 9.2°C being recorded on the early morning of 31st.

Mean daily temperature 16.1°C (+0.3°C)
Rainfall (provisional) 21.1 mm (90 %)

February

The month of February was on balance somewhat cooler and drier than normal. The mean air temperature was 0.8°C lower than normal at 15.1°C and the monthly total rainfall of 33.1 mm was 31 percent below the 1961-90 normal of 48 mm. However, the month was characterized by two distinctly different periods with generally fine and dry weather dominating the first half but cloudy and rainy conditions prevalent in the second.

With the continued influence of the winter monsoon the month started cold and cloudy although temperatures rose slightly as the wind gradually turned east. A northerly surge reached the coast on 4th bringing with it sunny and very dry conditions which lasted for a couple of days. During this time minimum temperatures fell progressively with the month's minimum temperature of 10.4°C being reached on the early morning of 6th. Milder conditions returned over the next three days before the arrival of a fresh easterly airflow early on 10th brought strong winds and generally fine conditions. Over the next two days winds moderated but continuing fine, sunny weather raised daytime maximum temperatures to the month's high of 22.3°C on the afternoon of 12th. A trough of low pressure crossed the coast on the evening of 13th bringing rain and thunderstorms and unsettled weather that night and the following morning. The rain eased off in the afternoon of 14th but the weather remained cool and cloudy with some rain until 17th. The arrival of a maritime airstream on 18th brought humid and misty conditions before the return of cool, rainy conditions on 19th which lasted until the end of the month.

Mean daily temperature 15.1°C (-0.8°C)
Rainfall (provisional) 33.1 mm (69 %)

Meeting Reviews

Sixth Annual Meeting 1995

Venue: Royal Observatory, Kowloon

Date: 11 March, 1995

The Annual Meeting of the Society was held at 12 noon on Saturday 11 March, 1995 at the Royal Observatory, Nathan Road, Kowloon.

The outgoing Chairman, Dr. Bill Kyle, welcomed members and guests to the AGM and thanked the members of the 1994-95 Executive Committee for their service to the Society and the membership for their support of the Executive Committee throughout the year. He then presented his annual report for 1994-95 highlighting the following matters.

On 28 February, 1995 membership of the Society stood at 212, comprising 124 Fellows, 50 Associate Members, 26 Student Members and 12 Corresponding Members.

During the year various activities were organized for members and invited guests. Two Research Forums, the Ninth and Tenth to be scheduled by the Society, were held during the year. The Ninth Forum, on the topic of "Meteorology and Environment" was held prior to the Fifth Annual Meeting on 12 March 1994 at the Royal Observatory, Kowloon and attracted a total of 44 participants. The Tenth, was held at The City University of Hong Kong on 10 December 1994. The topic "Probability and Statistics in the Atmospheric Sciences" drew 24 participants.

Other activities included the attendance of an official Society delegation at the Atmospheric Science Conference held in Beijing from 5-8 October, 1994 to commemorate 70th anniversary of the founding of the Chinese Meteorological Society, a visit to OWWS Operation Centre at HKUST and a social hike to Sunset Peak.

During the year two issues of the Hong Kong Meteorological Society Bulletin, Volume 4, Numbers 1 and 2 were published by the Editorial Board. The former was a Special Issue on Severe Weather and was very favourably received by the membership.

The Society's sixth year was also a relatively quiet one although the fairly full programme of activities organized by such a small society, not to mention the production of two issues of the Society Bulletin warranted commendation to those whose efforts made it possible. We also broke the 200 member barrier and we continue to grow and prosper.

This was his final year as Chairman, a post he held for the past 4 years, as he believed it was time for new blood to take over the helm of the Society. He thanked all those who supported him during his time in office and encouraged members to offer the same support to his successor.

The Hon. Treasurer, Mr. Y.K. Chan, then presented the audited accounts of the Society for the year. These were adopted unanimously.

Election of Office Bearers of the Society and appointment of the Honorary Legal Advisor and Honorary Auditor for 1995-96 resulted in the following:

Chairman	Dr. Johnny C.L. Chan
Vice Chairman	Mr. C.Y. Lam
Hon. Secretary	Ms. Olivia S.M. Lee
Hon. Treasurer	Mr. Y.K. Chan
Committee:	Ms. Julie Evans-Dowsley
	Dr. S.C. Kot
	Dr. W.J. Kyle
	Dr. C.N. Ng
	Dr. Y.Y. Yan
Hon. Legal Advisor	Ms. Venus Choy
Hon. Auditor	Mr. John C.T. Wu

The meeting agreed to continue waiver of the

Entrance Fee for all new members for 1995. On the proposal of the outgoing Executive Committee the following revision of the annual subscriptions was adopted unanimously:

HK$200	for Fellow
HK$150	for Associate Member
HK$ 50	for Student Member
HK$500	for Institutional Member
US$ 30	for Corresponding Member

Research Forum 11

Venue: Royal Observatory, Kowloon

Date: 11 March, 1995

Subject: Impacts of Hazardous Weather

An eleventh research forum was held at the Royal Observatory, Kowloon with the theme of *Impacts of Hazardous Weather*. The forum was organized by Mr. Y.K. Chan of the Royal Observatory who was also the forum chairman.

Two papers were delivered in the first session as listed.

ADVERSE WEATHER CONDITIONS AND FLIGHT OPERATIONS SAFETY

by Captain Wratten, Cathay Pacific Airways

TRAINS IN THE RAIN

by Mr. R.T. Kynaston, Deputy Operations Director, Mass Transit Railway Corporation

Following a break for refreshments two more papers were delivered in a second session as listed.

FLOODING AND SEVERE RAINSTORMS IN HONG KONG

by Mr. R.T.K. Cheung, Chief Engineer Land Drainage, Drainage Services Department, Hong Kong Government

THE IMPACT OF DROUGHT IN HONG KONG

by Dr. M.R. Peart, Department of Geography and Geology, The University of Hong Kong

---

Calendar of Coming Events

This section is intended for the publication of forthcoming events organized by the Society or by other organizations with similar aims. If members wish to notify the Society of any such events they should mail or fax such information to the Editor-in-chief along with their name(s) and membership number(s).

1995

Boulder, CO, USA **July 2 - 14**

21st IUGG General Assembly.

Boulder, CO, USA **July 3 -7**

Joint IAHAS.IAMAS Symposium on
"HJ1 Clouds, Convection and Land Surface Processes".

Breckenridge, CO, USA **July 17 -21**

7th American Meteorological Society Conference on
"Mountain Meteorology".

Toulouse, France **July 17-21**

CALMET 95 _ Computer Aided Learning and Distance Learning in Meteorology.

Beijing, China **July 20 -22**

International Symposium on Environment and Biometeorology.

Heidelberg, Germany **July 24 - 27**

3rd International Symposium on
"Air-Water-Gas Transfer".

Trieste, Italy **July 31 - August 4**

International Symposium on
"African Drought".

Toulouse, France **July 24 -28**

WMO Symposium on
"Education and Training - Curriculum".

Honolulu, HI, USA **August 5 - 12**

21st Annual General Assembly of International Association of the Physical Sciences of the Oceans.

Mendoza, Argentina **August 13 - 27**

IGU COC Workshop & Field Experiment on
"Climatology and Air Pollution".

Sao Paulo, Brazil **August 21 - 25**

3rd International Symposium on
"Hydrological Applications of Weather Radar".

Edinburgh, Scotland, UK **September 4 - 7**

5th British Hydrological Society National Symposium.

Hamburg, Germany **September 4 - 8**

3rd International Conference on
"Modelling of Global Climate Change and Variability".

North Weald, England, UK **September 5 - 8**

Met-X '95 International Meteorological Exhibition.

Syracuse, NY, USA **September 13 - 15**

4th US / Canada Workshop on
"Great Lakes Operational Meteorology".

Seattle, WA, USA **September 18 - 22**

3rd Thematic Conference on
"Remote Sensing for Marine and Coastal Environments".

Kansas City, MO, USA **September 19 -22**

4th NWS National Workshop on
"Winter Weather Forecasting".

Toulouse, France **September 25 - 29**

ECAM '95 2nd European Conference on
"Applications of Meteorology".

Pretoria, South Africa **October**

2nd International Conference of the
African Meteorological Society.

Vail, CO, USA **October 9 - 13**

27th American Meterorological Society Conference on
"Radar Meteorology".

Beijing, China **October 23 - 27**

International Workshop on
"Limited-Area and Variable Resolution Models".

Baltimore, MD, USA **November 6 - 10**

21st International Technical Meeting on
"Air Pollution Modelling and its Application".

Hanover, NH, USA **December 5 - 9**

International Conference for Arctic Research Planning.

1996

Orlando, FL, USA, **January 4 - 8**

CONSERV96 Conference and Exposition.

Atlanta, GA, USA, **January 28 - February 2**

76th American Meteorological Society Meeting.

5th American Meteorological Society Symposium on
"Education".

7th American Meteorological Society Symposium on
"Global Change Studies".

8th American Meteorological Society Conference on
"Satellite Meteorology and Oceanography".

9th Joint AMS/AWMA Conference on
"Applications of Air Pollution Meteorology".

12th American Meteorological Society
International Conference on
"Interactive Information and Processing Systems for Meteorology, Oceanography and Hydrology".

12th American Meteorological Society Conference on
"Biometeorology and Aerobiology".

22nd American Meteorological Society Conference on
"Agricultural and Forest Meteorology".

American Meteorological Society Symposium on
"Planned and Inadvertent Weather Modification".

American Meteorological Society Symposium on
"Coastal Oceanic and Atmospheric Prediction".

San Francisco, CA, USA **February 19 - 23**

18th American Meteorological Society Conference on
"Severe Local Storms".

13th American Meteorological Society Conference on
"Probability and Statistics".

Hong Kong **March 16**

7th Hong Kong Meteorological Society Annual Meeting.

Edinburgh, Scotland, UK **July 22 - 26**

4th International Conference on
"School and Popular Meteorology Education".

Boston, MA, USA **Summer**

25th American Meteorological Society Conference on
"Broadcast Meteorology".

Ljubljana, Slovenia **September 1 - 8**

14th International Congress of Biometeorology.

Reading, England, UK **September 9 - 13**

7th International Conference on
"Mesoscale Processes"

HONG KONG METEOROLOGICAL SOCIETY

INFORMATION FOR CONTRIBUTORS TO THE BULLETIN

Technical or research articles, as well as reviews and correspondence of a topical nature are welcome. In general contributions should be short, although exceptions may be made by prior arrangement and at the discretion of the Editorial Board. Copyright of material submitted for publication remains that of the author(s). However, any previous, current or anticipated future use of such material by the author must be stated at the time of submission.

Manuscripts must be accurate and preferably in the form of a floppy diskette containing an electronic version in one of the common word processing formats such as Word, Wordstar or Wordperfect. Whether or not an electronic form is submitted, two complete printed manuscript copies of the article should be submitted. These should be preceded by a covering page stating the title of the article, the full name of the author(s), identification data for each author (position and institution or other affiliation and mailing address). An abstract of about 150 words should be included. Manuscripts should be double-spaced, including references, single side only on A4 paper with a 2.5 cm margin on each side, and be numbered serially in pencil.

All references should be arranged in alphabetical and chronological order. In the text, in brackets, author's surname(s) followed by the date; in the reference list at the end, the author's surname(s) and initials followed by the date and the title of the work. If a book, this should be followed by the publisher's name, place of publication and number of pages; or, if a journal article, by the title of the periodical, volume and page numbers.

Originals of tables should be neatly drawn as they will be reproduced directly. Diagrams should be in black on tracing material or smooth white paper, with a line weight suitable for any intended reduction from the original submitted size. Black and white photographs should be clear with strong contrasts. Colour photographs are also acceptable by prior arrangement with the Editorial Board. Please contact the Editor-in-chief for details. Originals of all illustrations should be numbered consecutively with captions printed on separate sheets of paper and should be clearly identified with the author's name(s) on the back. All copyright materials to be published must be cleared by the contributor(s).

The principal author will be sent proofs for checking prior to publication. The Society does not provide authors with free offprints of items published in the Bulletin, but may be able to obtain quotations on behalf of authors of technical articles who express, at the time of submission, a wish to purchase offprints from the printer.

Enquiries and all correspondence should be addressed to the Editor-in-chief, Hong Kong Meteorological Society Bulletin, *c/o* Department of Geography and Geology, The University of Hong Kong, Pokfulam Road, Hong Kong. *(Telephone: + (852) 2859-7022; Telefax: + (852) 2559-8994 or + (852) 2549-9763; email: billkyle@hkucc.hku.hk or billkyle@hkuxa.hku.hk).*

香港氣象學會

HKMetS BULLETIN, Vol. 5, Number 1, 1995

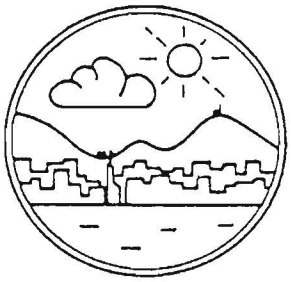

HONG KONG METEOROLOGICAL SOCIETY

BULLETIN

CONTENTS

Single Copy Price: HK$ 150
(for subscription rates see inside front cover)